Synthesis and immobilisation of unsaturated, functional phosphorus ligands and their metal complexes

Von der Fakultät Chemie der Universität Stuttgart
zur Erlangung der Würde eines
Doktors der Naturwissenschaften (Dr. rer. Nat.)
genehmigte Abhandlung

vorgelegt von

Samith Komath Mallissery
aus Kerala (Indien)

Hauptberichter:	Prof. Dr. Dietrich Gudat
Mitberichter:	Prof. Dr. Wolfgang Kaim
Tag der mündlichen Prüfung:	22.07.09

Institut für Anorganische Chemie der Universität Stuttgart

2009

Dedicated to my Pappa and my Aunt...............

Research is to see what everybody else has seen, and to think what nobody else has thought

…………..Albert Szent Gyorgyi

Acknowledgements

Thanks to Frau Angelika for being friendly and cheerful in all our trips and outings and making those lively and comfortable. Thanks a lot to Sreekumar, Sumi, Mathan, Atanu and Dinesh for their helping hand during my stay at Stuttgart. I thank my friends at Stuttgart who made my stay here wonderful and memorable that I would like to cherish in my memories.

I feel privileged and lucky to be associated with this great and wonderful institution and to work along with the best people. I wish the very best for all these people in their future endeavours.

Special thanks to my M.Tech project supervisor Dr. T. P. Mohandas at NCL and Dr. S. Prathapan at CUSAT for all the help that I needed for coming to Stuttgart for pursuing my research work. I thank the staffs of the Chemistry department of CUSAT for supporting me during my project work.

My special thanks to Rajesh Shenoi at NCL for all the help and support in the labs at NCL.

I would like to express my thanks to my professors at S. N. College, Kannur for motivating me to do higher studies and looking curiously to see my progress while I did my masters course. Thanks to Prof. Prasannan who taught me the basics of chemistry and his endless effort to observe my good future.

I would like to thank my friends Santhosh Paul, Radhakrishnan, Biju Devassya, Muthu Krishnan, Hemanth, John, Ramanathan, Harikrishnan, Sreejith, Shijo for their support and enquiries about the research work and for their wishes.

I cannot recall but with awe my mother for supporting me in all my endeavours and standing by me in all difficulties. I would like to thank my sister Samitha and brother-in-law Rohit for their support and care and the special person, my little lovely niece Suhani whom I am eager to see, for bringing new spirit and joy in our lives. I use this oppurtunity to thank my cousins Sreejith and Sreenish for helping me always.

Symbols and abbrevations

NMR - Nuclear Magnetic Resonance

HR MAS - High Resolution Magic Angle Spinning

MO - Molecular orbital

HOMO - Highest occupied molecular orbital

LUMO - Lowest occupied molecular orbital

σ - Sigma

π - Pi

CP MAS - Cross polarization Magic angle spinning

Fig - Figure

d - Doublet

δ - Chemical shift

δ_{iso} - Isotropic chemical shift

DCM - Dichloromethane

M - Multiplets

Me - Methyl

m/e - Mass to charge ratio

HMQC - Heteronuclear multiple quantum coherence

HSQC - Heterospin quantum coherence

tht - Tetrahydrothiophene

thf - Tetrahydrofuran

CSA - Chemical shift anisotropy

XPS - X ray photoelectron spectroscopy

υ_{rot} - Rotational frequency

ns - Number of scans

dmf - Dimethylformamide

$[M]^{+}$ - Molecular ion

2D - Two dimensional

m.p. - Melting point

RT - Room temperature

s - Second

min - Minute

HP Dec - High power Decoupling

BET - Brunauer, Emmett and Teller

K - Kelvin

ICP - Inductively coupled plasma

ms - millisec

efg - Electric field gradient

hrs - hours

ESI - Electron spray ionization

EI - Electron ionization

TABLE OF CONTENTS

6. Immobilisation of monophosphaferrocene derivatives on silica

7. Experimentals

1. Introduction

1.1 Immobilisation of metal complexes

Remarkable developments have taken place in homogenous and heterogenous catalysis over the past few decades. Traditionally a comparison between these two catalyses point out a number of strong and weak points[1]. The definition of the active site at the molecular level and the variability in design are considered as significant advantages for homogenous catalysis, while limited activity and stability usually represent its weak points. On the other hand, ease of separation, recovery, recycling and stability of catalysts are in favour of heterogenous catalysis. Difficulties in the characterization at the molecular level, complexity and reproducibility in preparation, negative effects on selectivity resulting from the occurance of diffusion limitations, are doubtless disadvantageous when designing heterogenous processes.

For this reason, there have been many approaches for heterogenizing homogenous metal complexes by attaching well defined molecular species on supports which can be inorganic materials or organic polymers- in other words.

immobilising molecular complexes

In principle, immobilised metal complexes enjoy all the advantages of homogenous and heterogenous systems[2]. Immobilisation of metal complexes on inorganic supports has opened many tracks to more practical fine chemical processes[3]. Several methods of immobilisation which have been proposed are covalent tethering, adsorption, electrostatic retention and encapsulation. Immobilisation via covalent attachment of a ligand to the support **(scheme 1)** is the most popular and versatile approach and has a broad applicability[4], but normally requires redesign of the ligand to get the appropriate functionalization. An important property of such heterogenized systems is that complexes attached to the support via stable bonds experience no leaching. Some typical examples using this approach are the silica and

1 H. U. Blaser, B. Pugin and M. Studer, *In Chiral Catalyst Immobilization and Recycling*. D. E. De Vos, I. F. J Vankelecom, and P. A. Jacobs, (eds) Wiley-VCH, Weinheim. **2000**, 1-15.
2 W. C. Finch, R. D. Gillespie and D. Hedden, T. J. Marks, *J. Am. Chem. Soc*. **1990**, *112*, 6221.
3 S. Abramson, N. Bellocq and M. Lasperas, *Top. Catal*. **2000**, *13*, 339.
4 A. Kinting, H. Krause and M. Capka, *J. Catal*. **1985**, *25*, 152.

MCM-41 immobilised copper-bis(oxazoline) for Friedel crafts reactions[5], silica immobilised rhodium-diphosphine complex for hydroformylation[6] and silica immobilised chromium (II) salen complexes for the asymmetric ring opening of epoxides[7].
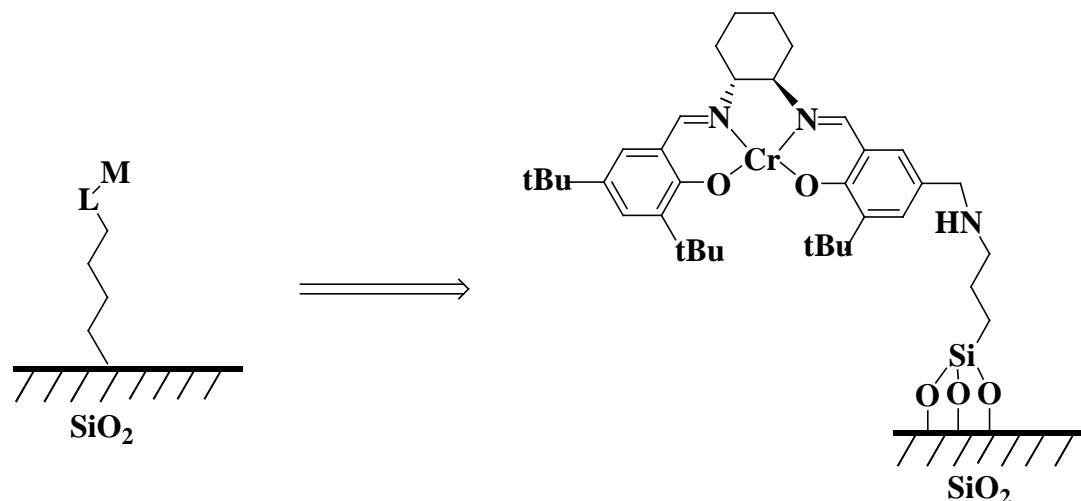
scheme 1: Covalent tethering

Occasionally, immobilisation via adsorption is possible, provided the complex is not removed from its support as a result of competing interactions with solvents. As immobilisation by adsorption can rely on weak van der Wals interactions, the stability of the supported catalyst can be improved by modifying the catalyst and support for hydrogen bonding to occur. Chiral rhodium catalysts have been immobilised in this way **(scheme 2)** where a phosphine ligand was modified to incorporate sulfonic acid groups which are hydrogen bonded with the silanols present on the surface[8].

[5] A. Corma, H. Garcia, A. Mousaif, M. J. Sabatier, R. Zniber and A. Redouane, *Chem. Commun*. **2002**, 1058.

[6] J. S. Albertus, Joost, N. H. Reek, Paul, C. J. Kamer and P. W. N. M van Leeuwen, *J. Am. Chem. Soc*. **2001**, *123*, 8468- 8476.

[7] C. Baleizao, B. Gigante, M. J. Sabatier, H. Garcia and A. Corma*, Appl. Catal. A*. **2002**, *288*, 279.

[8] C. Bianchini, P. Barbaro, V. Dal Santo, R. Gobetto, A. Meli, W. Oberhause, R. Psaro and F. Vizza, *Adv. Synth. Catal*. **2001**, *41*, 343.
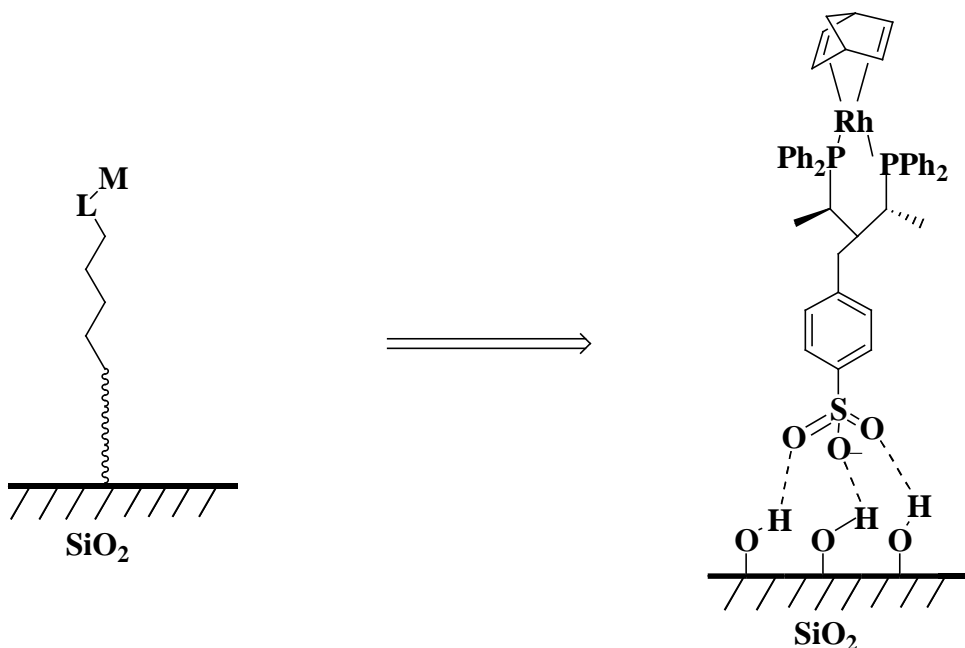
scheme 2: Adsorption

Solid support ion exchange capacity can be applied to immobilise charged complexes through ion pair formation or electrostatic retention. Even though the competetion with ionic substrates and salts in solution is obvious, cheap inorganic cations as well as anion exchangers are readily available, namely zeolites and clays, and layered double hydroxides, respectively. Historically, the first strategy in this respect was the immoblilisation of Box-copper complexes **(scheme 3)** through ionic exchange on anionic supports and has been thoroughly investigated by Mayoral and co-workers[9] since 1997.
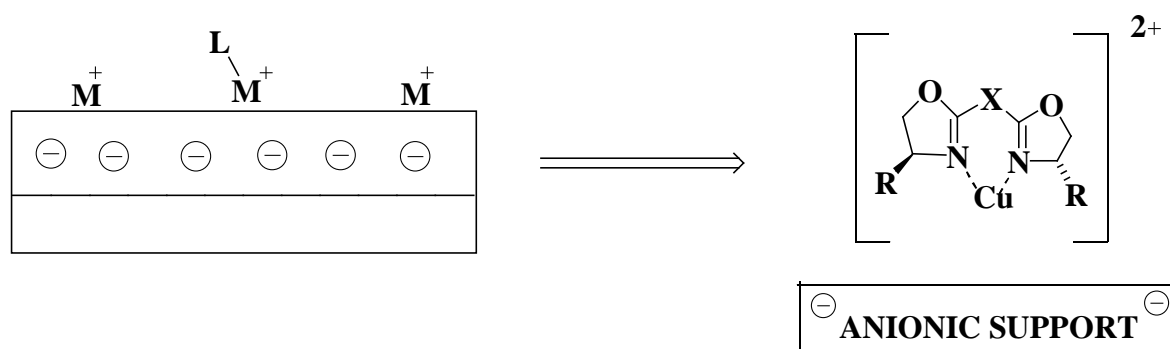
scheme 3: Electrostatic retention

Immobilisation is also possible by steric inclusion, or entrapment of the active transition metal complex in microporus supports. Encapsulation of a metal complex in the cages of a support

---

[9] J. M. Fraile, J. I. Garcia, J. A. Mayoral and T. Tarnai, *Tetra. Asymm.* **1997**, *8*, 2089.

fully depends on the (respective) size of the complex and the cage in which it is held sterically to prevent leaching during the reaction. As catalyst retention requires the encapsulation of a relatively large complex into cages only accessible through windows of molecular dimensions, the term ´´ship-in-a-bottle`` (**scheme 4)** has been used for this methodology. Intrinsically the size of the window not only determines the retention of the complex, but also limits the substrate size that can be used. This method is particularly employed to immobilise metal salen complexes within supercages of faujasite type zeolites[10,11].

Mn^{III} complex in zeolite
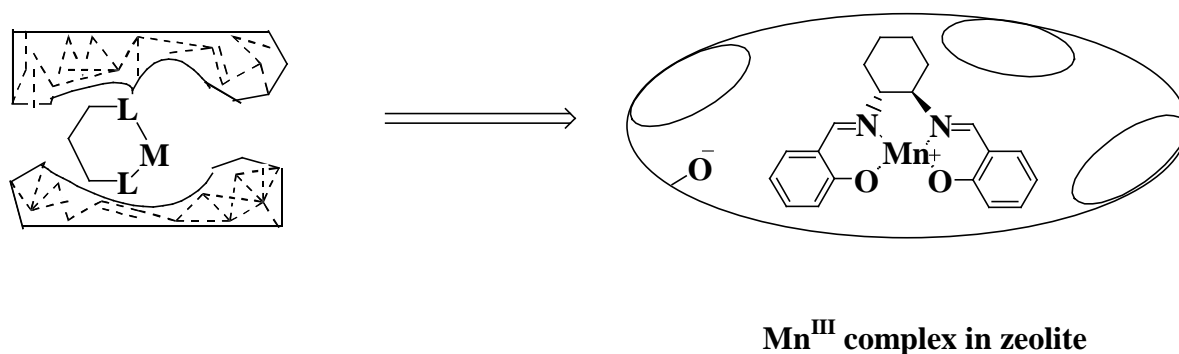
scheme 4: Encapsulation

Of the four methodologies described, only two, namely covalent tethering and electrostatic interaction, have shown to provide reasonably stable supported systems. Adsorption methodology provides relatively non-stable catalysts, even though it offers a relatively facile method of immobilisation.

The topic of immobilisation has been the subject of several hundred publications and several reviews. Graham J. Hutchings and coworkers[12] highlighted that immobilised catalysts can give higher enantioselection when compared with non-immobilised counterparts and addressed how high enantioselection in immobilised systems is achieved. H. Papp and T.Lutz[13] demonstrated the covalent bonding technique as the most effective approach for peptide bound immobilisation of Mn(III)-salen complex and investigated the catalytic epoxidation reaction. Pioneering work of Jose A. Mayoral et al.[14] on supported oxazoline based complexes for a wide variety of enantioselective reactions; detected the surface effects,

[10] S. B. Ogunwami and T. Bein, *Chem. Commun*. **1997**, 901.
[11] M. J. Sabatier, A. Corma, A. Domenech, V. Fornes and H. Garcia, *Chem. Commun*. **1997**, 1285.
[12] P. M. Morn and G. J. Hutchings, *Chem. Soc. Rev*. **2004**, *33*, 108-122.
[13] T.Lutz and H. Papp, *Kinteics and catalysis*. **2007**, *48*, 176-182.
[14] J. M. Fraile, J. I. Garcia and J. A. Mayoral, *Coord. Chem. Rev*. **2008**, *252*, 624-646.

which opened the door to developments in new stereochemical features of heterogenously catalysed enantioselective reactions. A bidentate phosphine complex anchored onto mesoporous molecular sieve demonstrated by Cathleen M. Crudden[15] shows that the activity of a catalyst for alkene hydrogenation was dependent on the method of grafting. Furthermore, immobilisation is persumed to be a hot area in the arena of biochemistry. A widespread interest for enzyme immobilisation[16] has been noticed in recent years. The driving force for this interest in enzyme immobilisation is enhanced stability, repeated use, facile separation from reaction mixture and the prevention of enzyme contamination in products. Encapsulated enzymes serve as useful building blocks for construction of biofunctional thin films with high enzyme loadings[16].

Before 1980, characterization of the immobilised material at the molecular level was a great barrier for the researchers. However, laterly with the increasing availabilty of solid state NMR techniques, the task of characterising the immobilised species was made easier. To the best of our knowledge, the first classical publication for studying the immobilised complexes formed via linkers with the use of solid state NMR was by Fyfe and coworkers[17]. Recently Blümel et al.[18] described the immobilisation of phosphine linkers and their complexes with various methodolgies; they pointed out that the structural integrity and mobility of the immobilised metal complexes with respect to phosphine linkers are easy to investigate by classical solid state NMR and high resolution magic angle spinning (HR MAS) NMR techniques. Even elecrostatic bonding to the support via phosphonium ion and leaching effects in the presence of solvents could be probed by (HR MAS) NMR under realistic conditions.

.

[15] C. M. Crudden, D. Allen, M. D. Mikoluk and J. Sun, *Chem. Commun*. **2001**, 1154-1155.
[16] Y. Wang and F. Caruso, *Chem. Mater*. **2005**, *17*, 953-961.
[17] L. Berni, H. C. Clark, J. A. Davies, C. A. Fyfe and R. E. Wasylishen, *J. Am. Chem. Soc*. **1982**, *104*, 438.
[18] C. Merckle, S. Haubrich, J. Blümel, *J. Organomet. Chem.* **2001**, 627, 44-54.

1.2 Phosphinines and their metal complexes:

The ligands having an sp^2 hybridized phosphorus atom are an interesting area of phosphorus chemistry[19,20]. The reason lies in the difference in electronic properties of these ligands as compared to their nitrogen counterparts and classical tertiary phosphines[21]. One class of such phosphorus heterocycles are phosphinines (formerly called λ^3 – phosphorines or phosphabenzenes)[22]. The bonding situation and possible aromaticity of phosphinines have been disputed for a long time. In 1974 the structure of phosphinine was established with the use of electron diffraction and microwave study[23,24] and proved to be planar. The P=C bond strength was estimated as nearly 60 - 70% of that of C=C bond as a result of symmetry allowed overlap between the p_z orbitals[25]. Later, spectroscopic studies and physicochemical investigations clearly indicated the aromaticity of phosphinines[26]. Due to the lower electronegativity of phosphorus, the P atom bears a positive charge where as the α-carbons bear negative charge[27,28]. The opposite is observed in the case of pyridines. The P atom in phosphinines behaves as a sigma donor towards the carbocyclic C_5 system but as an acceptor in π sense. Phosphinines exhibit weak basic, or nucleophilic character[29]. This lack of basicity has been accounted for by considering geometrical factors. The internal C-P-C angle takes a value of 100° while pyridine has 117°. The closing of this angle, results from the lengthening of the carbon the hetero atom bond (P-C: 1.73 Å; C-N: 1.35 Å) which also reflects the difficulty of the hetero atom in achieving sp^2 hybridization. The recent calculations have assessed that the lone pair in pyridine has 29.1% s character versus 63.8% in phosphinines[27]. Consequently for a strong bond to form with an added proton, the lone pair must gain an important p character and be directional. This rehybridization is disfavored by the strain imposed on the C-C-C angles that block the opening of the internal C-P-C angle[30]. Correlation between core-ionization energies and proton affinities support this assumption. Due to the lack of basicity, phosphinines do not form classical lewis acid - base adducts.

[19] P. Le Floch, *Coord. Chem. Rev.* **2006**, *250*, 627-681.
[20] L. Weber, *Angew. Chem. Int. Ed*. **2002**, *41*, 563-572.
[21] J. Waluk, H. P. Klein, A. J. Ashe, III and J. Michl, *Organometallics*. **1989**, *8*, 2804.
[22] G. Märkl and C. Martin, *Angew. Chem. Int. Ed. Engl*. **1974**, *13*, 408.
[23] A. J. Ashe III, *Acc. Chem. Res*. **1978**, *11*, 153.
[24] T. C. Wong and L.S. Bartell, *J.Chem. Phys*. **1974**, *61*, 2840.
[25] P. D. Burrow, A. J. Ashe, III, D. J. Belville, and K. D. Jordan, *J. Am. Chem. Soc*. **1982**, *104*, 425.
[26] M. J. S. Dewar and A. Holder, *Heterocycles*. **1989**, *28*, 1135.
[27] P. Rosa, N. Mezailles, F. Mathey and P. Le Floch, *J. Org. Chem*. **1998**, *63*, 4826.
[28] L. Nyulazzi and G. Keglevich, *Heteroatom. Chem*. **1994**, *5*, 131.
[29] H. Oehling and A. Schweig, *Phosphorus*. **1971**, 203.
[30] D. J. Berger, P. P. Gaspar, and J. F. Liebman, *J. Mol. Struct. (Theochem)*. **1995**, *51*, 338.

Phosphinines can be oxidized under classical conditions leading to the disruption of aromaticity. Owing to high reactivity, isolation of the corresponding oxides in pure form remained unsuccessful[31].

Nucleophiles usually attack at the electropositive P atom in phosphinines to give phosphacyclohexadienyl anions **(scheme 5)**. This particular electronic situation has considerably hampered the synthetic development of phosphinines for a long time since commonly used methodologies for the derivitization of arenes and N,O,S heterocycles (proton abstraction, metal-halogen exchange) are not duplicable.
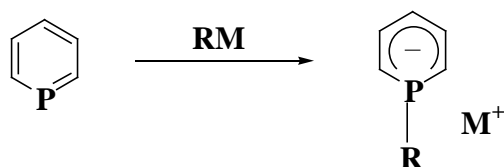
scheme 5

The first synthetic method for phosphinines was laid down by Markl[32] in 1966 who synthesized 2,4,6-triphenyl phosphinine from the corresponding pyrylium salt mediated by O^+/P exchange; with the source of PH_3, which can be relatively diverse ($P(CH_2OH)_3$[33], $P(SiMe_3)_3$[34]) **(scheme 6)**. Their successful synthesis unambiguously demonstrated that the reactive Phosphorous carbon double bond could be thermodynamically stabilized by incorporation into aromatic structure. Recently D. Vogt and C. Müller demonstrated the synthesis of various donor-functionalized phosphinines, that introduced specific substituents into the desired position of heterocyclic framework[35] .

[31] A. Hettche and K. Dimroth, *Chem. Ber.* **1973**, *106*, 1001.

[32] G. Märkl, *Angew. Chem. Int. Ed. Engl.* **1966**, *5*, 846.

[33] K. Dimroth, N. Greif, W. Stade and F. W. Steuber, *Angew. Chem. Int. Ed. Engl.* **1967**, *6*, 711.

[34] G. Märkl, F. Lieb and A. Merz, *Angew. Chem. Int. Ed. Engl.* **1967**, *6*, 458.

[35] 1) C. Muller, E. A. Pidko, A. J. P. M. Staring, M. Lutz, A. L. Spek, R. A. van Santen and D. Vogt, *Chem. Eur. J.* **2008**, *14*, 4899-4905. 2) C. Muller, L. G. Lopez, H. Kooijman, A. L. Spek and D. Vogt, *Tetra. Lett.* **2006**, *47*, 2017-2020.
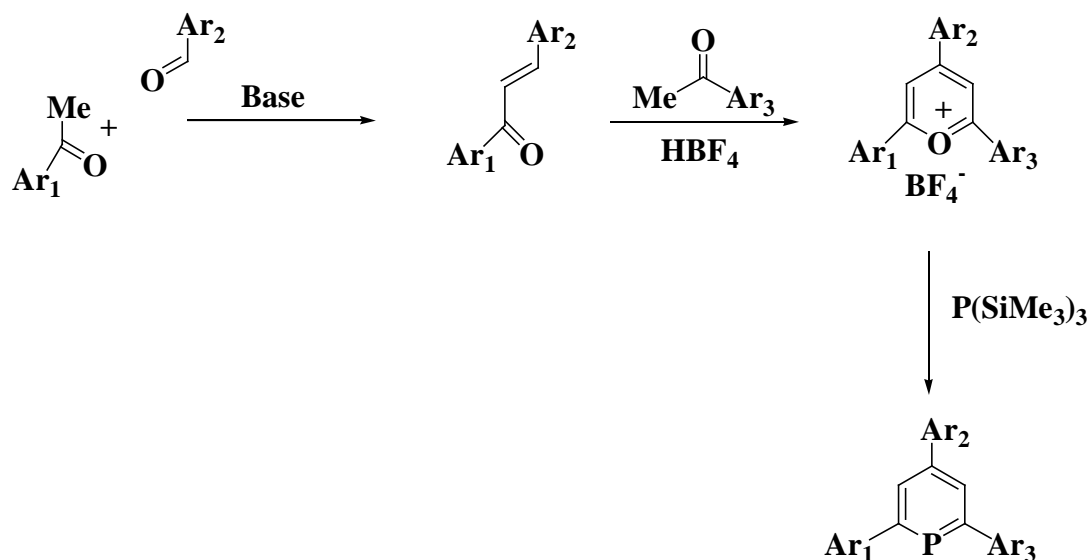
scheme 6

For some time 2,4,6-triaryl substitiuted phosphinines remained the only easily accessible derivatives. The development of new methods allowed the synthesis of different functional derivatives. Among these, ring expansion of phospholes[36] and thermolysis of tris(allyl)phosphine[37] are frequently employed for developing phosphinines. As will be shown later, titanacycle transfer reactions are an attractive and promising field of investigations in the development of polyfunctional phosphinines[38,39]. 1,3,2-diazaphosphinine (**scheme 7**) obtained from

[36] C. Charrier, H. Bonnard and F. Mathey, *J. Org. Chem.* **1982**, *47*, 2376.

[37] P. Le Floch and F. Marthey, *J. Chem. Soc., Chem. Commun*. **1993**, 1295.

[38] N. Mezailles, N. Avarvari, L. Ricard, F. Mathey and P. Le Floch, *Inorg. Chem.* **1998**, *37*, 5313-5316.

[39] N. Avarvari, P. Le. Floch and F. Mathey, *J. Am. Chem. Soc*. **1996**, *118*, 11978.

scheme 7

Cp₂Ti(Me)₂
1) 2RCN
2) PCl₃
3) Et₃N
→ (1,3,2-diazaphosphinine, R, R, N, P, N)
R₁CCR₂ →
(bicyclic intermediate: R, N, R, N–P, R₂, R₁)

–RCN ↓

R₄, R₂, R₃, P, R₁ ← R₃CCR₄, –RCN ← R, R₂, N, P, R₁, –RCN

R = ᵗBu
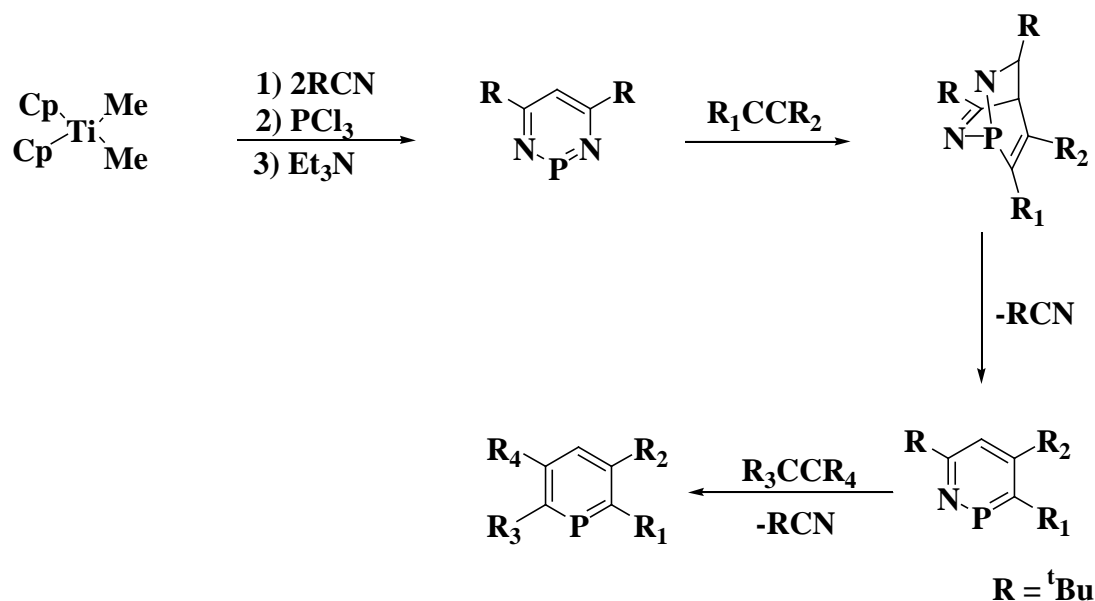
1,3,2- diazatitanacyclohexadienes[40] initially synthesized by Doxsee et al[41,42,43] , turned out to be an efficient precursor for 2,3,5,6-tetrafunctional phosphinines via a N-Ti and N-P bond metathesis[44]. The two significant advantages of this route are firstly, the precursor 1,3,2-diazaphosphinine can be obtained in fairly good yields in a single pot reaction from Cp_2TiMe_2 and need not to be isolated before reacting with alkynes. Secondly, the reaction with alkynes procceed under mild condition due to the high polarity of the formal 1,4 dipole –P=N-C=C.

The coordination chemistry of these P=C bond systems is remarkably different from that of classical C, N, P based systems. Thus considering solely coordination through the P lone pair (η^1 coordination), phosphinines are known to act as weaker σ donors than most of the classical sp^3 hybridized phosphines featuring three P-C bonds. Based on MO calculations the lone pair orbital is only the third highest occupied orbital in phosphinines whereas it is the HOMO in pyridine[45,46,47]. Conversely σ donor ability of phosphinine is sharply reduced. Neverthless, having a LUMO of lower energy, phosphinines will act as better π acceptor ligands[19]. Obviously this particular electronic configuration confers a very unusual organic

[40] K. M. Doxsee and J. B. Farahi, *J. Am. Chem. Soc*. **1988**, *110*, 7239.
[41] K. M. Doxsee and J. B. Farahi, *J. Chem. Soc, Chem. Commun*. **1990**, 1452.
[42] K. M. Doxsee, J. B. Farahi and H. Hope, *J. Am. Chem. Soc*. **1991**, *113*, 8889.
[43] K. M. Doxsee, J. J. J. Juliette, J. K. M. Mouser and K. Zientara, *Organometallics.* **1993**, *12*, 4682.
[44] N. Avarvari, P. Le. Floch, L. Ricard and F. Mathey, *Organometallics.* **1997**, *16*, 4089.
[45] J. Waluk, H. P. Klein, A. J. Ashe III, and J. Michl, *Organometallics*. **1989**, *8*, 2804.
[46] T. Veszpremi, L. Nyulaszi, P. Varnai and J. Reffy, *Acta Chim. Hung.-Models Chem*. **1993**, *130*, 691.
[47] P. D. Burrow, A. J. Ashe III, D. J. Belville and K. D. Jordan, *J. Am. Chem. Soc*. **1982**, *104*, 425.

and coordination chemistry on phosphinines. The transition metal complexes of phosphinines with $\eta^1(\sigma)$ and $\eta^6(\pi)$ coordination mode are widely known[19] and the last few decades reseachers have a great input in their application to homogenous catalysis like hydroformylation, enantioselective catalysis, Diels-Alder reaction etc[48,49]. Phosphinines also behave as π donor ligands. Interestingly, this low coordinated phosphorus ligand can accommodate various bonding modes and combinations of bonding modes due to the presence of the phosphorus atom lone pair and a reactive π and π^* system (**Fig 1**).
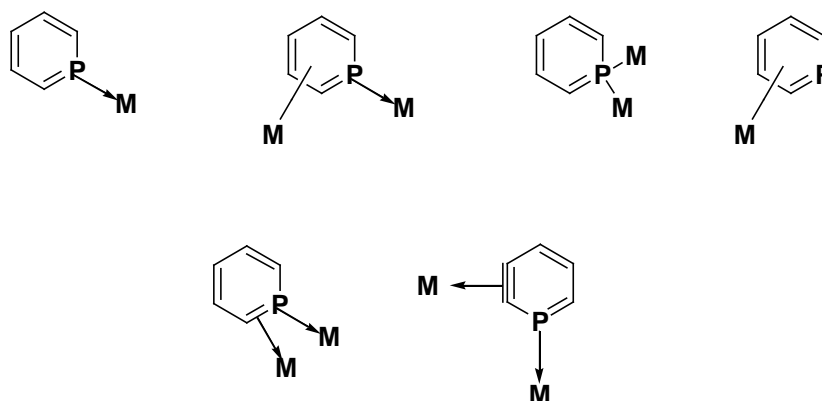
Fig 1

As mentioned, the most important electronic characteristic of phosphinines is their strong π accepting capacity which makes them ligands suitable to the stabilization of electron rich transition metal complexes. Thus it is evident that formation of η^1 complexes of phosphinines (2e-donor) is favoured by transition metals in low oxidation states. A nice illustration for the exceptional ability of phosphinines to stabilize metals in low oxidation state was given by Elschenbroich et al. who synthesised and characterized homoleptic complexes[50] [Ni(η^1-$C_5H_5P)_4$], [Cr(η^1-$C_5H_5P)_6$][51] and [Fe(η^1-$C_5H_5P)_5$][52]. Historically, tetrakis (phosphinine) Ni(0) is the first example (**Fig 2**).

[48] B. Breit, R. Winde, T. Mackewitz, R. Paciello and K. Harms, *Chem. Eur. J.* **2001**, *7*, 3106.

[49] E. F. DiMauro and M. C. Kozlowski, *J. Chem. Soc. Perkin. Trans*, **2002**, *1*, 439.

[50] C. Elschenbroich, M. Nowotny, A. Behrendt, W. Massa and S. Wocaldo, *Angew. Chem. Int. Ed.* **1992**, *31*, 1343.

[51] C. Elschenbroich, S. Voss, O. Schiemann, A. Lippek and K. Harms, *Organometallics*, **1998**, *17*, 4417.

[52] C. Elschenbroich, M. Nowotny, A. Behrendt, K. Harms, S. Wocaldo and J. Pebler, *J. Am. Chem. Soc.* **1994**, *116*, 6217.
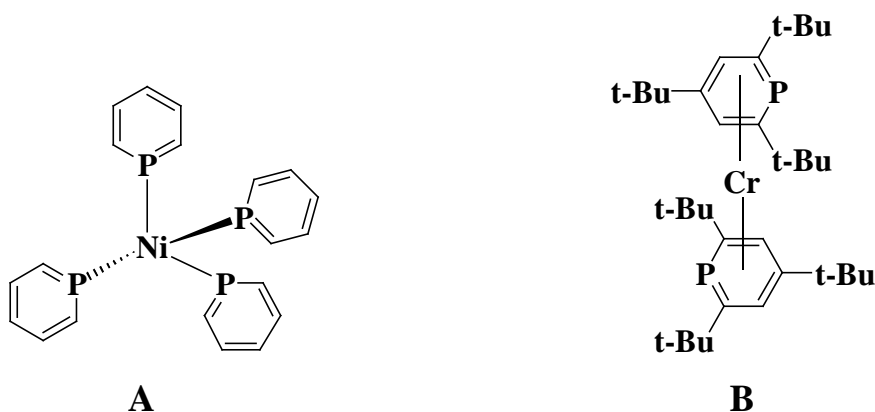
Fig 2

Whereas the late transition metals prefer the η^1 coordination, the η^6 mode predominates with the early transition metals[19]. Further in the chemistry of phosphinines, the substitution scheme of the ring plays a determinant role on the outcome of the complexation. A suitable example to illustrate this is the synthesis of sandwich complex of chromium(0) of the bulky 2,4,6-tri(tert-butyl)phosphinine[53] (**Fig 2**). With iron, the introduction of only one bulky trimethylsilyl group is sufficient to adopt η^6 coordination[54]. Also with group 8 metals, a η^6 ruthenium complex of 2,6-bis(trimethylsilyl)phosphinine was formed by reacting the ligand with the [Ru(η^5-Cp*(η^4-C$_4$H$_{10}$)Cl] complex in the presence of AgBF$_4$ as chloride abstractor. During the same study it was found that with poorly substituted phosphinines like the 2-bromo-4,5-dimethylderivative (C$_7$H$_8$PBr) a cationic classical η^1 [Ru(η^5-Cp(C$_7$H$_8$PBr$_3$)][BF$_4$] complex is formed [55]. Cationic complexes of the [M(COD)](M = Rh, Ir) with η^6 coordinated heterocycles were also obatined with group 9 metals when a 2,6-bis(trimethylsilyl)phosphinine was used as a ligand. Interestingly, η^1 coordination to give a cationic complex occurs when only one trimethylsilyl group is present [56].

A few other unusual bonding modes were also reported for phosphinines. A first example was given with the synthesis of stable phosphabenzyne zirconocene complex[57] (**Fig 3**). The synthetic methodology for this complex is similar to that used for the synthesis of classic η^2 benzyne zirconocene complex and relies on a β-abstraction followed by the elimination of benzene or methane from the corresponding Zr(1V) derivative. μ, η^2 coordination mode (two

[53] P. L. Arnold, F. G. N. Cloke, K. Khan and P. Scott, *J. Organomet. Chem.* **1997**, *77*, 528.

[54] F. Knoch, F. Kremer, U. Schimdt, U. Zenneck, P. Le. Floch and F. Mathey, *Organometallics.* **1996**, *15*, 2713.

[55] P. Le. Floch, F. Knoch, F. Kremer, F. Mathey, J. Scholz, K. H. Thiele and U. Zenneck, *Eur. J. Inorg. Chem.* **1998**, 119.

[56] N. Mezailles, L. Ricard, F. Mathey and P. Le. Floch, *Organometallics.* **2001**, *20*, 3304.

[57] P. Le. Floch, L. Ricard and F. Mathey, *J. Chem. Soc., Chem. Commun.* **1993**, 789.

electrons given by the lone pair of phosphorus and two electrons by phosphorus carbon double bond) was seen in the complex[58] **(Fig 3)** which results from the reaction of a phosphinine with a $[Os_3H_3(CO)_{10}]$ cluster[59].

R = H, SiMe$_3$ or t-Bu
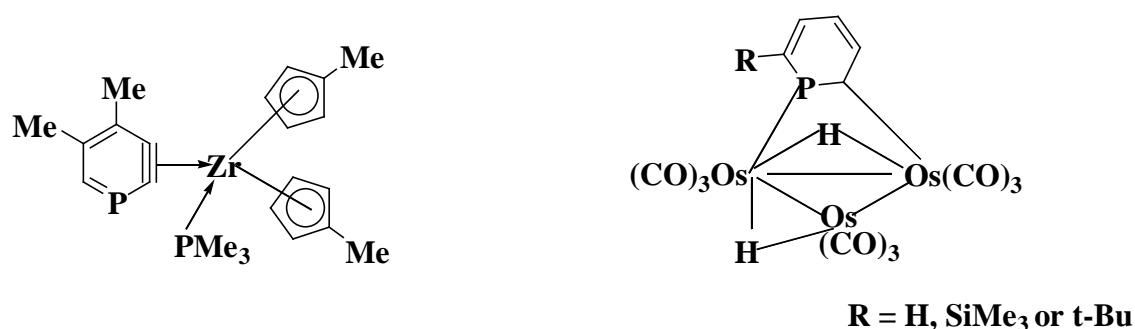
Fig 3

The outcome of the reaction proved to be highly dependent on the amount of phosphinine used and the substitution scheme of the ring. Polydentate ligands featuring phosphinines have also found application in coordination chemistry. Thus, classical Mn(I), Fe(I), Mo(I) bis(2-phosphinyl)phosphinines were reported by reacting the ligands with appropriate metal precursors, $[Mn_2(CO)_{10}]$, $[Fe(\eta^5-Cp)(CO)_2]_2$, $[MoCp(CO)_2]$ respectively[60].

It has been seen that stability of phosphinine ligand was found to be very dependent on the oxidation state of the metal[19]. A prerequiste for an efficient catalyst is the ability of the ligand, or part of them (in case of hemilabile system), to accommodate variable oxidation states involved in the catalytic cycle. In this regard it could be expected that phosphinines are not well-tailored for the development of efficient catalyst systems, but still reports are made of the successful application of the ligands in catalysis. Breit et al showed that phosphinine rhodium(I) complexes could be considered a useful hydroformylation catalyst for olefines[61] **(scheme 8)**. It was also shown that the phosphinine ligands could successfully address the

[58] P. Le Floch, A. Kolb and F. Mathey, *J. Chem. Soc., Chem. Commun.* **1994**, 2065.

[59] A. J. Arce, A. J. Deeming, Y. de Sanctis and J. Manzur, *J. Chem. Soc., Chem. Commun.* **1993**, 325.

[60] K. Waschbusch, P. Le. Floch, L. Ricard and F. Mathey, *Chem. Ber. Recl*, **1997**, *130*, 843.

[61] B. Breit, R. Paciello, B. Geisler and M. Röper, (BASF, A-G), Ger. Pat, 19621967, *Chem. Abstr.* **1999**, *130*, 129496.

difficulty of hydroformylation of internal olefines which is of particular interest in both synthetic organic and industrial contexts.
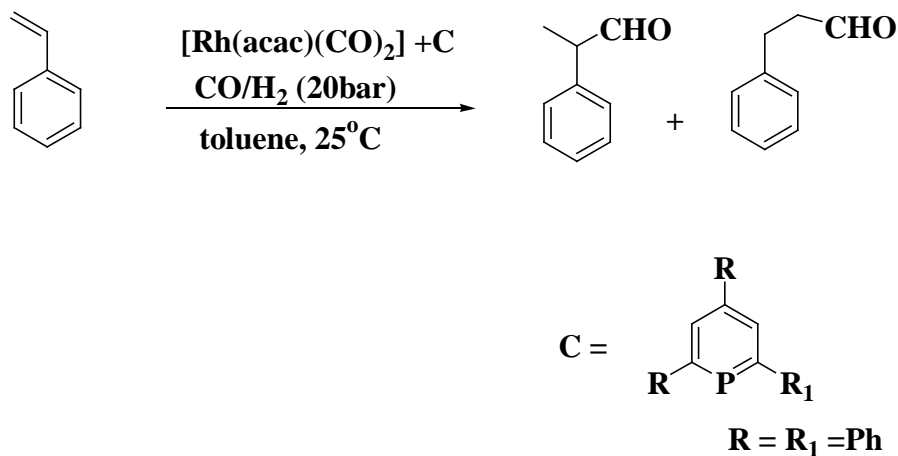
scheme 8

η^1 phosphinine complexes of Ni(0) were employed as a catalyst in Wender`s type [4+2] cycloadditions. The only report based on catalysis by η^6 complexes was made by Zenneck and coworkers who showed that is the use of η^6 Fe(0) complex of 2-trimethylsilyl-4,5-dimethylphosphinine catalyzes the cyclotrimerization of alkynes to form pyridines[62]

---

[62] D. Böhm, H. Geiger, F. Knoch, S. Kummer, P. Le Floch, F. Mathey, U. Schimdt and U. Zennck, *Phosphorus, Sulfur, Silicon*, **1996**, *109*, 173.

1.3 Phosphaferrocenes

Phosphaferrocenes, the first example of phosphametallocenes, are considered to be the most easily available low coordinate phosphorus ligands as the phosphorus atom in the phosphaferrocene molecule is still nucleophilic enough to act as a Lewis base to metal centres[63] and thereby constitute a very important class of compounds. The compound 3,4-dimethyl-1-phosphaferrocene **(Fig 4)** was first prepared by Mathey and coworkers[64] in 1977. Mathey conducted a detailed study of this and related compounds[65,66].
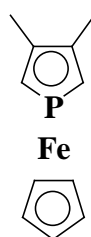
Fig 4

With the sp^2 phosphorus atom as part of an aromatic phospholyl system coordinated to a CpFe fragment, phosphaferrocenes constitute rather unique ligands which differ considerably from the phosphine ligands having sp^3 hybrid phosphorus atoms in both electronic and steric properties. Theoretical investigations revealed phosphaferrocene derivatives to be weakly σ donating and strongly π accepting ligands. This is due to the fact that their electron lone pair is energetically low-lying and their LUMO possesses largely p_z character at the phosphorus atom.

Unlike ferrocenes which can be deprotonated and are readily accessible to attack by a variety of electrophiles, phosphaferrocenes cannot be deprotonated. This obstructs an easy and general access to functional derivatives of phosphaferrocene. Electrophilic substitution is the only known method for introducing substituents on the phospholyl ring of phosphaferrocene moiety. The formylation[67], acylation[64] and carboxylation[68] of 3,4-dimethylphosphaferrocene in Friedel crafts or Vilsmeyer reactions have been found to

[63] F. Mathey, *J. Organomet. Chem.* **1990**, *149*, 400.

[64] F. Mathey, A. Mitschler and R. Weiss*, J. Am. Chem. Soc.* **1977**, *99*, 3537.

[65] X. Sava, L. Ricard, F. Mathey and P. Le Floch, *Organometallics.* **2000**, *19*, 4899-4903.

[66] F. Mathey, J. Fischer and J. H. Nelson, *Struct. Bonding*. **1983**, *55*, 154.

[67] G. deLauzon, B. Deschamps, J. Fischer, F. Mathey and A. Mitschler, *J. Am. Chem. Soc*. **1980**, *102*, 994.

[68] G. deLauzon, B. Deschamps and F. Mathey, *Nouv. J. Chim*, **1980**, *4*, 683.

procceed selectively at the phosphole ring, thereby forming monofunctionalized products with the additional substituents at the ortho-position of pholpholyl ring. The deactivating nature of formyl, acyl and carboxylic ester functionality prevents the formation of disubstituted derivatives. On the basis of pioneering work laid down by Mathey[69], phosphaferrocene constitutes an excellent building block for the development of chiral bidentate ligands by introduction of an appropriate donor substituent into the alpha position of the phospholyl ring, thereby incorporating chirality into the system by breaking the planar symmetry of phosphametallocene. Unlike ferrocene based ligands in which bidentate coordination to a metal centre is by two donor substituents, phosphaferrocene coordinates via the ring P atom[70,71,72,73] **(Fig 5)**.
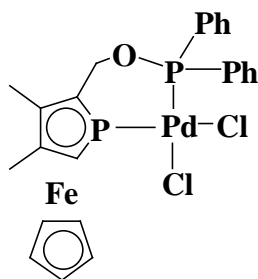
Fig 5

The steric properties of the molecule may be tuned by introducing substituents on the Cp ring, and the donor substituent on the phospholyl ring can be widely modified on the basis of steric bulk, the mode of donor function and the length of the backbone. The group of Ganter[74] has ilustrated that formyl derivatives of phosphaferrocene are convenient building blocks for the synthesis of various enantiomerically pure ligands. They succeeded in the separation of enantiomers. Other bidentate ligands like bis(phosphaferrocenyl)ferrocene[75] and systems featuring side functional arms were also prepared. The group of Fu [76] produced very efficient phosphaferrocene-based catalysts and mixed phosphaferrocene-oxazoline ligands **(Fig 6)**.

[69] C. Ganter, L. Brassat, C. Glinsböckel and B. Ganter, Organometallics. **1997**, *16*, 2862-2867.

[70] L. Brassat, B. Ganter and C. Ganter, *Chem. Eur. J*. **1998**, *4*, 2148-2153.

[71] C. Ganter, L. Brassat and B. Ganter, *Chem. Ber*. **1997**, *130*, 1771-1776.

[72] H. Willms, W. Frank and C. Ganter, *Organometallics*. **2009**, *28*, 3049-3058.

[73] J. Bitta, S. Fassbender, G. Reiss, W. Frank and C. Ganter, *Organometallics*. **2005**, *24*, 5176-5179.

[74] C. Ganter, *J. Chem. Soc., Dalton. Trans*. **2001**, 3541-3548.

[75] C. Ganter, C. Kaulen and U. Englert, *Organometallics*. **1999**, *18*, 5444.

[76] R. Shintani, M. M. C. Lo and G. C. Fu, *Org. Lett*. **2000**, *2*, 3695.
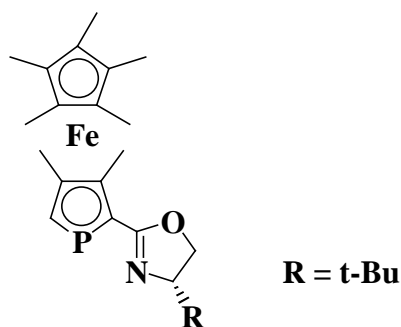
Fig 6

The group of Hayashi[77] elaborated the study of phosphaferrocenes with the synthesis of phosphanyl substituted phosphaferroecenes via the use of enantiomerically pure chiral phospholyl ligands. Palladium and platinum (II) dichloride complexes were also characterized in the same context. Since d_{Π}-p_{Π} back bonding is not possible for s and p block elements adduct bonds between main group compounds are normally weak. Mathey[78] recently came out with the structural characterization of the ionic complex [octa-n-propyl-diphosphaferrocene/GaCl$_2$]$^+$ GaCl$_4^-$. Roberts and Silver[79] have provided NMR spectroscopic evidence of a 3,3',4,4'-tetramethyl-1,1'-diphosphaferrocene/BF$_3$ adduct in CDCl$_3$ solution. Phosphaferrocene was also incorporated in tridentate ligands with two pentadant phosphinine ligands[80]. Fewer efforts were achieved in the development of diphosphaferrocene so far. In 1988, Fu and coworkers[81] succeeded in the separations of two enantiomers of (2-phenyl-3,4-dimethyl)diphosphaferrocene.

Even though the organic chemistry of phosphaferrocenes has been widely studied on their use as ligands, detailed investigation of their coordination chemistry is still continuing. Phosphaferrocenes usually behave as two electron donor ligands, however very recently it was demonstrated that the central iron atom can also coordinate to transition metal centres. For example the ligand shown in **(Fig 7)**, acts as a four electron donor - two electrons being given by the lone pair and two additional by a non-bonding orbital at iron[82].

[77] M. Ogasawara, K. Yoshida and T. Hayashi, *Organometallics*. **2001**, *20*, 3913.

[78] X. Sava, M. Melaimi, N. Mezailles, L. Ricard, F. Mathey and P. Le Floch, *New. J. Chem*, **2002**, *26*, 1378-1383.

[79] R. M. G. Roberts, J. Silver and A. S. Wells, *Eur. J. Inorg. Chem.* **2003**, 2049-2053.

[80] X. Sava, N. Mezailles, N. Maigrot, F. Nief, L. Ricard, F. Mathey and P. Le Floch, *Organometallics*, **1999**, *20*, 4205.

[81] S. Qiao, D. A. Hoic and G. Fu, *Organometallics*, **1998**, *17*, 773.

[82] X. Sava, L. Ricard, F. Mathey and P. Le Floch, *Chem. Eur. J.* **2001**, 3159.
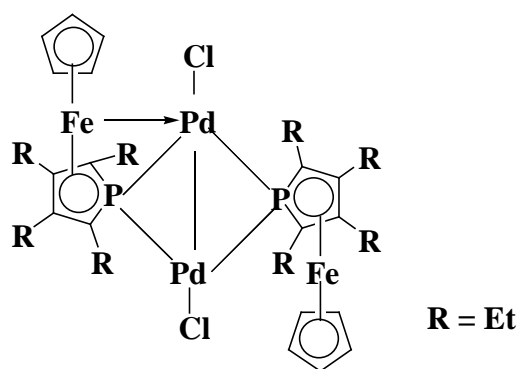
Fig 7

The most interesting applications of these low coordinate phosphorus ligands are in homogenous catalysis. Fu and coworkers were the first to report the use of phosphaferrocenes in homogenous catalysis. In 2000 it was shown that the application of [Rh(COD)(**A**)]PF$_6$ can be applied as a catalyst in the enantioselective isomerization of allylic alcohols to the corresponding aldehydes **(scheme 9)**.
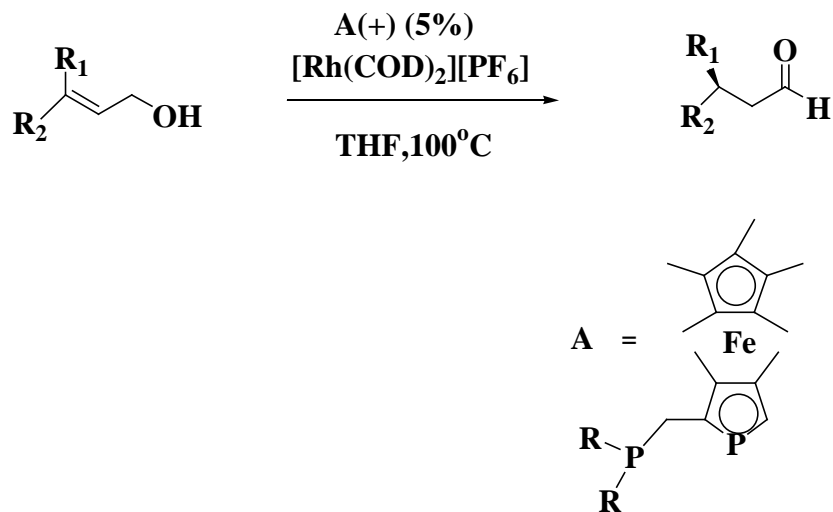
scheme 9

The enantiopure phosphaferrocene oxazoline ligands **B** have shown significant application in enantioselective allylic alkylation catalyzed by palladium salts **(scheme 10)**. In 2001, Hayashi et al made a phosphinyl substituted bidentate ligand which was successfully applied in the asymmetric alkylation of rac-1,3-diphenyl-2-propenyl acetate[77]. Ganter and his group designed enantiomerically functionalized phosphaferrocenes in various asymmetric reactions.
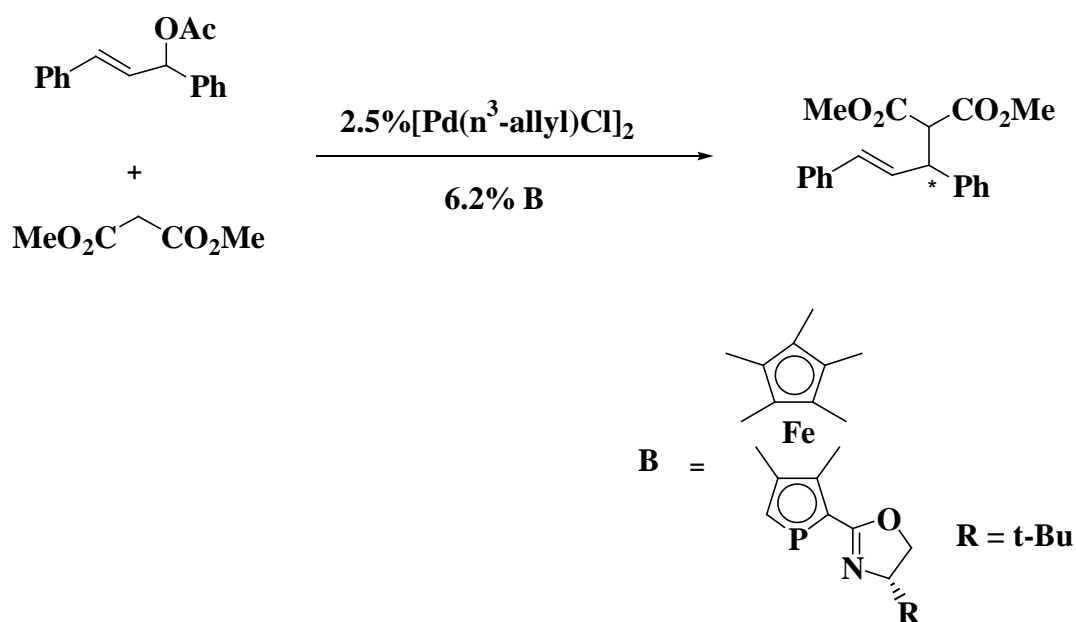
scheme 10

They have shown that the palladium catalyzed allylic alkylation proceeds with a 78% conversion yield and an enantiomeric excess of 79%[75]. Copper(I) complexes of phosphaferrocne - oxazoline ligands[83] incorporating a chiral phosphaferrocene moiety have also shown an interesting activity in the asymmetric conjugative addition of diethylzinc to acyclic enones to obtain the corresponding ketones. These ligands were also shown to be successful in the Kinugasa reaction that affords the synthesis of beta lactams from the intramolecular cyclisation of alkyne-nitrone derivatives[84].

---

[83] R. Shintani and G. C. Fu, *Org. Lett*. **2002**, *4*, 3699.
[84] R. Shintani and G. C. Fu, *Angew. Chem. Int. Ed*, **2003**, *42*, 4082.

2. Goals

In recent years genuine breakthroughs for immobilising phosphorus containing ligands, especially functionalized phosphines, and the corresponding complexes on inorganic surface[85,86,87,88,89] came out as they can, in principle, combine all the advantages of homogenous and heterogenous catalysts: we learned, how solid state NMR and suspension NMR spectroscopy served as a potent motor for investigating the amorphous solids. Low coordinated phosphorus heterocycles such as phosphinines[61,62] and phosphaferrocenes[77,83,84] show interesting properties in homogenous catalysis. This makes it worth investigating their immobilisation to further improve their catalytic performance.

For better erudition of the previous reports on the immobilisation of palladium catechol phosphines on TiO_2 surface[90], it is aimed to immobilise the newly reported palladium catechol phosphines on different specimens of TiO_2. It is proposed to study the behaviour of these immobilised species in various solvents by suspension NMR as the surface bound complexes are possibly used in catalytic process in which the complexes are in contact with the solvents.

It is also aspired to develop complexes of phosphinines having similar functionality as catechol phosphines and immobilise them on TiO_2 surface (**Fig 8**). The auxiliary aim is to select silica as the carrier material for anchoring functionalized phosphinines (**Fig 9**) via the covalent tethering method.

85 C. Merckle, S. Haubrich and J. Blümel, *J. Organomet. Chem.* **2001**, *44*, 627.
86 C. Merckle and J. Blumel, *Adv. Synth. Catal.* **2003**, *345*, 584.
87 C. Merckle and J. Blumel, *Top. Catal.* **2005**, *34*, 5.
88 G. Tsiavaliaris, S. Haubrich, C. Merckle and J. Blümel, *Synlett.* **2001**, 391.
89 F. Piestert, R. Fetouaki, M. Bogza, T. Oeser and J. Blümel, *Chem. Commun.* **2005**, 1481.
90 N. T. Lucas, J. M. Hook, A. M. Mc Donagh and S. B. Colbran, *Eur J. Inorg. Chem.* **2005**, 496-503.
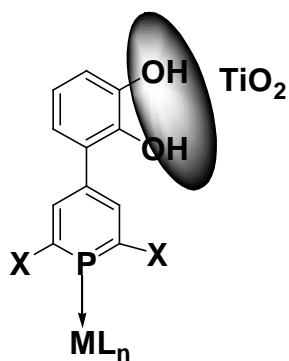
Fig 8
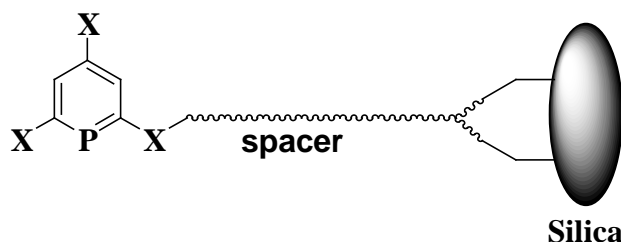
Fig 9

Metal nanoparticles have recieved particular attention for potential application in catalysis and biochemistry. Gold nanoparticles stabilized by phosphinines have been reported in the literature[91], but the knowledge of the ligand coordination on the gold surface remained unclear. Thus another area of interest is to synthesis phosphinine stabilized gold nanoparticles **(Fig 10)** and characterize them for the first time by ^{31}P MAS NMR spectroscopy together with gold(I) phosphinine complexes as model compounds; which would possibly furnish a conclusive model of the mode of ligand coordination on the gold surface.
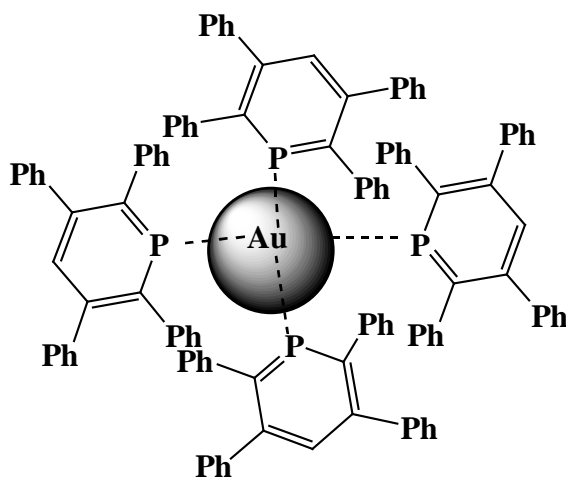
Fig 10

With an sp^2 hybridized phosphorus atom as part of the aromatic phospholyl system coordinated to the CpFe fragment, the monophosphaferrocene[83] constitutes a rather unique ligand system with moderate σ-donor and good π-acceptor properties. As per understanding,

---

[91] A. Moores, F. Goettmann, C. Sanchez and P. Le Floch, *Chem.Commun.* **2004**, 2842-2843.

no report has been found based on immobilised monophosphaferrocene. Thus it is projected to anchor monophosphaferrocene on silica as the support, which may open the gate for heterogenised monophosphaferrocenes **(Fig 11)**.
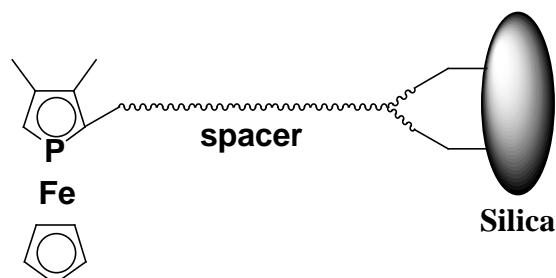
Fig 11

In brief, the current study aims **(i)** to synthesise novel functionalized phosphinines and their complexes capable to anchor and to immobilise them on inorganic supports**, (ii)** to immobilise reported palladium catechol phosphines on TiO_2 and study the immobilised species and their remobilisation in various solvents by suspension NMR. **(iii)** to prepare some novel gold(1) phosphinine complexes and phosphinine stabilized gold nanoparticles and study the mode of ligand coordination on the gold surface by ^{31}P NMR spectroscopy. **(iv)** to develop and anchor suitable functional derivative of monophosphaferrocenes onto inorganic surface by covalent tethering method and to study the anchoring process by CP MAS NMR spectroscopy.

3. Immobilisation of metal complexes of phosphines

Phosphines are very important ligands for immobilising complexes on oxidic supports[18]. For the immobilisation of transition metal complexes using functional phosphine ligands, several strategies have been developed[92,93]. The complexes of immobilised phosphines are employed in various catalytic reactions[92]. For example, rhodium complexes of phosphine ligands immobilised on silica supports via covalent tethering have often been extensively used for hydroformylation reactions[94]. Blumel et al described how the proper choice of functional phosphine linkers can fruitfully be applied to the immobilisation of metal complexes[85,86,87]. They also investigated the properties of various inorganic oxides like SiO_2, TiO_2, Al_2O_3 as support materials for the immobilisation of bifunctional phosphine ligands and by using multi nuclear solid state NMR spectroscopy as analytical tools, and described wether the ligand can be immobilised cleanly and how strong the covalent bonding to the support is [95].

3.1 Immobilisation of palladium catechol phosphines on titania

In view of recent reports describing the synthesis of complexes [90,96] **1 (scheme 11)** containing a catechol phosphine ligand and demonstrating the use of catechol moieties to immobilise these complexes on TiO_2 nanoparticles, it was anticipated that catechol units in complexes **2** and **3** should likewise allow a similar interaction with the solid surface.
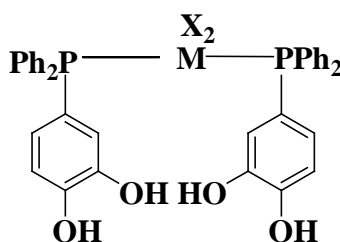
scheme 11:   1: MX_2 = $PdBr_2$, $PtCl_2$

[92] S. A. Raynor, J. M. Thomas, R. Raja, B. F. G. Johnson, R. G. Bell and M. K. Mantle, *Chem. Commun.* **2000**, 1925-1926.

[93] N. J. Meehan, M. Poliakoff, A. J. Sandee, J. N. H. Reek, P. C. J. Kamer and P. W. N. M. van Leeuwen, *Chem. Commun.* **2000**, 1497-1498.

[94] A. J. Sandee, J. N. H. Reek, P. C. J. Kamer and P. W. N. M. van Leeuwen, *J. Am. Chem. Soc.* **2001**, *123*, 8468 -8476.

[95] C. Merckle and J. Blümel, *Chem. Mater*. **2001**, *13*, 3617-3623.

[96] N. T. Lucas, A. M. McDonagh, I. G. Dance, S. B. Colbran and D. C. Craig, *Dalton Trans.* **2006**, 680-685.

The complexes **2** and **3** were prepared as descibed in the literature[97]. In order to verify the initial hypothesis the deposition of the complexes **2** and **3** was studied and the resultant materials characterised by solid state NMR spectroscopy. Immobilisation of the complexes **2** and **3** was accomplished by stirring CH_2Cl_2 solutions of **2** and **3** with solid TiO_2 and filtering off the supernatant liquid **(scheme 12)**. The immobilisation experiments were carried out with two different solid phases, viz. neutral titania (Merck, TiO_2 p.a., denoted as TiO_2; pH of 10% dispersion in water ~ 7) and pyrogenic TiO_2 nanoparticles (Degussa TiO_2 P25, denoted as NP-TiO_2) with a slightly acidic surface (pH of 4% dispersion in water ~ 3.5 - 4.5). Loading of the complex onto the support was calculated from the results of the elemental analysis of the materials obtained as 60 mg/g of **2**/TiO_2, 48 mg/g of **3**/TiO_2, and 45 mg/g of **3**/NP-TiO_2.

The successful deposition of both complexes on the solid carriers was readily monitored by solid-state ^{31}P NMR spectroscopy. The $^{31}P\{^1H\}$ CP MAS spectra of the surface modified materials are very similar to those of the pure, polycrystalline complexes **(Fig 12)** and display a single intense sideband manifold with nearly unchanged positions of the isotropic line. The spectra of samples of **2**/TiO_2 and **3**/TiO_2 showed additional broad signals of low intensity centered around -9 ppm, signals which were absent in the spectra of the pure complexes **(Fig 12)** and indicated a small amount of a second surface-bound species to be present.
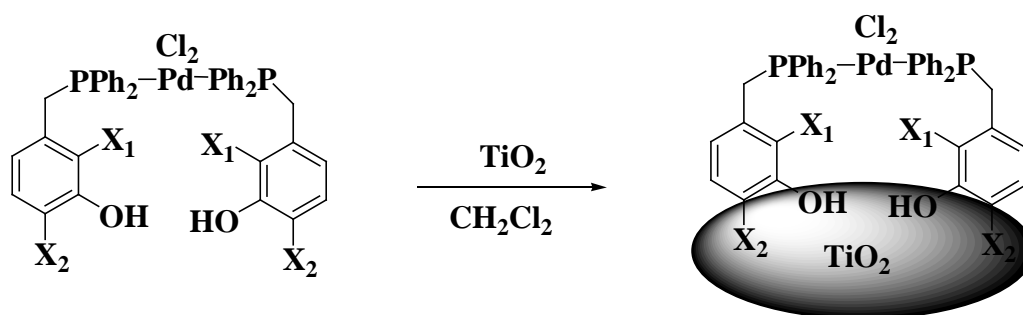
	X_1	X_2
2	OH	H
3	H	OH

scheme 12: Immobilisation of palladium catechol phosphines **2** and **3** on TiO_2.

[97] S. Chikkali and D. Gudat, *Eur. J. Inorg. Chem.* **2006**, 3005-3009.

The line widths of the signals for the surface - bound complexes on TiO_2 were somewhat larger (in case of **2**) or similar (in case of **3**) as those for the pure crystalline complexes whereas the NP-TiO_2-supported complexes displayed an increase in linewidths by nearly an order of magnitude **(Fig 12)**. Similar effects have been repeatedly observed for surface-bound phosphine complexes[98] and also phosphine oxide **POL2** (or **POL3**) derived from the corresponding ligand **L2** (or **L3**) of complex **2** (or **3**) but not for ligand itself nor its complex **2** (or **3**) **(Table 1)**. The major contribution to this broadening is presumably a substantial chemical shift dispersion which arises as a consequence of disordered surface environments. The isotropic shifts of the second surface bound species are close to the chemical shifts of the respective
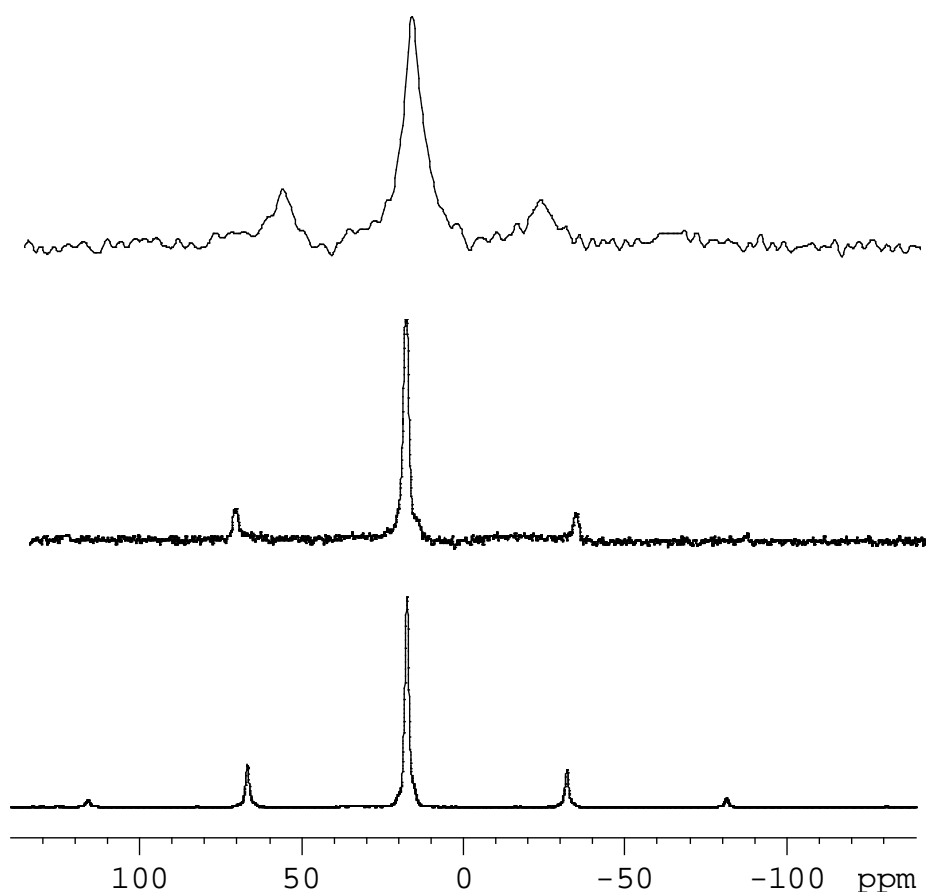
Fig 12: $^{31}P\{^{1}H\}$ CP MAS NMR spectra of pure crystalline **3**, υ_{rot}: 7 kHz, ns: 64, contact time: 1 ms, pulse delay: 5 s (bottom trace) and of **3** immobilised on neutral titania, υ_{rot}: 8 kHz, ns: 539, contact time: 5 ms, pulse delay: 6 s (TiO_2, middle trace) and on TiO_2 nanoparticles, υ_{rot}: 8 kHz, ns: 539, contact time: 1 ms, pulse delay: 6 s (NP-TiO_2, top trace).

---

[98] L. Bemi, H. C. Clark, J. A. Davies, D. Drexler, C. A. Fyfe and R. Wasylishen, *J. Organomet. Chem.* **1982**, 224, C5.

ligands (-13 to -15 ppm)[97] and since the spectrum of a sample prepared by immobilisation of the ligand of **3** on TiO_2 contained an identical line as the only signal, these lines were assigned to the surface - bound phosphines. Their formation can be explained by cleavage of the metal from **2** and **3**, and the observation of such decomplexation suggests that **2** and **3** are presumably less robust towards displacement of the phosphine ligands than **1** for which no similar behavior has been observed[90].

Table 1. Solid-state ^{31}P NMR isotropic chemical shifts (δ_{iso}), linewidths ($\Delta \nu_{1/2}$) and principal components of the CSA tensor (δ_{ii}) for complexes **2** and **3**.

Compound[a]	δ_{iso}	$\Delta \nu_{1/2}$ [Hz]	δ_{11} [ppm]	δ_{22} [ppm]	δ_{33} [ppm]	Ω [b]
2	22.4	120	97	22	-50	147
2/TiO_2	20.8	300	72	28	-38	110
PO**L2**	40.5	112	-	-	-	-
2/TiO_2/CH_2Cl_2	20.4	86	77	28	-43	120
2/TiO_2/CH_3CN	22.5	130	73	32	-40	113
3	17.5	160	80	23	-50	130
L 3	-10.8	115	15	-12	-33	45
3/TiO_2	17.7	100	82	19	-50	132
3/TiO_2/CH_2Cl_2	16.8	150	81	17	-50	131
3/NP-TiO_2	18.4	1100	-	-	-	-
3/NP-TiO_2/$CH_2 Cl_2$	19.1	600				
3/NP-TiO_2/CH_3CN	18.7	700				
3/NP-TiO_2/MeCN-amine[c]	17.2	900	-	-	-	-

[a] TiO_2 = neutral titania (Merck p.a.), NP-TiO_2 = titania nanoparticles (Degussa P25).
[b] $\Omega = \delta_{11} - \delta_{33}$.
[c] CH_3CN/NEt_3 (9:1).
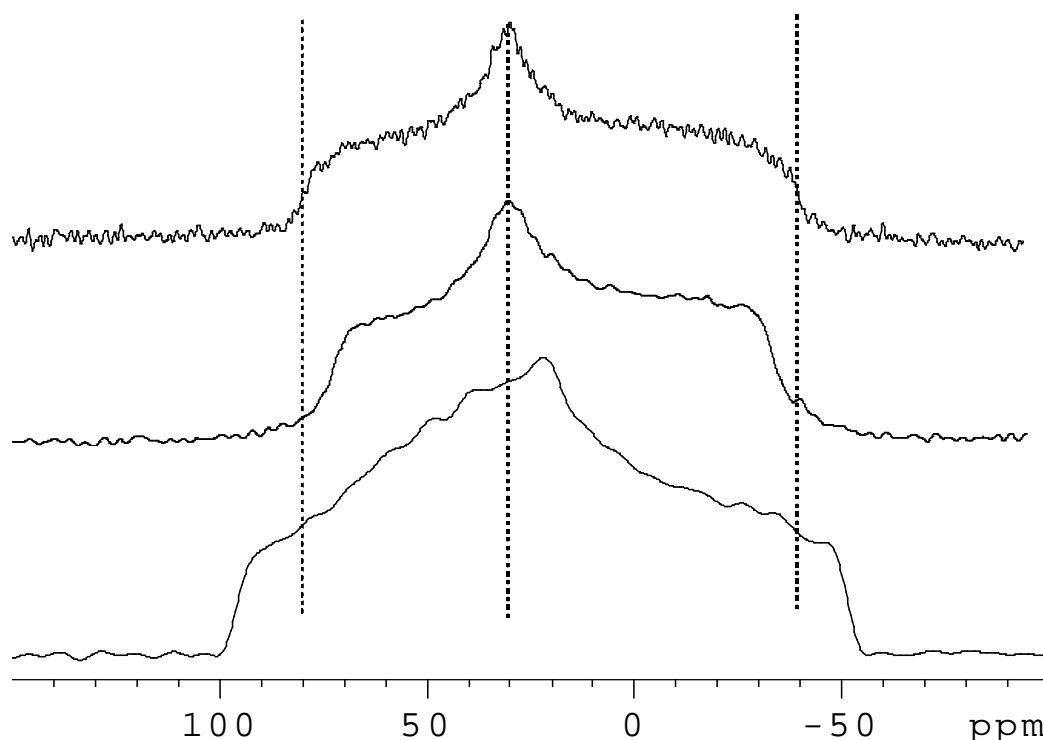
Fig 13: $^{31}P\{^1H\}$ CP NMR spectra of non spinning samples of crystalline **2,** ns: 2048, contact time: 1 ms, pulse delay: 5 s (bottom), **2** on TiO_2, ns: 2048, contact time: 1 ms, pulse delay: 5 s (middle) and a suspension of **2** on TiO_2/CH_2Cl_2, ns: 6144, contact time: 1 ms, pulse delay: 4 s (top). The vertical lines were drawn for better comparison and illustrate the values of δ_{ii} of the top trace.

Solid-state $^{31}P\{^1H\}$ CP NMR spectra of non spinning samples of pure and surface-bound **2** and **3** on neutral TiO_2 displayed characteristic powder patterns which enabled deduction of the principal components δ_{ii} of the magnetic shielding tensors. Meaningful static spectra of samples on NP-TiO_2 could not be obtained since the discontinuities in the line shapes were blurred by the large chemical shift dispersion. The chemical shift parameters of pure **3** and **3**/TiO_2 **(Table 1)** do not differ appreciably whereas **2**/TiO_2 displays a markedly lower shielding anisotropy than pure crystalline **2 (Fig 13)**. An explanation for this observation will be given in section **3.2.**

3.2 The study of immobilised - remobilised species by suspension NMR

The classical analytical method for studying the immobilised complexes **2** and **3** is solid state NMR[18]. However, based on Yesinowski`s pioneering work on suspension NMR of modified hydroxyapatite powders[99], this easy and practical method becomes more and more popular

---

[99] J. P. Yesinowski, *J. Am. Chem. Soc*. **1981**, *103*, 6266.

among chemists in various fields of surface chemistry. High-resolution magic angle spinning (HR MAS) NMR spectroscopy combines the mobilising influence of the solvent with the line narrowing effect of MAS[100]. The equipment needed for HR MAS suspension NMR spectroscopy are rotors which are equipped with spacers and a screw with a small hole to remove the surplus solvent. Therefore, HR MAS is the method of choice of any sort of mobile, but not homogenous species. With respect to the possible use of surface bound complexes in catalysis[101], it was proposed to typify the behaviour of the materials under conditions that mimic those of a catalytic process in which the complexes are in contact with the solvents and, especially in the case of C-C cross coupling reactions, a large excess of strong base[90]. It was therefore intended to measure slow spinning HR MAS NMR spectra of suspensions of the immobilised complexes **2** and **3** in different solvents.

In CH$_2$Cl$_2$

The slow-spinning ^{31}P {^{1}H}CP MAS NMR spectra of suspensions of **2**/TiO$_2$ and **3**/TiO$_2$ in CH$_2$Cl$_2$ display sideband manifolds with practically the same chemical shifts as the dry samples **(Fig 14)**. Likewise, the anisotropic chemical shift parameters δ_{ii} of **3**/TiO$_2$ obtained from a ^{31}P{^{1}H}CP NMR spectrum of a non spinning sample **(Table 1)** are the same as in the dry material and in pure **3**. In the case of **2**/TiO$_2$, however, the solvent induces a perceptible increase in the CSA and the span Ω of the CSA tensor in **2**/TiO$_2$/CH$_2$Cl$_2$ is midway between that in **2**/TiO$_2$ and crystalline **2** **(Fig 13**, **Table 1)**. It is unlikely that these changes arise from a solvent-induced increase in the mobility of the surface-bound complex since this should lower the effective CSA. Instead, it is suggested that the effect reflects variations in molecular conformations which accompany the interaction of the complex with the surface. A possible scenario, which has also been discussed for **1**[96], is that tethering of the OH- moieties to the surface enforces changes in the orientation of the catechol units relative to crystalline **2**, thus explaining the difference between **2** and dry **2**/TiO$_2$. Addition of a solvent might then either induce further conformational changes or the observed deviations may be interpreted as directly reflecting the effects of solvation. For **3**, the different arrangement of the OH moieties is considered to induce a larger spatial separation of the metal-phosphine unit from the surface, and conformational changes are clearly less pronounced than in **2** and have no visible impact on the chemical shift.

---

[100] J. Blümel, *Coord. Chem. Rev.* **2008**, *252*, 2410-2423.
[101] S. Chikkali, D. Gudat and M. Niemeyer, *Chem. Commun.* **2007**, 981-983.
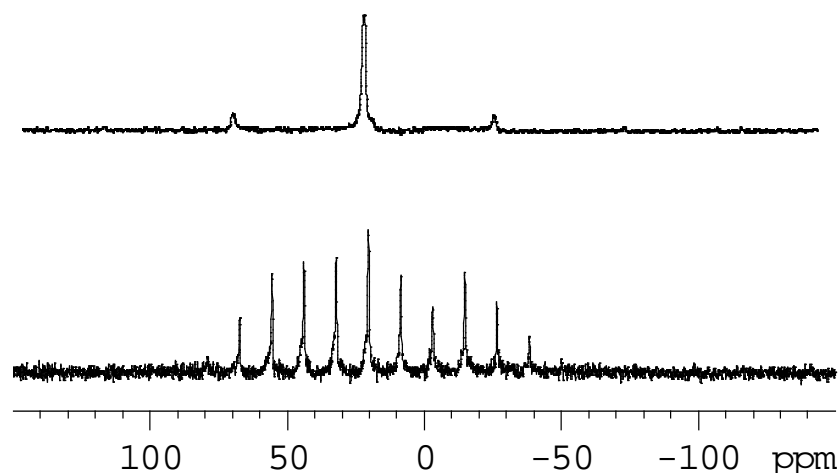
Fig 14: ^{31}P {^{1}H} CP MAS NMR spectra of **2** immobilised on neutral titania, υ_{rot}: 8 kHz, ns: 256, contact time: 1 ms, pulse delay: 8 s (top trace) and on TiO$_2$/CH$_2$Cl$_2$ (bottom trace), υ_{rot}: 1.5 kHz, ns: 128, contact time: 1 ms, pulse delay: 4 s.

In DMF

In contrast with the suspension in CH$_2$Cl$_2$, the ^{31}P CP MAS NMR spectra of **2**/TiO$_2$ or **3**/TiO$_2$ in dmf displayed no signals at all (**Fig 15**, top trace). However, ^{31}P{^{1}H}MAS NMR spectra recorded with direct excitation of ^{31}P showed two sharp lines that were not accompanied by any rotational sidebands. ^{31}P chemical shifts of **2**/TiO$_2$/dmf are 34.3 and 18.6 ppm relative signal intensities of 1:1.5 while **3**/TiO$_2$/dmf was observed at $\delta(^{31}$P) = 32.4 and 18.8 ppm with relative intensities of 1:0.7. The chemical shifts are similar to those of the cis and trans isomers of complexes **2** and **3** in solution. The occurrence of accidental unwanted oxidation can be excluded as the P oxides of **2** and **3** exhibt different isotropic chemical shifts [$\delta(^{31}$P) = 40 - 41 ppm both in solution[97] and as surface adsorbed species]. Acquisition of spectra of non - spinning samples did not indicate any marked changes except a moderate broadening of both lines (**Fig 15**, bottom trace). The spectrum of **2**/TiO$_2$/dmf displayed two further broad lines of low intensity at δ = 79.4 and 26.6 ppm. The pairwise appearance of these signals in this and in other spectra suggests that they belong to a single species which must then bear two distinguishable phosphine ligands but further structural assignment is unfeasibile.
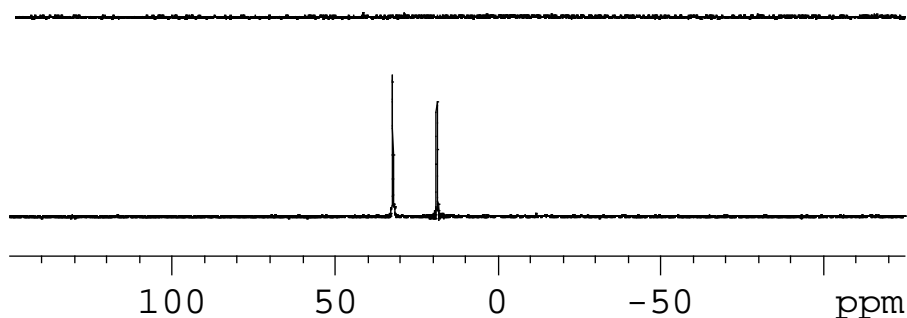
Fig 15: $^{31}P\{^{1}H\}$ NMR spectra of a non spinninig sample of **3** on TiO_2/dmf recorded with cross polarisation, υ_{rot}: 1.5 kHz, ns: 256, contact time: 1 ms, pulse delay: 4 s (top trace) and direct excitation of the ^{31}P nuclei, υ_{rot}: 1.5 kHz, ns: 64, contact time: 1 ms, pulse delay: 4 s (bottom trace).

Both the failure of the cross polarisation scheme and the line narrowing in the static spectra are typical for species undergoing isotropic motion and suggest that the complexes have become detached from the surface and are dissolved in the solvent. This hypothesis is in accord with earlier results indicating that phosphines immobilised on TiO_2 are highly prone to leaching[102], and was independently confirmed by the finding that the same signals were observable in ^{31}P NMR spectra of solutions prepared by extracting the immobilised complex with a larger volume of an appropriate solvent and subsequent filtration.

In CH₃CN

Measurement of ^{31}P NMR spectra of suspensions of **3**/TiO_2 in acetonitrile produced similar results to those obtained in dmf. In contrast, studies of the system **2**/TiO_2/CH_3CN led to the remarkable observation that ^{31}P CP MAS NMR spectra displayed spinning sideband manifolds similar to those found for **2**/TiO_2/CH_2Cl_2 (**Fig 16**, middle trace and **Table 1**) whereas ^{31}P NMR spectra recorded without cross polarisation showed, at the same time, two narrow isotropic lines (**Fig 16**, bottom trace) with similar chemical shifts $[\delta(^{31}P) = 32.0, 18.3$ ppm] as **2**/TiO_2/dmf. As expected, the spectrum of a nonspinning sample recorded under cross-polarisation displayed a powder lineshape, which is characterised by values of δii similar to those of **2**/TiO_2/CH_2Cl_2, whereas the corresponding spectrum recorded with direct ^{31}P excitation remained unchanged apart from an insignificant line broadening. These findings are in agreement with previously published studies on TiO_2 - immobilised phosphine complexes[103] and can be readily explained by assuming that the surface-bound complex **3**

---

[102] C. Merckle and J. Blümel, *Chem. Mater.* **2005**, *17*, 586.
[103] C. Merckle and J. Blumel, *Chem. Mater.* **2001**, *13*, 3617.

completely dissolves in acetonitrile, whereas, in the case of **2**, only partial dissolution occurs and a fraction of the complex remains on the carrier. The fact that the signal of the complexes in solution under cross - polarisation conditions cannot be observed is due to the averaging of the dipolar coupling, whereas the suppression of the signal of the surface-bound species under direct excitation of ^{31}P can be rationalised by assuming effective saturation of this resonance due to a much longer ^{31}P T_1 relaxation time.
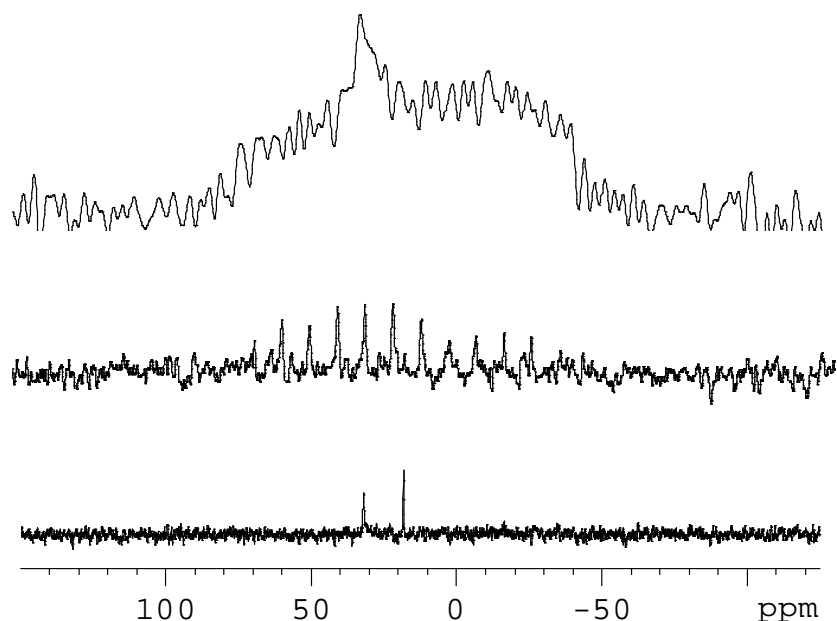
Fig 16: ^{31}P{^{1}H}NMR spectra of **2**/TiO$_2$/CH$_3$CN recorded (a) under cross polarisation with a non spinning sample, ns: 256, contact time: 1 ms, pulse delay: 4 s (top trace), (b) under cross-polarisation and MAS, υ_{rot}: 1.5 kHz, ns: 128, contact time: 1 ms, pulse delay: 4 s (middle trace) and (c) with MAS and direct excitation of the ^{31}P nuclei, υ_{rot}: 1.5 kHz, ns: 128, contact time: 1 ms, pulse delay: 4 s (bottom trace).

The validity of this assumption was confirmed by the finding that the signals of surface - bound and dissolved species were in fact both visible in a spectrum recorded under direct excitation pulses and longer relaxation delays.

In CH$_2$Cl$_2$ or DMF containing 10 vol% Et$_3$N

As palladium catalysed reactions are often carried out in the presence of bases[90,101], NMR spectroscopic studies were extended to suspensions of **2**/TiO$_2$ and **3**/TiO$_2$ in CH$_2$Cl$_2$ or dmf containing 10 vol % of triethylamine. It was noted that under these conditions complete detatchment of the complexes from the surface took place and that all signals detected were now attributable to species in solution. The observed chemical shifts revealed further that **2** and **3** had been transformed into new products. Samples containing **2** displayed a single sharp

line at 61.0 (in CH_2Cl_2/Et_3N) or 56.8 ppm (in dmf/Et_3N) which was assigned, on the basis of the similarity with the data of analogous compounds[104], to the bis(chelate) complex **4** **(scheme 13)**. This hypothesis is further corroborated by the finding that formation of the same product was likewise observed upon treatment of a solution of **3** with excess triethylamine.
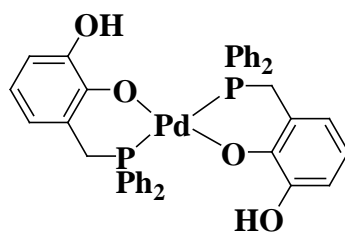
4

scheme 13

Samples containing **3** gave complicated spectra indicative of the presence of a mixture of several species which could not be further assigned. As intramolecular dehydrohalogenation and formation of a chelate ring is in this case, prevented by the unfavourable positioning of the OH groups, it is likely that an intermolecular condensation pathway leading to the formation of oligonuclear complexes is followed.

Analogous NMR spectroscopic studies of suspensions of **3**/NP-TiO_2 produced spectra showing a single spinning sideband manifold which is characterized by a chemical shift that is identical to that of the dry material, but the signal has a slightly reduced linewidth (see **Table 1**). In contrast to the previously described results, these findings give no evidence for either detatchment of the immobilised complexes from the surface, or the occurrence of similar base induced reactions as had been observed for **2**/TiO_2 or **3**/TiO_2. The line narrowing effects are well known in NMR spectra of suspensions of immoblised phosphine complexes[105,106] and are, in the first place, attributable to the increased librational mobility of surface bound species that are in contact with the solvent;[103] the rather moderate extent of the line narrowing in the case (in comparison to known cases of precedence[103,102]) is persumably due to the presence of a rather rigid molecular skelton in the phosphine ligand employed.

[104] D. J. Brauer, M. Hingst, K. W. Kottsieper, C. Liek, T. Nickel, M. Tepper, O. Stelzer and W. S. Sheldrick, *J. Organomet. Chem.* **2002**, *645*, 14-26.
[105] T. Posset and J. Blümel, *J. Am. Chem. Soc*. **2006**, *128*, 8394.
[106] S. Brenna, T. Posset, J. Furrer and J. Blümel, *Chem. Eur. J*, **2006**, *12*, 2880.

Summarising the results of the NMR studies presented, it can be stated that the behaviour of the surface - bound complexes depends on both the molecular structures of the complexes **2** and **3** and, to an even larger extent, the properties of the carrier material. Thus, deposition of both complexes on neutral TiO_2 is feasible but the complexes can be easily eluted by polar solvents. Judging from the different solubilities in acetonitrile, **3** is slightly more mobile than **2**. On the other hand, **2** displays a larger sensitivity of the anisotropic chemical shift data to environmental influences, which correlates with a closer proximity of the catechol OH groups (as potential surface binding sites) to the phosphorus atom and may be indictive of a closer interaction between the phosphine complex and the surface. The reactivity of the surface - bound complexes in the presence of a base reveals that the catechol moieties are available for chemical reactions and in connection with the easy detatchment of the surface - bound complexes, it was possible to conclude that the surface binding operates presumably by means of adsorptive hydrogen - bonding interactions. This was also in accord with previous findings on the behaviour of TiO_2-tethered phosphine complexes[103]. In contrast, the immobilised complexes on slightly acidic TiO_2 nanoparticles (NP-TiO_2) are definitely more tightly bound and gave no spectroscopic evidence for either the occurrence of leaching or of any base-induced dehydrochlorination. Both findings are compatible[96] with the view that the catechol OH groups support an ester like interaction with metal atoms on the surface which is persumably more covalent in nature. Although it was not yet possible to give a definite explanation for this at first glance surprising behaviour (it could be expected that formation of the surface esters should be more favoured on the more basic surface) several arguments to support the given interpretation can be proposed: in addition to the common place assumption that the surfaces of nanoparticles often exhibit enhanced reactivity due to the larger concentration of defect sites, one can argue that esterification on NP-TiO_2 benefits from acid catalysis. Furthermore, the formation of catecholate esters in a weakly acidic environment is no contradiction in itself as it is well known that chelate formation may increase the acidity of the free OH functions. Regardless of the nature of the interaction, however, the NMR spectroscopic studies indicate that the surface-bound complexes exist in the same manner as the pure crystalline materials, ie exclusively as trans configured complexes whereas in solution an equibilirium mixture of cis and trans isomers exists.

3.3 Investigation of catalytic activity of immobilised palladium catechol phosphines

The persistent attachment of the phosphine complex to the surface stimulated to explore the catalytic activity of **3**/NP-TiO$_2$. **3**/NP-TiO$_2$ was investigated as a catalyst for the Sonogashira coupling of 4-iodo-nitrobenzene and phenyl acetylene. Combining both components for 24hrs at room temperature in triethylamine in the presence of copper iodide as cocatalyst and 10 mol% of the immobilised complex **3** on NP-TiO$_2$ produced, after chromatographic workup, the expected coupling product in 70% yield **(scheme 14)**. The catalyst was recovered and has been used for the second run which gave a yield of 68% of the coupling product. The catalyst recovered after the second run was again reused for the further run, but the yield of the coupling product dropped to 10%.
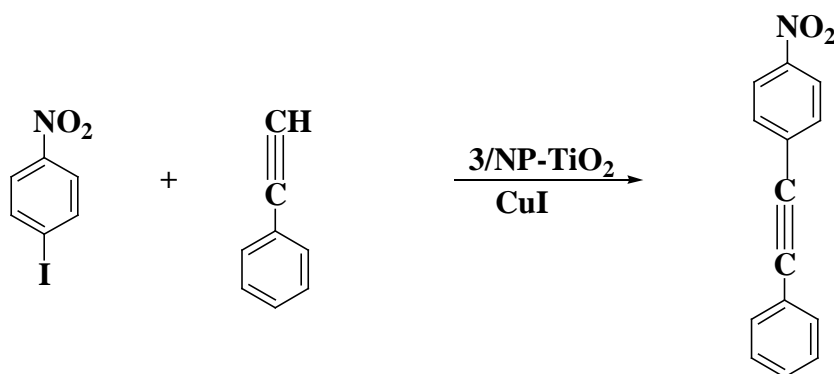
scheme 14: Sonogashira coupling of 4-iodo-nitrobenzene and phenylacetylene using **3**/NP-TiO$_2$ as the catalyst.

ICP analysis of the solid recovered after each run disclosed Pd loadings of 4.6, 2.6 and 2.6 mg (corresponding to 43, 24 and 24 µmol) of Pd g^{-1} NP-TiO$_2$. These results revealed that the loading of Pd dropped significantly after the first run indicating the occurrence of catalyst leaching during the reaction. However as the Pd loading in the second and third run was the same, the observed drop in the catalytic performance cannot be attributed to leaching alone. Presumably, chemical degradation of the complex is also responsible for this sudden drop in catalytic performance. These results indicated that **3**/NP-TiO$_2$ can, in principle, be applied as immobilised as it seems to be more tightly bound to the surface of the support than the related complex **1**[90] and its use seems to offer no advantage when compared with the homogenous

reaction with the related complex **2** as a precatalyst which gave a yield of 90% of the same product in the same reaction time and with a comparable catalyst loading[101].

To conclude, it has been demonstrated that catechol phosphine complexes **2** and **3** can be deposited on the surface of both neutral TiO_2 and slightly acidic TiO_2 nanoparticles. The characterisation of both dry specimens and suspensions by ^{31}P HR MAS NMR experiments with or without the use of cross-polarisation revealed that, in the first case, the action of polar solvents is sufficient to accomplish partial or even complete detachment from the surface. This finding is in accord with the assumption that the complexes are predominantly adsorbed by means of hydrogen interactions. In contrast, complexes deposited on TiO_2 nanoparticles with a slightly acidic surface showed more resistance to leaching and failed to undergo base-induced dehydrochlorination, thus suggesting a tighter bounding mode which is presumably more covalent in nature. The use of the heterogenised complex as catalyst in a carbon - carbon cross coupling reaction was also demonstrated in this context.

4. Immobilisation of phosphinine derivatives on inorganic supports

4.1 Synthesis of silyl alkoxy functionalized phosphinines

As one objective of the project is to immobilise phosphinine units, it is planned to synthesise phosphinines with silyl alkoxy functionalized linker that could dish up a proper candidate for anchoring onto silica support. The requisite silyl alkoxy functionalized phosphinines can be synthesized based on the method which uses 1,3,2-diazaphosphinine **5 (scheme 15)** as the precursor and relies on its high reactivity with alkynes. The very reactive 1,3,2-diazaphosphinine, was prepared an orange-red oil according to the literature procedure from 1,3,2-diazatitanacyclohexadienes by reaction with PCl_3 and excess triethylamine via N-Ti / Cl-P bond metathesis[44]. The 1,3,2-diazatitanacyclohexadiene[40] was initially prepared by the reaction of pivalonitrile with Cp_2TiMe_2 in toluene. Due to the high sensitivity of 1,3,2-diazaphosphinine, it could not be isolated before reaction with alkynes and was only characterized by its $^{31}P\{^1H\}$ NMR shift at 272 ppm. The molarity of the toluene solutions obtained was determined by integeration of $^{31}P\{^1H\}$ NMR signals after addition of a specific amount of triphenylphosphine as the internal standard. The compound was obtained in nearly 40% yield.
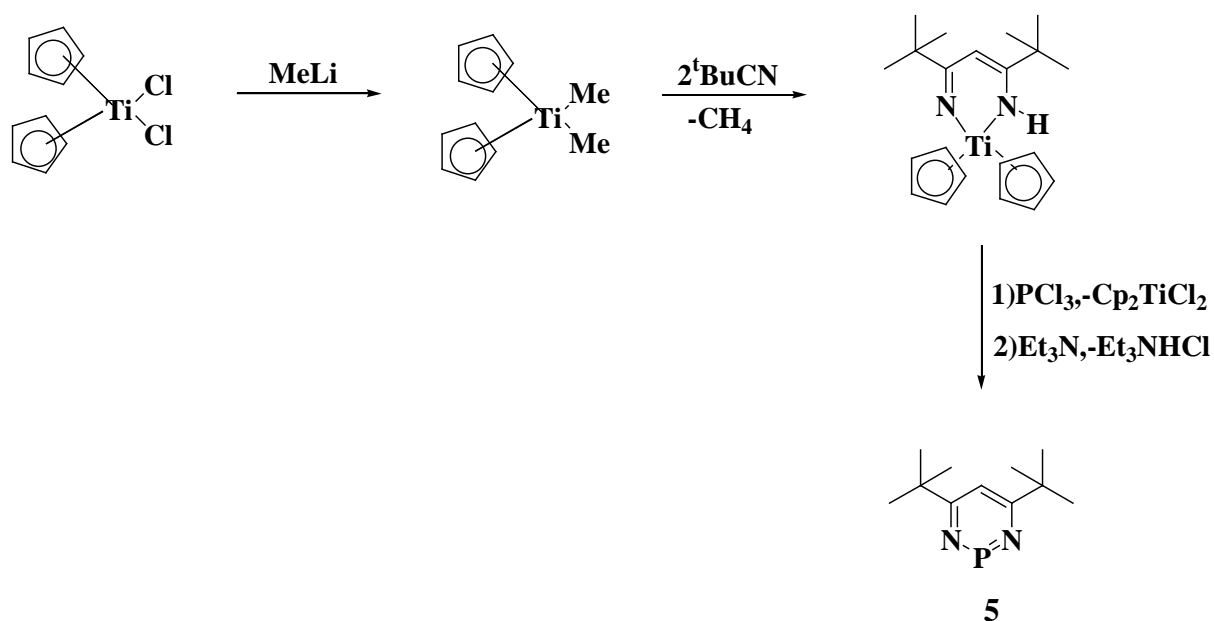
scheme 15: Synthesis of 1,3,2-diazaphosphinine

To attain the requisite functionalized phosphinine, appropriate silyl alkoxy functionalized alkyne has to be developed primarily. The facile synthesis of such alkyne **6** is shown in **scheme 16**[107]. The initial hydrosilylation of allyl triethoxy silane in the presence of Karstedt's catalyst (3-3.5% platinum in a vinyl terminated polydimethylsiloxane) gave 1-triethoxy silyl-3- chlorodimethylsilylpropane, the spectroscopic data of which were identical with those reported in the literature[107]. Hydrosilylation was followed by the dropwise addition of phenylacetenyl lithium to 1-triethoxysilyl-3-chlorodimethylsilylpropane at −78°C in dichloromethane. The solution was concentrated after the removal of precipitated lithium chloride to obtain a brownish yellow oil which was distilled to afford **6** as yellow oil in nearly 70% yield. The alkyne **6** was characterized by routine solution NMR techniques. The ^{1}H NMR spectrum of **6** showed a signal at 0.01 ppm which was attributable to the dimethyl silyl protons. The multiplets at 0.65 and 1.6 ppm were assigned to the propyl protons. The triplet at 1.15 ($^3J_{HH}$ = 7.2 Hz) and quartet at 3.7 ppm ($^3J_{HH}$ = 8.1 Hz) were attributed to the methylene and methoxy protons of the ethoxy group respectively. The ^{13}C NMR spectrum of **6** displayed the resonances of dimethyl silyl carbons at 1.2 ppm and those of propyl carbons at 14.89, 17.85 and 20.58 ppm. Signals at 18.65 and 58.65 ppm were attributed to the silyl alkoxy carbons. The triple bonded carbons were resonated in the lowfield regions at 93.75 and 106.03 ppm. Aromatic carbons were observed further downfield at 123.59, 128.50 and 132.29 ppm. The structure of **6** was confirmed by electron ionization mass spectroscopy which showed a molecular ion peak at m/e = 364.2 [M] $^+$.
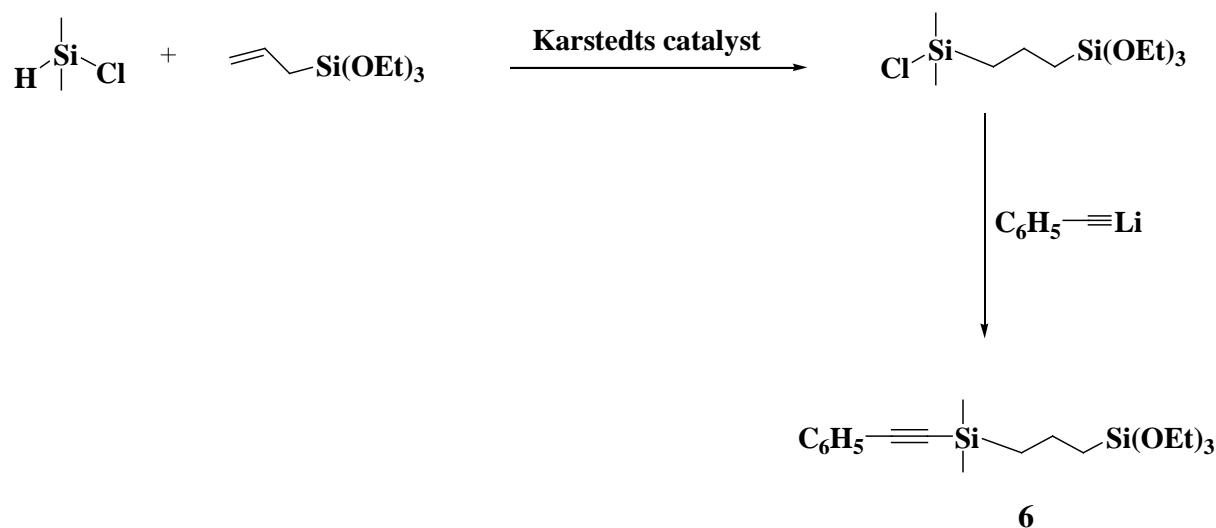
scheme 16: Synthesis of silyl alkoxy functionalized alkyne **6**

107 F. J. LaRonde, A. M. Ragheb and M. A. Brook, *Colloid. Polym. Sci.* **2003**, *281*, 391-400.

So formed alkyne **6** was then allowed to react with **5** in equimolar amounts via [4+2] addition/retro addition sequence to produce a 1,2-monoazaphosphinine, which was not isolated. The complete transformation was checked by ^{31}P NMR spectroscopy which exhibits signal at 306 ppm along with a signal of low intensity at 300 ppm. The intermediates were then reacted with phenylacetylene, at a higher temperature, in another [4+2] addition/retro addition sequence (**scheme 17**). The crude mixture showed ^{31}P{^{1}H} NMR signals of a major isomer at 240 ppm, which was however accompanied with other minor isomers with ^{31}P{^{1}H} NMR shifts at 232, 208 and 201 ppm. All attempts to isolate these isomers by column chromatography were not successful. The structure of the major isomer was assigned by running ^{1}H,^{31}P-HMQC and ^{1}H,^{29}Si-HSQC NMR spectra. The 2D-NMR spectra allowed to assign a doublet of doublet at 8.86 ppm ($^2J_{HP}$ = 37.5 Hz and $^4J_{HH}$ = 1.5 Hz) in the ^{1}H NMR spectrum to the major isomer, which is attributable to the ortho proton in the phosphinine ring. Furthermore, a doublet at 0.23 ppm ($^4J_{HP}$ = 1.5 Hz) was assigned to the protons of dimethylsilyl group, proving that the silyl alkoxy functionality is attached to the ortho carbon atom in the phosphinine ring. The protons of two phenyl rings appeared as multiplets in the downfield regions 7.10 - 7.24 ppm and 7.28 - 7.41 ppm. This major isomer showed further ^{29}Si NMR resonances at -46.5 and -2.5 ppm attributed to the ethoxy siliyl and dimethyl silyl groups, respectively. Based on these data, the structure was depicted as shown in (**scheme 17**). The attempt to ellucidate the structure of other isomers was not successful. The similar observation of isomeric products was previously reported in the synthesis of other functionalized phosphinines by the use of unsymmetrical alkyne like phenyl acetylene[91].

If these isomeric mixtures are planned to immobilise on silica, then it would give a mixture of phosphinine ligands on the surface which would be rather difficult to characterize. Therefore the present methodolgy of preparing functionalized phosphinines capable to anchor on inorganic surface could not be pursued further for the creation of heterogenized phosphinines.
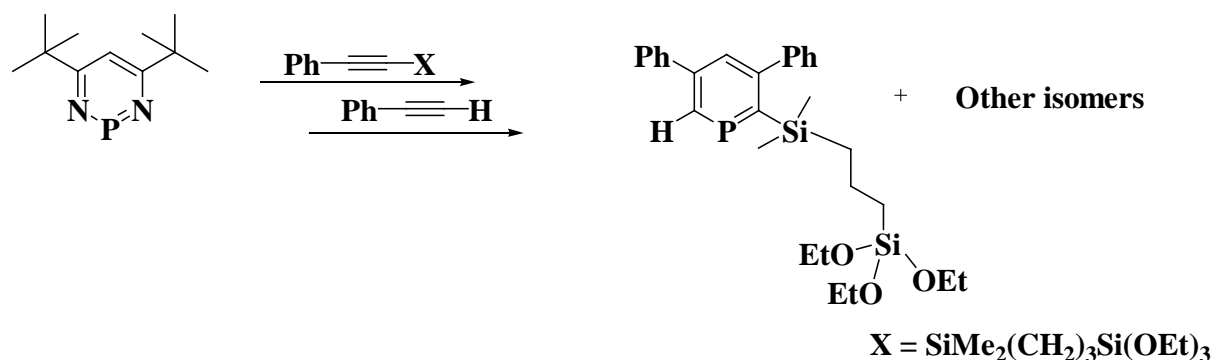
scheme 17: Synthesis of silyl alkoxy functionalized phosphinine.

4.2 Synthesis of hydroxy functionalized phosphinines

In the previous study the use of bifunctional catechol phosphine compounds to anchor transition metal complexes ligated via the P atom to TiO_2 bound by the catecholate group was investigated, and by ^{31}P CP MAS NMR successful deposition of palladium catechol phosphines on TiO_2 was observed. Based on these results, it was aspired to develop similar functionalized phosphinines having hydroxy groups in vicinal positions of aromatic moiety that might perform in a similar way as palladium catechol phosphines ie soft phosphorus donor preferentially coordinate to soft metal centres and the OH functionalities could bind to hard Ti^{1V} metal centres. The modular synthetic route elaborated by D. Vogt and C. Müller[35] was adapted here for the requirement that lead to hydroxy functionalized phosphinines. This involves the initial synthesis of alkoxy functionalized phosphinines via pyrylium salt[34], followed by the deprotection of alkoxy groups leading to the requisite hydroxy functionalized phosphinines.

Synthesis of chalcone derivatives

Pyrylium salts[34], precursor for phosphinines could be readily achieved from chalcones **(scheme 18)** obtained by aldol condensation of aromatic aldehyde with appropriate acetophenones in basic medium. Chalcone **7a** was made according to the reported literature[108] and the same method has been adapted for the preparation of two other derivatives **7b** and **7c**. Chalcones **7a** and **7c** were obtained as yellow solids and **7b** as yellow oil.

---

[108] Vogel, *Organic syntheses*. **1941**, *1*, 78.
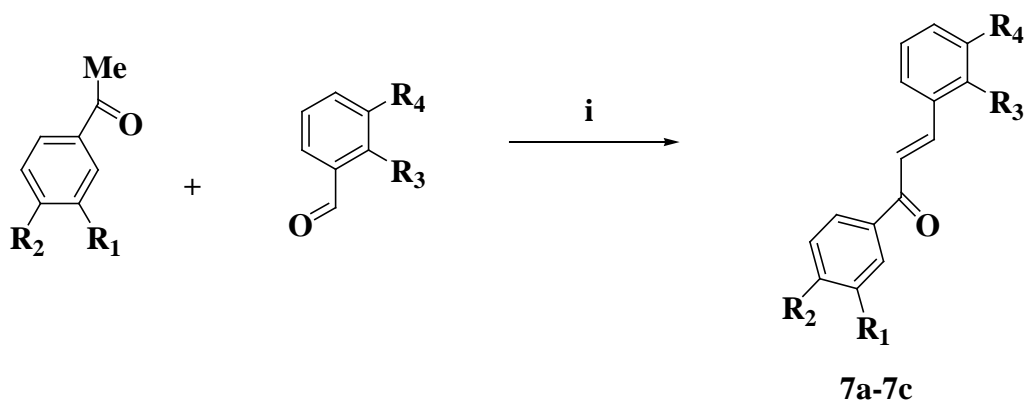
	R_1	R_2	R_3	R_4
7a	H	H	H	H
7b	H	H	OMe	OMe
7c	OMe	OMe	H	H

scheme 18: i) NaOH, Ethanol-water mixture

All these chalcone derivatives were characterized by routine NMR spectroscopy and other analytical techniques.

Synthesis of aryl pyrylium salts

Aryl pyrylium salts **8a – 8c** required were then obtained as yellow to orange solids by tetrafluroboric acid mediated condensation of an appropriate chalcone with a suitable acetophenone derivative **(scheme 19)**. Thus, tetrafluorboric acid (52% ethereal solution, 2.2 equiv) was added to a solution of the chalcone (2.2 equiv) and acetyl derivative (1 eqiv) in 1,2-dichloroethane at 70°C. The addition of three-fold amount of ether to the cooled reaction mixture after refluxing for 5hrs led to precipitation of the pyrylium salts. All these pyrylium salts **8a – 8c** were characterized in detail by NMR, mass spectroscopy and elemental analyses. As a represenative of pyrylium salts, **8a** 2-(3',4'-dimethoxy phenyl)-4,6-diphenyl pyrylium tetrafluoroborate was obtained as orange solid of m.p. 248°C in 58% yield from benzal acetophenone and 3,4-dimethoxy acetophenone. The positive mode electron spray ionization mass spectrum of **8a** showed the ion peak at m/e = 369.1 Dalton. The ^{1}H NMR of **8a** showed two different methoxy protons as singlets at 4.03 and 4.04 ppm. The two meta hydrogens of the pyrylium ring were observed as doublets at 8.06 ppm ($J_{HH} = 2.1$ Hz) and 8.35 ppm ($J_{HH} = 2.2$ Hz). The multiplets at 7.72 - 7.86 ppm, 8.44 - 8.48 ppm and 8.54 - 8.58 ppm accounting for nine protons are assigned to phenyl groups.
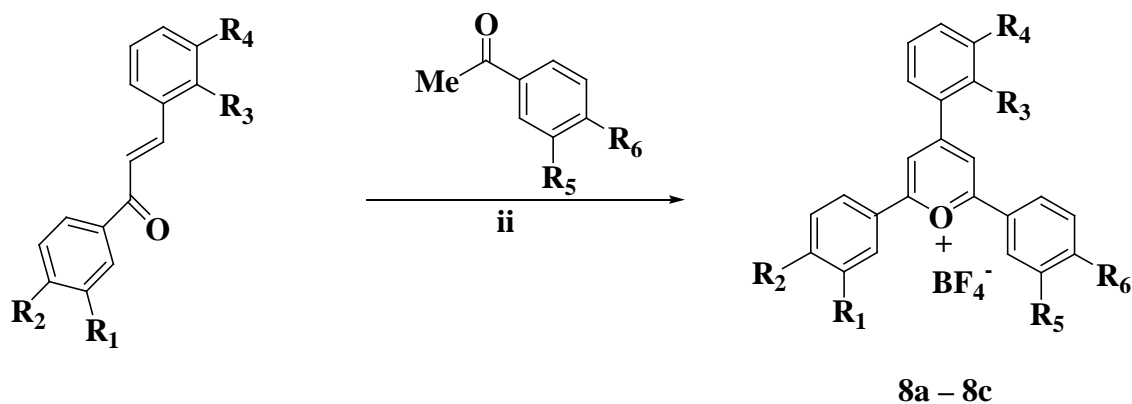
	R_1	R_2	R_3	R_4	R_5	R_6
8a	H	H	H	H	OMe	OMe
8b	H	H	OMe	OMe	H	H
8c	OMe	OMe	H	H	OMe	OMe

scheme 19: ii HBF$_4$ (52% ethereal solution), 1,2-dichloroethane, reflux, 5hrs.

Synthesis of methoxy functionalized phosphinines

The pyrylium tetrafluroborates **8a – 8c** were then reacted with excess P(SiMe$_3$)$_3$ in acetonitrile at reflux temperature to give phosphinines which were isolated as pale yellow to yellow solids 20-36% yield after flash chromatographic workup with hexane and ethylacetate (10:1) as eluants **(scheme 20)**. All phosphinines were characterized by routine solution NMR techniques and mass spectra as well as by elemental analyses.

scheme 20: Synthesis of methoxy functionalized phosphinines via aryl pyrylium tetrafluroborates.

	R₁	R₂	R₃	R₄	R₅	R₆
9a	H	H	H	H	OMe	OMe
9b	H	H	OMe	OMe	H	H
9c	OMe	OMe	H	H	OMe	OMe

As a representaive, phosphinine **9a** (m.p.147°C) was isolated in 32% yield after chromatographic workup. The $^{31}P\{^1H\}$ NMR spectrum displayed a singlet at 182 ppm. The ^1H NMR spectrum displayed singlets at 3.41 ppm and 3.44 ppm corresponding to the protons of the methoxy groups. The two distinct doublet of doublets observed at 8.11 ppm ($^3J_{HP}$ = 5.9 Hz, $^4J_{HH}$ = 1.1 Hz) and 8.21 ppm ($^3J_{HP}$ = 5.8 Hz, $^4J_{HH}$ = 1.2 Hz) were attributed to the aryl protons in meta positions of the phosphinine ring. The multiplets displayed at 7.18 - 7.36 ppm, 7.45 - 7.50 ppm, 7.71 - 774 ppm were assigned to the phenyl groups. The two ortho carbon atoms of phosphinine ring resonated as doublets at 171.9 ($^1J_{CP}$ = 52.5 Hz) and 172 ppm ($^1J_{CP}$ = 52.1 Hz) in the ^{13}C NMR spectrum of **9a**. Two further doublets observed at 131.39 ppm ($^2J_{CP}$ = 11.3 Hz) and 131.63 ppm ($^2J_{CP}$ = 11.2 Hz) were assigned to the meta carbons of phosphinine ring. The doublet at 142.65 ppm ($^3J_{CP}$ = 3.1 Hz) was assigned to the para carbon in phosphinine heterocyclic ring. The C-α of two phenyl groups were resonated as doublets at 136.5 ppm ($^2J_{CP}$ = 24.7 Hz) and 143.69 ppm ($^2J_{CP}$ = 24.5 Hz). The two singlets at 55.47 ppm and 55.50 ppm were assigned to the two methoxy carbons. Electron ionization mass spectrum of **9a** gave a molecular ion peak at m/e = 384.1 Dalton. The single crystals
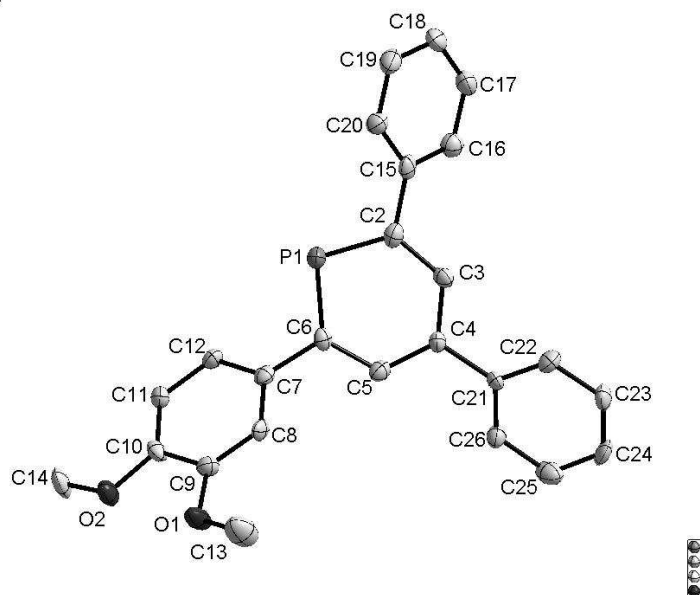
Bond length (Å)	Bond angle (Å)
C(6)-P(1) 1.751(6)	C(2)-P(1)-C(6) 101.6(3)
C(2)-P(1) 1.746(6)	C(3)-C(2)-P(1) 123.6(5)
C(2)-C(15) 1.495(8)	C(15)-C(2)-P(1) 118.0(4)
C(6)-C(7) 1.480(8)	C(3)-C(2)-C(15) 118.4(5)

Fig 17: ORTEP representation of the molecular structure of **9a** in the crystal with some selected bond lengths and bond angles; the crystallographic labelling is different from numbering used for assignments of NMR spectra.

of **9a** and **9c** suitable for X-ray analysis were grown by slow diffusion of hexane into a concentrated dichloromethane solution of the compound. The compound **9a** crystallized in a monoclinic unit cell with space group P(2)1/c. The molecular structure along with the selected bond lengths is shown in **Fig 17**. Here, the three phenyl rings are coplanar with the phosphorus containing ring. The C(6)-P(1) and C(2)-P(1) bond lengths are are 1.751 Å and 1.756 Å respectively. C(2)-P(1)-C(6) bond angle is 101.6^o and for C(3)-C(2)-P(1) is 123.6^o. The molecule shows weak CH, O hydrogen bonds C(13)-H(13)---O(2): 2.53 Å and C(14)-H(14)---O(1): 2.58 Å. Similar values of bond lengths and bond angles were also observed in other phosphinines[109].

[109] P. Le Floch, D. Carmichael, L. Ricard and F. Mathey, *J. Am. Chem. Soc*. **1993**, *115*, 10665-10670.

The compound **9c** crystallized in triclinic unit cell with space group P-1 **(Fig 18)**. The C(6)-P(1) and C(2)-P(1) bond lengths are 1.746 Å and 1.750 Å respectively. The C(2)-P(1)-C(6) bond angle is 101.88° and for C(3)-C(2)-P(1) is 123.34°. Here, also the molecule shows weak CH, O hydrogen bonds C(63I)-H(63A)---O(24): 2.61 Å and C(5)-H(5)---O(63): 2.55 Å.
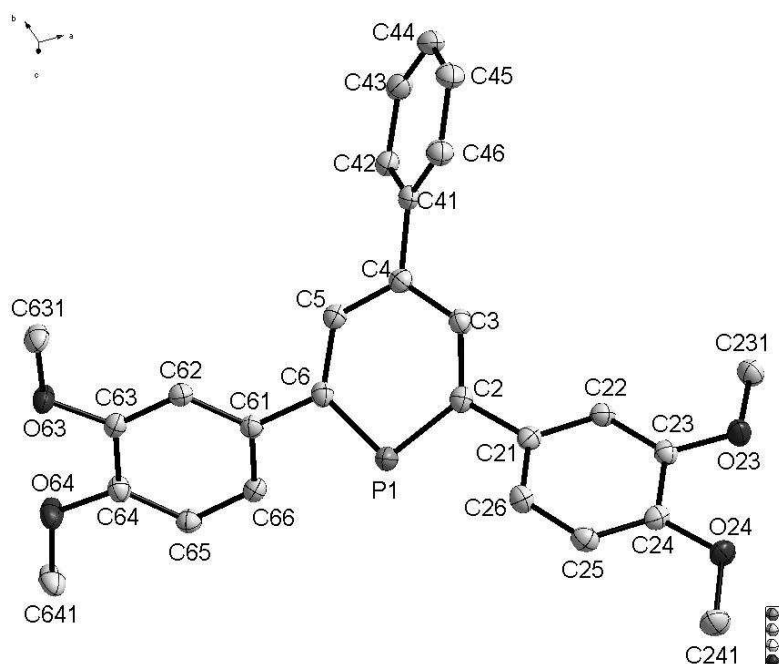
Bond length (Å)	Bond angle (Å)
C(6)-P(1) 1.7461(13)	C(2)-P(1)-C(6) 101.88(6)
C(2)-P(1) 1.7500(13)	C(3)-C(2)-P(1) 123.34(10)
C(2)-C(21) 1.4911(17)	C(21)-C(2)-P(1) 115.83(9)
C(6)-C(61) 1.4912(17)	C(3)-C(2)-C(21)120.78(11)

Fig 18: ORTEP representation of the molecular structure of **9c** in the crystal with some selected bond lengths and bond angles; the crystallographic labelling is different from numbering used for assignments of NMR spectra.

Deprotection of methoxy functionalized phosphinines

The slow addition of excess BBr$_3$ in CH$_2$Cl$_2$ at low temperature to the solution of alkoxy functionalized phosphinines in CH$_2$Cl$_2$ followed by overnight stirring at room temperature is a known literature method[35] for the conversion of the methoxy groups in phosphinines to hydroxy groups. The phosphinines **10a** and **10b** were isolated after aqueous work up as air sensitive yellowish white powders in pure form from the crude mixture after flash column
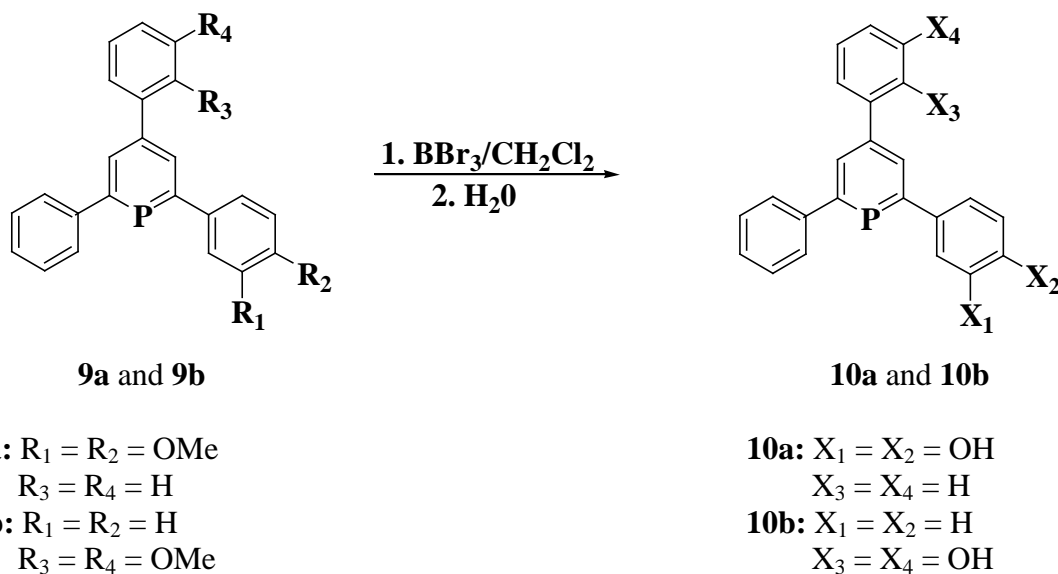
scheme 21: Deprotection of methoxy functionalized phosphinines

chromatography with hexane: dichloromethane (1:1) as eluant **(scheme 21)**. All the hydroxy functionalized phosphinines were characterized by solution NMR spectroscopy and elemental analyses. Furthermore, their molecular formulae were confirmed by electron ionization mass spectroscopy. As a representative, the hydroxy functionalized phosphinine **10b**, which melts at 165°C, was obtained as a white solid in 62% yield and displayed a singlet at 185.3 ppm in $^{31}P\{^1H\}$ NMR spectrum. The disappearance of methoxy signals in ^1H and ^{13}C NMR spectroscopy established the successful deprotection. A doublet observed at 8.08 ppm ($^3J_{HP} = 5.7$ Hz) was attributed to the meta protons in the heterocyclic ring. The multiplets at 6.58 - 6.81 ppm, 7.18 - 7.23 ppm, 7.65 - 7.68 ppm were assigned to the thirteen aromatic protons of phenyl groups. The ^{13}C NMR spectrum of **10b** exhibited a doublet at 171.87 ppm ($^1J_{CP} = 52.8$ Hz) which was assigned to the ortho carbons of phosphinine ring. The two meta carbons of phosphinine ring resonated as doublet at 133.42 ppm ($^3J_{CP} = 12.0$ Hz). The signal observed as doublet at 141.53 ppm ($^3J_{CP} = 1.8$ Hz) was assigned for the para carbon with respect to phosphorus in the hetero moiety. Further the structure of **10b** was confirmed by mass spectral analysis. The Electron ionization mass spectrum of **10b** gave a molecular ion peak at m/e = 356.1 Dalton.

4.3 Preparation of transition metal complexes of phosphinines

In surveying the coordination chemistry of phosphinines[19], it is easily recognised that known phosphinine complexes of group 11 are rather rare. Some copper(I) complexes were reported[110], but a very little is known for silver and gold derivatives. Schmidbaur et al[111] was the first who came out with a gold(I) phosphinine complex, however, its spectroscopic and structural data remained unknown. Later, the coordination behaviour of 2,6-disilyl-substituted phosphinines towards gold(I) was examined by F. Mathey and Le Floch[112] who successfully characterized the resultant gold(I) complexes by spectroscopic and X-ray crystal structural analyses. The formation of both η^1 and η^6 complexes was normally encountered for most metals [113]. The two main factors that defined the preferred coordination mode are the nature of metal precursor and substitution pattern of the ligand. As the ultimate aim is to immobilise the complexes of newly made hydroxy functionalized phosphinines, the metal complexes should be available as isolated compounds since otherwise the study of the immobilised complexes on the surface may lead to uninterpretable. Since gold is known to make linear complexes with a single neutral P- donor ligand[112] and not having problem with other mode of coordination, gold(I) precursor is a suitable candidate for forming complexes with the newly synthesized phosphinines.

Gold (I) complex of methoxy functionalized phosphinines

The reaction of phosphinines **9a – 9c** with AuCl(tht) in dichloromethane was monitored and procceeded cleanly at room temperature within 15 min **(scheme 22)**. The completion of the reaction was checked by ^{31}P NMR spectroscopy. The complexes **11a – 11c** were obtained as pale yellow solids after precipitation with hexane.

[110] P. Le. Floch, L. Ricard and F. Mathey, *Bull. Soc. Chim. Fr*, **1996**, *133*, 691.
[111] K. C. Dash, J. Eberlein and H. Schmidbaur, *Synth. Inorg. Met. Org. Chem.* **1973**, *3*, 375.
[112] N. Mezailles, L. Ricard, F. Mathey and P. Le. Floch, *Eur. J. Inorg. Chem.* **1999**, 2233-2241.
[113] M. Doux, L. Ricard, F. Mathey, P. Le. Floch and N. Mezailles. *Eur. J. Inorg. Chem.* **2003**, 687-698.

scheme 22: Synthesis of gold(I) complexes of methoxy functionalized phosphinines
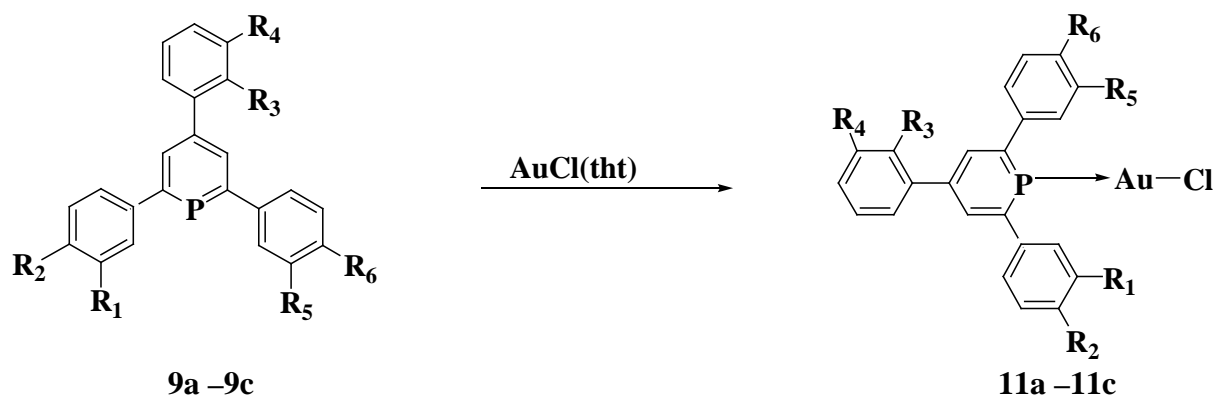
	R_1	R_2	R_3	R_4	R_5	R_6
9a	H	H	H	H	OMe	OMe
9b	H	H	OMe	OMe	H	H
9c	OMe	OMe	H	H	OMe	OMe
11a	H	H	H	H	OMe	OMe
11b	H	H	OMe	OMe	H	H
11c	OMe	OMe	H	H	OMe	OMe

The complex **11a**, which melts at 142°C, was obtained in 96% yield. The $^{31}P\{^1H\}$ NMR of **11a** displayed a singlet at 152.39 ppm. The large quadrupolar moment of ^{197}Au shortens the relaxation time of this nucleus, thereby no $^1J(^{197}Au\text{-}^{31}P)$ coupling was observed for complex **11a**. As expected, the coordination shift for the ^{31}P signal is negative ($\Delta\delta$ = -30 ppm) in **11a**. This was in accordance with the reports as obtained for 2,6-disilyl-substituted phosphinine gold(I) complexes[112]. The meta protons (3,3', -H) in ^1H NMR of **11a** resonated as doublet of doublet at 8.40 ppm ($^3J_{PH}$ = 22.7 Hz, $^4J_{HH}$ = 1.7 Hz) and 8.49 ppm ($^3J_{HP}$ = 22.7 Hz, $^4J_{HH}$ = 1.6 Hz). As expected for other Au complexes, metal coordination is accompanied by a usual increase of $^3J_{PH}$ with respect to the free ligand ($^3J_{PH}$ = 22.7 Hz (**11a**) vs 5.8 Hz (**9a**)). The multiplets at 7.41 - 7.42 ppm, 7.49 - 7.59 ppm, 7.70 - 7.74 ppm, 7.78 - 7.83 ppm account for phenylic protons. The two singlets at 3.93 and 3.99 ppm were attributed to the protons of two methoxy groups. In the ^{13}C NMR spectrum, the α-carbon atoms display a similar coordination shift ($\Delta\delta$ = -14) as had been observed in the ^{31}P NMR spectrum. The coordination shift of the para carbon C-4 is negligible upon complexation. And also the $^1J_{PC}$ varied from 52 Hz in **9a** to 36 Hz in **11a**. The loss of lone pair effect (algebric increase of the coupling) and the high degree of coordination at P atom (decrease of the magnitude of coupling) are the two competing factors which generally observed in classical complexes of tertiary phosphines are

responsible for this large variation in the coupling constants[114]. It was also noted that a very large increase in the $^3J_{PC}$ coupling constant to the C-4 carbon from 3.2 Hz in **9a** to 26.3 Hz occurred in **11a**. Electron ionization mass spectrum of the compound **11a** gave molecular ion peak at m/e = 616.0 [M$^+$]. Another peak at 384.1 was corresponded to the free ligand [M-AuCl]$^+$. The other two gold complexes **11b** and **11c** were characterized by NMR analyses. The structures of **11b** and **11c** were further confirmed by electron ionization mass spectroscopy. **11b** and **11c** displayed the molecular ion peak at m/e = 676.1 and 616.8 respectively.

The structure of **11a** was confirmed by single X-ray crystal analysis. The single crystal of **11a** suitable for analysis was grown by the slow diffusion of hexane into a concentrated solution of the compound in dichloromethane.

---

[114] C. J. Jameson in Phosphorus-31NMR spectroscopy in stereochemical analysis (Eds: J. Verkade, L. D. Quin), VCH Publishers, Inc, Deerfield Beach, Florida. **1987**, 205-230.
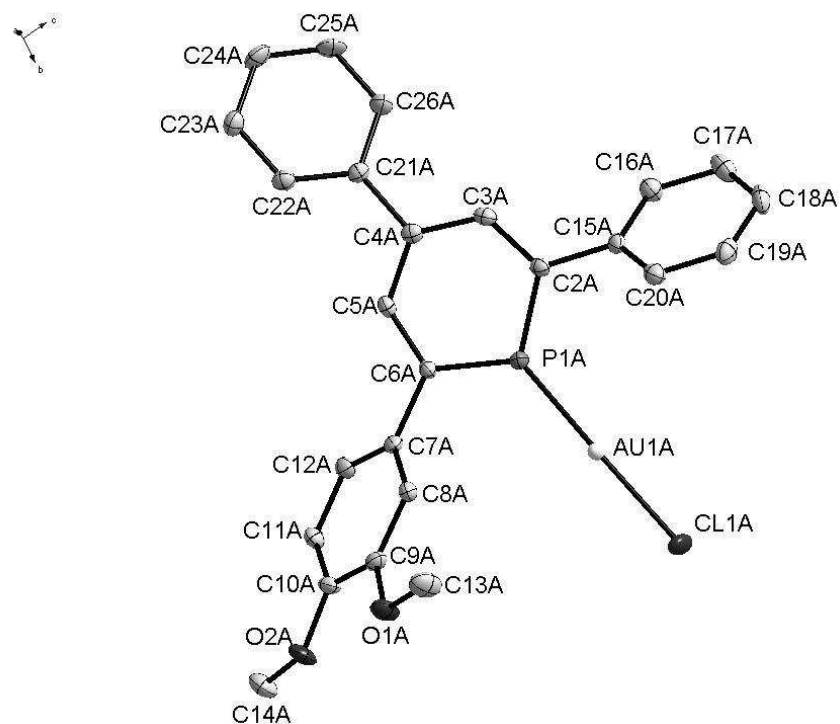
Bond lengths (Å)	Bond angles (Å)
Cl(1A)-Au(1A) 2.2766(8)	P(1A)-Au(1A)-Cl(1A) 175.88(3)
Au(1A)-P(1A) 2.2060(8)	C(6A)-P(1A)-C(2A) 107.13(15)
P(1A)-C(6A) 1.715(3)	C(6A)-P(1A)-Au(1A) 126.39(10)
P(1A)-C(2A) 1.721(3)	C(2A)-P(1A)-Au(1A) 126.45(11)
C(2A)-C(3A) 1.386(4)	C(3A)-C(2A)-C(15A) 121.5(3)
C(2A)-C(15A) 1.487(4)	C(3A)-C(2A)-P(1A) 120.0(2)
C(3A)-C(4A) 1.399(4)	C(15A)-C(2A)-P(1A) 118.5(2)

Fig 19: ORTEP representation of the molecular structure of **11a** in the crystal with some selected bond lengths and bond angles; the crystallographic labelling is different from numbering used for assignments of NMR spectra.

An ORTEP drawing of **11a** is presented in **Fig 19**. The compound crystallizes in triclinic with space group P-1. As expected for a LAuX complex, the complex adopts a linear geometry with bond angle of 175.9^{o} for P(1A)-Au(1A)-Cl(1A). The Au(1A)-Cl(1A) and Au(1A)-P(1A) bond lengths are 2.277(1) Å and 2.206(8) Å. The bond lengths and bond

angles in **11a** are in good agreement with those observed for bis(trimethylsilyl) phosphinine gold(I) chloride[112] having Au-Cl and Au-P bond distances are 2.281(2) Å and 2.211(2) Å respectively. The Au(1A)-P(1A) bond length is shorter as compared to that observed for AuCl in phosphine complexes (Au-P: 2.227(2) Å, Au-Cl: 2.288(2) Å) [115]. This shortening of bond length is attributable to different hybridization of the P atoms in the two species (formal sp^2 in **11a** vs sp^3 in tertiary phosphine) and thus quite normal. By examining bond lengths and bond angles it is possible to elucidate further interesting information. The internal angle C(2A)-P(1A)-C(6A) falls in the range 107.13^o which is quite large as compared to the parent phosphinine **9a** (C-P-C = 101.6^o). This type of similar increase in value of bond angles (C(2)-P(1)-C(6)) was also oberved for other phosphinines in general upon complexation [M(C_5H_5P)$_6$] (M = Cr, Mo, W)[116] and is a direct consequence of the shortening of the P=C bonds are shortened (1.721(3) Å and 1.715(3) Å) compared to the parent phosphinine (1.746(6) Å and 1.751(6) Å). This shortening has also been observed in other complexes such as bis(trimetylsilyl) phosphinine gold(I) chloride[112] and Mo(C_5H_5P)(CO)$_5$[117].

In addition to the neutral phosphinine- AuCl complexes **11a-11c**, also an ionic complex **11d** was readily obtained by treating two equivalents of ligand **9a** at low temperature with one equivalent of AuCl(tht), followed by addition of silver triflate as chloride abstractor (**scheme 23**).
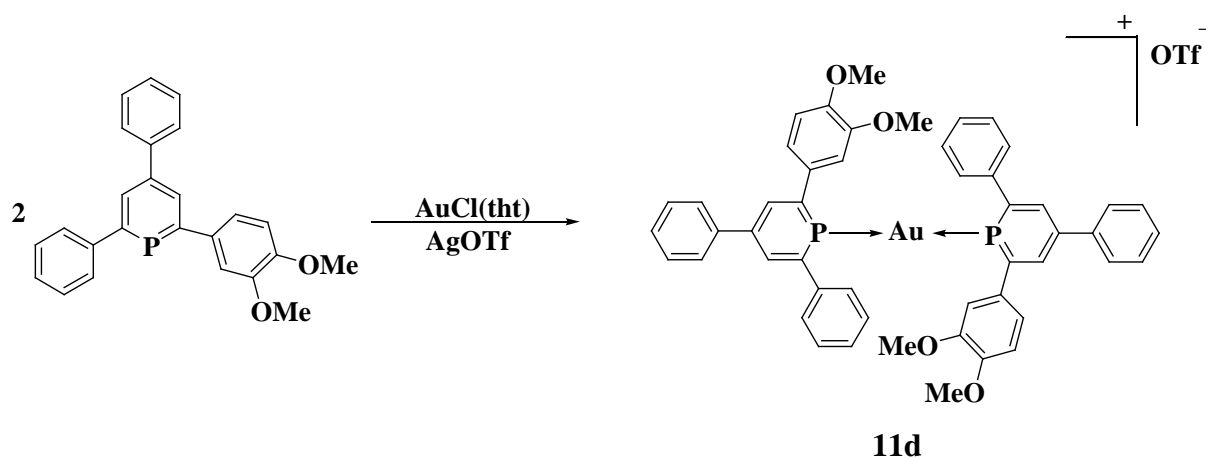
scheme 23: Synthesis of cationic gold phosphinine complex **11d**.

[115] S. Attar, W. H. Bearden, N. W. Alock, E. C. Alyea and J. H. Nelson. *Inorg. Chem.* **1990**, *29*, 425.

[116] P. Le. Floch, D. Carmichael, L. Ricard, F. Mathey, A. Jut and C. Amatore, *Organometallics*. **1992**, *11*, 2475.

[117] A. J. Ashe III, W. Butler, J. C. Colburn and S. Abu-Orabi, *J. Organomet. Chem*, **1985**, *282*, 233.

The complex was obtained in 86% yield as a pale yellow solid after hexane precipitation and displays a ^{31}P NMR shift at 169 ppm. Here also the coordination shift is still negative ($\Delta\delta$ = -13) but lower as in **11a**. The ^{1}H NMR spectrum in CD_2Cl_2 displayed two singlets at 3.89 and 3.91 ppm which were attributed to the methoxy protons in **11d**. The multiplets at 6.96 - 7.00 ppm, 7.27 - 7.31 ppm, 7.48 - 7.59 ppm, 7.70 - 7.75 ppm were assigned for aromatic protons in the phenyl rings. The two distinct doublet of doublet at 8.27 ($^{4}J_{HH}$ = 1.4 Hz, $^{3}J_{HP}$ = 13.6 Hz) and 8.29 ppm ($^{4}J_{HH}$ = 1.3 Hz, $^{3}J_{HP}$ = 13.7 Hz) were assigned to the meta protons in the heterocyclic ring. Finally, the composition of **11d** was confirmed by electron spin ionization mass spectroscopy which displayed a peak at m/e = 996.24 Dalton that can be assigned to a complex [Au(**9a**)$_2$(CH$_3$OH)]$^{+}$.

.

Gold (I) complex of hydroxy functionalized phosphinines:

Two positional isomers of hydroxy functionalized phosphinines **10a** and **10b** upon treatment with AuCl(tht) in thf at RT afforded the complexes **12a** and **12b** respectively **(scheme 24)**. The complexes were isolated as very pale yellow solids in nearly 90 - 97% yield by simple precipitation from the reaction mixture.

10a - 10b   **12a - 12b**
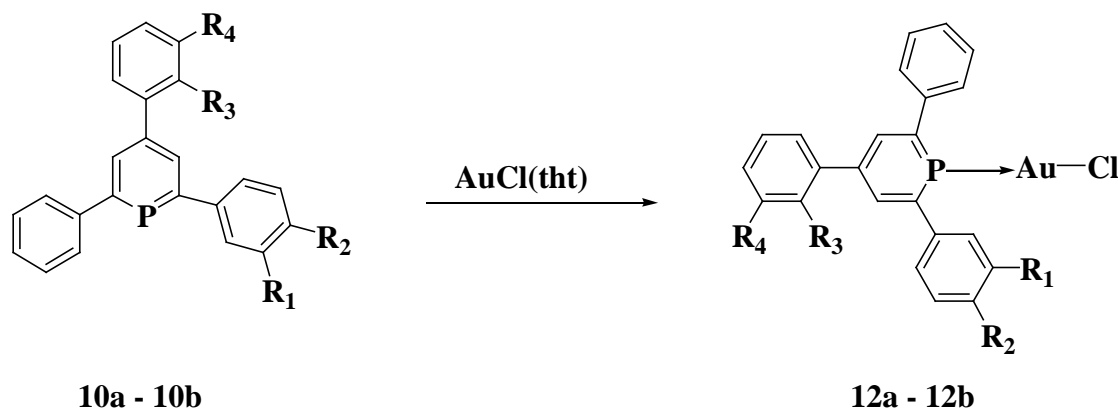
	R$_1$	R$_2$	R$_3$	R$_4$
10a	OH	OH	H	H
10b	H	H	OH	OH
12a	OH	OH	H	H
12b	H	H	OH	OH

scheme 24: Synthesis of gold(I) complexes of hydroxy functionalized phosphinines

The compound **12a,** which melted at 202°C, displayed a ^{31}P{^{1}H} NMR chemical shift at 152.40 ppm. The ^{1}H NMR spectrum of **12a** and **12b** exhibited similar signals like those faced

in **11a**. Likewise, a marked increase in the $^3J_{PH}$ coupling constant (from $^3J_{PH}$ = 10.0 Hz in **10a** to 22.4 Hz in **12a** and $^3J_{PH}$ = 5.7 Hz in **10b** to 22.7 Hz in **12b**) of meta protons (H at C-3 & C-5) was observed. The Protons of phenyl groups exhibit multiplets at 7.41 - 7.57 ppm, 7.77 - 7.88 ppm in **12a** and 7.45 - 7.57 ppm, 7.84 - 7.88 ppm in **12b**. Both **12a** and **12b** were analysed by electron ionization mass spectroscopy. While **12b** disclosed a peak at 587.02 corresponding to complex, **12a** gave only a peak at 356.1 corresponding to the free ligand. The successful completion of the reaction confirms that the ligand remains stable and that the activation of the phosphinine core by the electron withdrawing effect of the metal atom does not induce immediate addition of the acidic to the π-electron system.

4.4 Immobilisation of phosphinine metal complexes on titania

A study of the immobilisation of **12a** and **12b** on TiO_2 was undertaken. For this purpose, NP-TiO_2 was selected, in accord with the previous findings that immobilised phosphine complexes **2** and **3** are definitely more tightly bound on NP-TiO_2 than on neutral titania. Complexes **12a** – **12b** were stirred with previously preheated NP-TiO_2 in thf for 24 hrs at RT. After filtering off the supernatant liquid, the material was washed with several portions of thf and vacuum dried. The loading of the complexes on TiO_2 was estimated with the results obtained from elemental analyses as 12.9 mg/g of **12a**/NP-TiO_2 and 12.7 mg/g of **12b**/NP-TiO_2. The ^{31}P CP MAS NMR spectrum of **12a**/NP-TiO_2 displayed a high field signal at δ = 27 ppm with a small number of spinning side bands **(Fig 20)**. The line width of the resonance was found to be 2.9 k Hz and still larger than in gold(I) phosphinines. This increase in linewidth in the solid state can be attributed to the presence of observable unresolved splittings due to scalar and residual dipolar coupling to the ^{197}Au nucleus[118], which is absent in solution. A similar pattern was also seen for **12b**/NP-TiO_2. For better erudition, ^{31}P CP MAS NMR spectra of the free ligand, **9a** and the corresponding gold(I) complex, **11a** were also measured **(Fig 20)** and compared with those of **12a**/NP-TiO_2. The observed asymmetrical splitting of lines in **11a** was attributed to the coupling of the phosphorus with the gold (I = 3/2); similar pattern was also seen for Au-phosphine complex[115]. Even though the isotropic shift of the free complex and the TiO_2 supported complexes (**12a** or **12b**/NP-TiO_2) are different, the profile of the isotropic line is quite similar which supports the existence of Au to P coordination in **12b** or **12a**/NP-TiO_2.

---

[118] N. J. Clayden, C. M. Dobson and K. P. H. D. Michael, *J. Chem. Soc. Dalton Trans.* **1985**, 1811-1814.
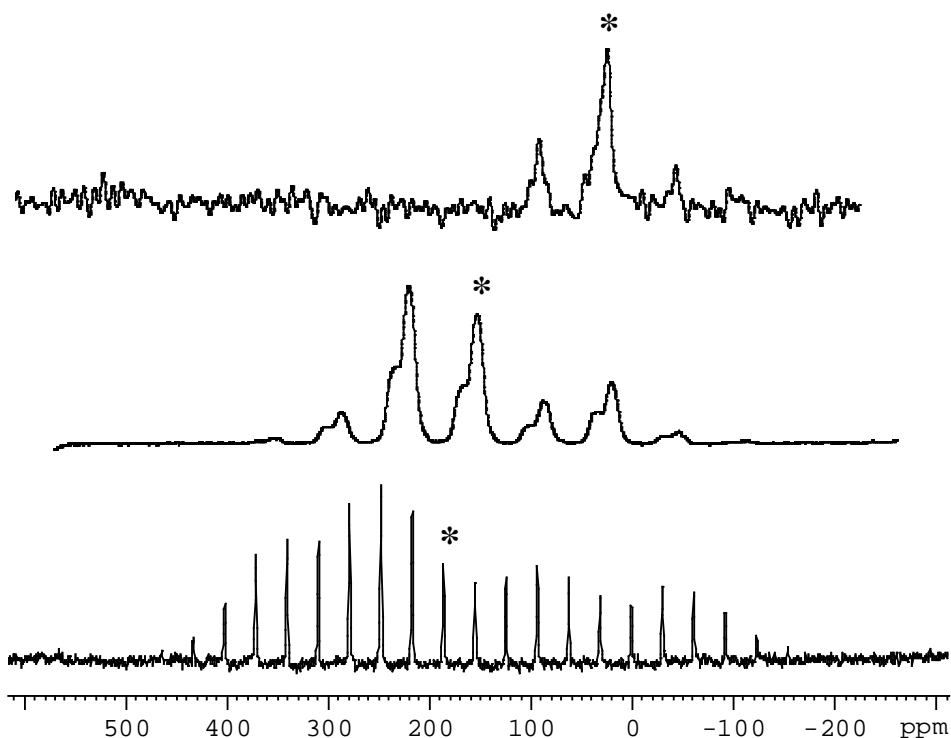
Fig 20: ^{31}P CP MAS NMR spectra of **12a**/NP-TiO$_2$, υ_{rot}: 8 kHz, ns: 2560, contact time: 1 ms, pulse delay: 6 s (top trace), **11a**, υ_{rot}: 8 kHz, ns: 512, contact time: 1 ms, pulse delay: 6 s (middle trace) and **9a**, υ_{rot}: 5 kHz, ns: 32, contact time: 1 ms, pulse delay: 6 s (bottom trace).

As only one ^{31}P isotropic shift was observed in the immobilised material it is clear that the process of immobilisation is clean and that no side products are observed. However, the high field position of the isotropic shift and the much smaller span of the chemical shielding tensor as compared to **11a** (δ = 152.40 ppm, **scheme 22**) implies that during the immobilisation process the phosphinine structure has been changed. **12a**/NP-TiO$_2$ or **12b** /NP-TiO$_2$ exhibit ^{31}P NMR signals in the upfield region like that of the anionic ligand in the complex reported by Floch et al[115,119] indicating that aromaticity within the ring has been disrupted. They suggested that the synthesis of anions involves nucleophilic attack at the electropositive P atom of phosphinine ring. Thus by correlating ^{31}P CP MAS NMR of **12a**/NP-TiO$_2$ or **12b**/NP-TiO$_2$ with previously reported literature[119], the surface bound phosphorus species was assigned as in **scheme 25**. The mechanism of the formation of the new species **13 (scheme 25)** on TiO$_2$ surface involves the attack of nucleophilic reagents that present in trace amount on the TiO$_2$ surface at the electropositive phosphorus centre of phosphinine, leading to the transformation of aromatic structure into phosphacyclohexadienyl gold complex. Although Au coordinated phosphinine is stable in the presence of -OH groups, the complex did not

---

[119] E. Deschamps, F. Mathey, C. Knobler and Y. Jeannin, *Organometallics*, **1984**, *3*, 1150-1157.

survive in immoblisation. Either the surface -OH groups be more reactive and attack to π-system or the attack is promoted by high acidity of NP-TiO$_2$.

13
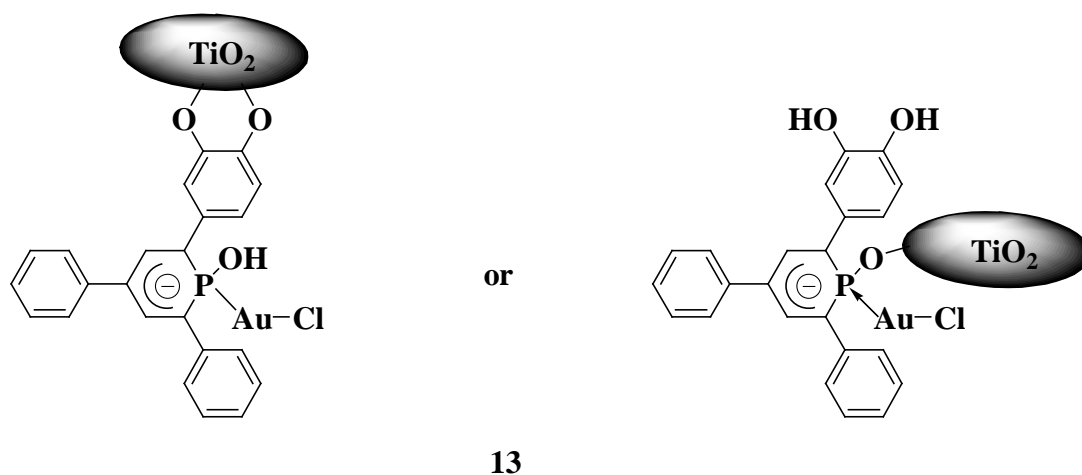
scheme 25

4.5 Immobilisation of phosphinine derivatives on silica

As the immobilisation of phosphinine gold(I) complexes on TiO$_2$ had not fulfilled the expectation, it was proposed to use silica as the carrier material. Covalent tethering is the most versatile approach for immobilisation in order to supress leaching of the immobilised ligands. Silica is a popular support as it is resistant against most solvents and also inexpensive and non toxic. The silica based inorganic mesoporous materials are more affordable for liquid phase reactions because they allow easy diffusion of reactants to the active sites[120,121]. Their surface silinol groups can be functionalized by using trialkoxysilanes with amine, thiol, carboxylic acid, phenyl, cyano groups. These materials can be easily characterized by NMR spectroscopic techniques. The silyl alkoxy functionalized phosphinines described in the section **4.1** would be suitable for anchoring them on silica. The described synthesis yielded however, mixtures of isomers that would have to be seperated by chromatography. It was already mentioned that such purification was not successful as the silyl alkoxy functionality reacted with the column material and ending up in decomposition products.

[120] P. M. Price, J. H. Clark and D. J. Macquarrie, *J. Chem. Soc; Dalton Trans.* **2000**, 101-110.
[121] K. Wilson, A. F. Lee, D. J. Macquarrie and J. H. Clark, *Appl. Cata. A.* **2002**, *228*, 127-133.

A slightly different approach can be made on this regard. This involves, designing of a phosphinine with an auxiliary group that permits the easy purification of ligands, and of a complementary carrier that can hold the newly designed ligand by covalent tethering. For this purpose, hydroxy functionalized phosphinine and halo alkyl functionalized silica were selected, which may easily be coupled to give a phenol ether function, thus immobilising phosphinine on the silica surface. The requisite hydroxy functionalized phosphinine can be synthesized by using the procedure of Vogt and Müller[35] mediated with pyrylium salt[34]. Hexagonal mesoporous silica (HMS)[121] was selected as the inorganic support as its preparation is straightforward does not require the need of strongly acidic conditions, is also cost friendly with the use of a cheap and neutral template and, the material can be readily functionalized with halo alkyl group.

Synthesis of hexagonal mesoporous silica

HMS which is less ordered than MCM-41 and SBA-15 was prepared according to the reported procedure[122], by adding tetraethoxysilane to a stirred solution of ethanol, water and 1-dodecylamine at ambient temperature. In order to remove the template (1-dodecylamine), the white precipitate obtained after 24 hrs stirring was calcined at $600^{o}C$ for 24 hrs **(scheme 26)**.
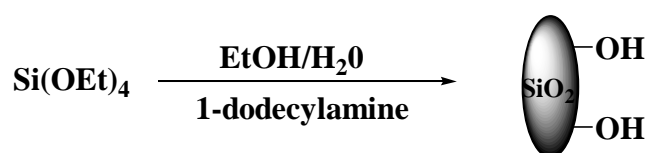
scheme 26: Synthesis of HMS

HMS was characterized by ^{29}Si CP MAS NMR. Unmodified HMS displayed two broad overlapping resonances at -110 and -102 ppm which correspond to Q^4 and Q^3 bands, respectively with Q^3 as major contribution of the bulk silica frame work [$Q^n = Si(OSi)_n(OH)_{4-n}$] **(Fig 22)**. Q^4 sites correspond to bulk silicon nuclei with $Si(OSi)_4$ group. A weak shoulder observed at -93 ppm is attributed to Q^2 species. The Q^3 sites are those with single Si-OH group that include both free and hydrogen bonded silanols and Q^2 corresponds to geminal

---

[122] P. T. Panev and T. J. Pinnavaia, *Science*, **1995**, *267*, 865-867.

silandiols. The assignments of Si resonances are similar to those observed in unmodified MCM-41[123].

Synthesis of chloropropyl functionalized HMS (ClPTESi-HMS)

A chloropropyl functionalization was introduced onto HMS by refluxing calcined HMS with (3-chloropropyl) triethoxy silane in toluene **(scheme 27)**. Functionalization onto HMS was verified by running ^{13}C CP MAS and ^{29}Si CP MAS spectroscopy.

calcined HMS
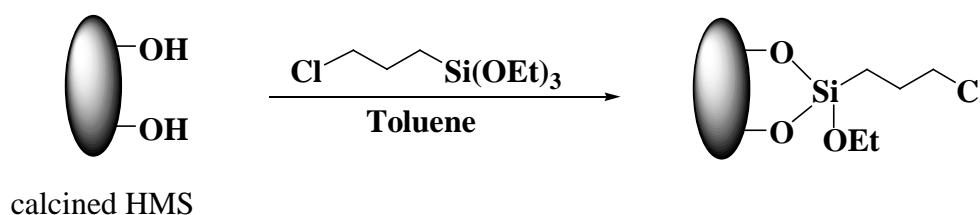
scheme 27: Synthesis of ClPTESi-HMS.

^{13}C CP MAS NMR spectrum of the material exhibits resonances at 8.1, 23.6 and 43.9 ppm (signals denoted as **a**, **b**, **c** in **Fig 21**) which were assigned to the three carbon nuclei of the grafted propyl chain, and signals at 13.0 and 57.6 ppm (denoted as *) which were assigned to the carbon nuclei of unreacted ethoxy groups attached to the silicon atom in the tether **(Fig 21)**. Similar assignments of ^{13}C NMR signals were observed in chloro propyl functionalized MCM-41[124] **(Table 2)**.

[123] S. M. Bruno, A. C. Coelho, R. A. S. Ferreira, L. D. Carlos, M. Pillilnger, A. A. Valente, P. R. Claro and I. S. Goncalves, *Eur. J. Inorg. Chem*. **2008**, 3786-3795.
[124] Sujandi, E. A. Prasetyanto, S. C. Lee and S. E Park, *Microporous and Mesoporous Materials*, **2009**, *118*, 134-142.
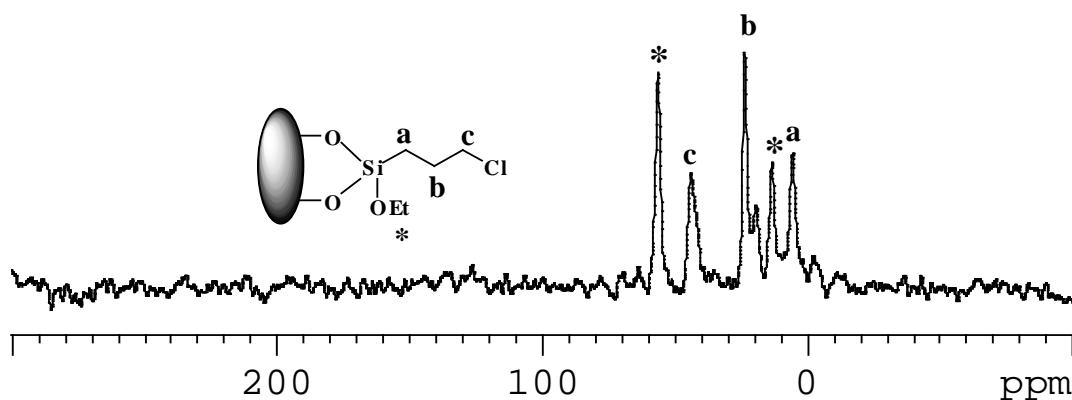
Fig 21: ^{13}C CP MAS NMR spectrum of ClPTESi-HMS, υ_{rot}: 8 kHz, ns: 4096, contact time: 1.8 ms, pulse delay: 5 s.

Table 2. ^{13}C CP MAS NMR chemical shifts [ppm] of silica supports

Compound	carbon atoms of propyl chain	ethoxy carbons
Chloropropyl triethoxy functionalized MCM-41	9.4, 21.0, 43.0	16.0, 58.0
ClPTESi-HMS	8.1, 23.6, 43.9	15.0, 57.6

The ^{29}Si CP MAS spectrum of modified HMS (ClPTESi-HMS), displayed signals of Q^4, Q^3 and Q^2 groups at –109, -101 and -90 ppm. The Q^3 resonance constitutes the major contribution in the bulk silica frame work **(Fig 22)**. This phenomenon is also observed in the case of chloropropyl functionalized MCM-41[123] species. The one additional less intense band at -53 ppm can be assigned to T^2 site of grafted organosilane species [T^m = $RSi(OSi)_m(OEt)_{3-m}$] **(Table 3)**. Since the intensity of Q^3 resonance is quite large as compared to Q^2 and Q^4 the chance for finding T^3 sites is little. This suggests that the products are best described by the structures shown in **Fig 21** which is formed by condensing two of the three alkoxy groups with surface -OH functions and represents the most frequently formed structural motif for immobilised trialkoxy silanes.
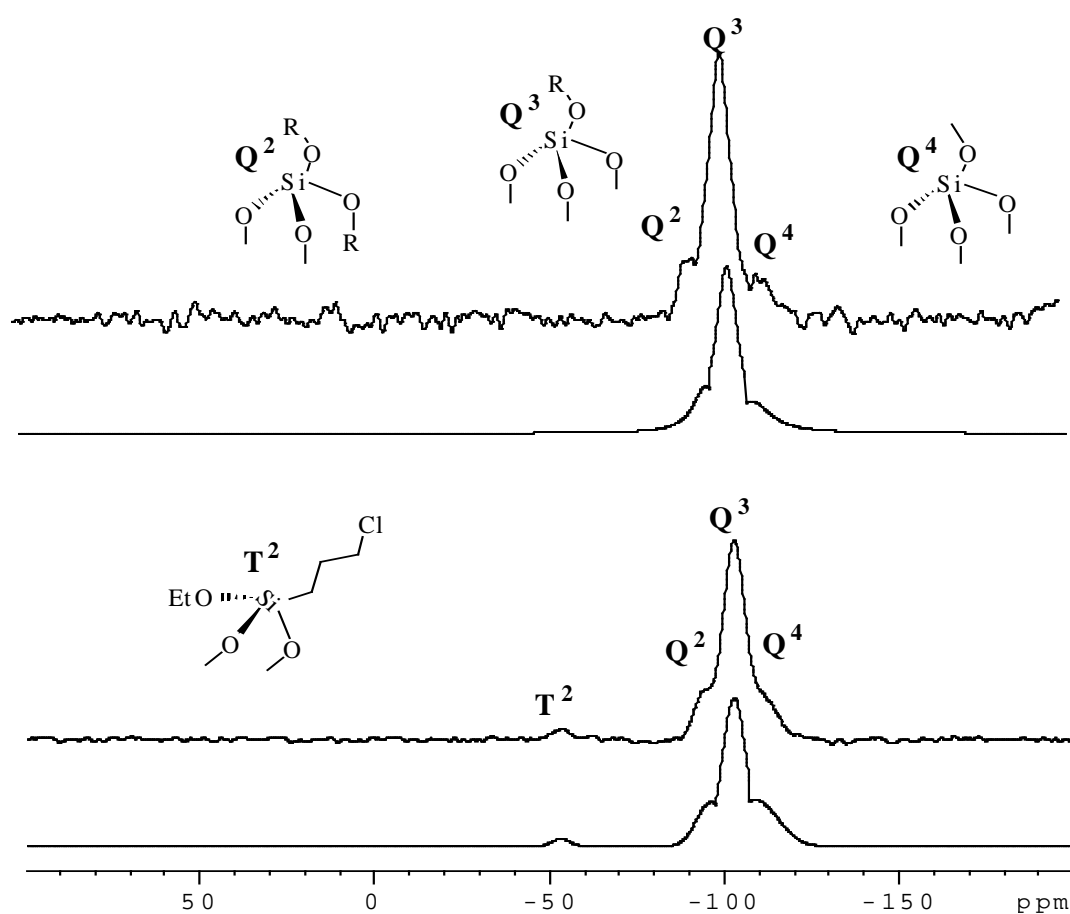
Fig 22: ^{29}Si CP MAS NMR spectra of HMS, υ_{rot}: 8 kHz, ns: 2048, contact time: 1 ms, pulse delay: 7.5 s (bottom trace) and ClPTESi-HMS, υ_{rot}: 9 kHz, ns: 3072, contact time: 1.4 ms, pulse delay: 7.5 s (top trace). **a**, **b**, **c** and **∗** represent carbon atoms of n-propyl group and ethoxy group respectively.

Table 3. ^{29}Si CP MAS NMR chemical shifts [ppm] of silica supports

Compound	Q^4	Q^3	Q^2	T^2
HMS (calcined)	-110	-102	-93	-
ClPTESi-HMS	-109	-101	-90	-53

Synthesis of hydroxy functionalized phosphinine

The hydroxy functionalized phosphinine was prepared by the method described in section **4.2**. Benzal acetophenone was initially treated with 3-methoxy acetophenone to form 2-(3'-methoxy phenyl)-4,6-diphenyl pyrylium tetrafluroborate, **8d** which on treatment with P(SiMe$_3$)$_3$, followed by flash chromatography with petrol ether - ethylacetate (2:1) as eluant to give the corresponding phosphinine **9d**. The NMR spectral results of both **8d** and **9d** were identical with those reported in the literature[48]. The methoxy group in **9d** was then deprotected with BBr$_3$ in dichloromethane, followed by flash column chromatography with hexane-dichloromethane mixture (50 : 50) after aqueous workup to give the requisite phosphinine **10d** as white solid in 61% yield **(scheme 28)**.
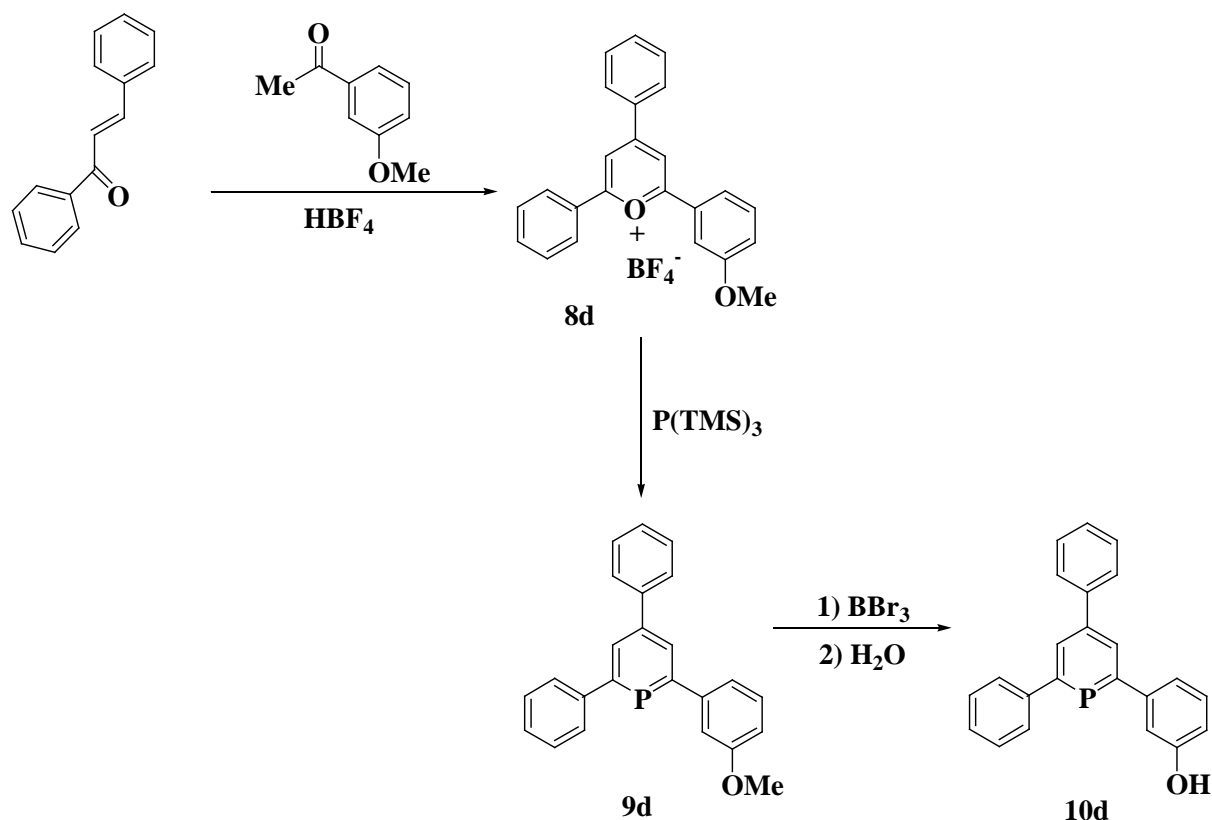
scheme 28: Synthesis of hydroxy functionalized phosphinine **10d**.

The compound which melted at 183°C displayed a singlet in ^{31}P{^{1}H}NMR spectrum. The disappearance of methoxy signals in ^{1}H and ^{13}C NMR spectroscopy confirmed the successful deprotection. A doublet at 8.08 ppm ($^{3}J_{HP}$ = 5.8 Hz) was assigned to meta protons in the phosphinine ring. The multiplets at 6.56 - 6.61 ppm, 6.97 - 6.99 ppm, 7.12 -7.28 ppm, 7.64 -

7.69 ppm were attributable to aromatic protons of the phenyl groups. The ^{13}C NMR spectrum of **10d** showed a doublet at 171.55 ppm ($^1J_{CP}$ = 52.3 Hz) and 171.87 ($^1J_{CP}$ = 52.5 Hz) which was assigned to ortho carbons of the phosphinine ring. The two meta carbons of phosphinine ring resonated as doublet at 131.83 ppm ($^2J_{CP}$ = 10.2 Hz) and 132 ppm ($^2J_{CP}$ = 10.2 Hz). The electron ionization mass spectrum of the compound gave a peak at 339.09 corresponding to the ligand.

Immobilisation of hydroxy functionalized phosphinine onto ClPTESi-HMS

The solution of **10d** in DCM was added dropwise at -78°C to a suspension of ClPTESi-HMS in toluene containing excess triethyl amine as base. The mixture is allowed to stir overnight at room temperature. The supernatant liquid was filtered off and the material **10d**/ ClPTESi-HMS was washed several portions of toluene and DCM successively. It was then dried under vacuum for 8 hrs **(scheme 29)**.

scheme 29: Immobilisation of phosphinine, **10d** onto ClPTESi-HMS

^{31}P NMR measurements of the isolated material with cross polarization led to grossly distorted signal intensities and thus rendered analysis of spectral results unreliable. Mobility of the linker having alkyl chain attached to the surface of HMS could be responsible for

obstructing signal intensities in ^{31}P CP MAS of **10d**/ ClPTESi-HMS. The phenomenon had also been detected in the case of phosphines immobilised on silica via linkers incorporating alkyl chains[100]. Therefore ^{31}P NMR spectra of **10d**/ClPTESi-HMS were measured with simple high power decoupling. The surface bound phosphinine together with other ill-defined side products were evident from ^{31}P HP Dec MAS NMR **(Fig 23)**.
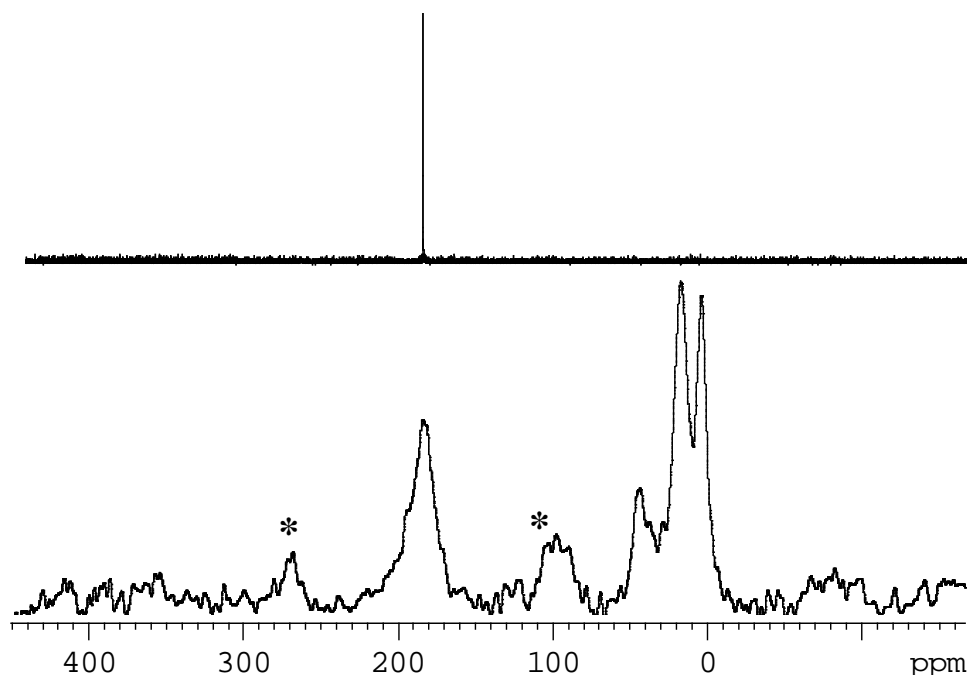

Fig 23: Solution ^{31}P{^{1}H} NMR of **10d** (top trace) and solid state ^{31}P {^{1}H} MAS NMR spectra of **10d**/ClPTESi-HMS, υ_{rot}: 9 kHz, HP [1]H Decoupling (bottom trace).

In ^{31}P MAS NMR, the signal observed at 183 ppm was attributed to immobilised phosphinine. The comparison of the line widths of immobilised and free phosphinine **9a** (**Fig 20**, bottom trace, in section **4.4,** $\Delta v_{1/2} = 0.3$ k Hz) showed a large increase for **10d**/ClPTESi-HMS ($\Delta v_{1/2} =$ 4.6 k Hz). The observed half width of the ligand in **10d**/ ClPTESi-HMS lies in the range of covalently bound phosphine linkers[100]. In addition to this, formation of major amounts of side products is visible by the observation of additional isotropic lines at 4.4, 18.2 and 45.1 ppm. From the integerals of ^{31}P NMR signals, it was found that only 25% of the ligand retains its identity in **10d**/ ClPTESi-HMS. The two main side products at 4.4 and 18.2 ppm are having similar intensities and also quite similar half widths with 1.3 and 1.5 k Hz respectively. The structural assignment of these side products was unfeasible. However, the origin of these side products in the immobilised material could be that alkoxy groups present

on the tether might attack at the electropositive P atom of the ligand leading to the disruption of phosphinine moiety.

To conclude, some novel functionalized phosphinines bearing hydroxy (or methoxy) groups in the vicinal positions on the aromatic moiety were synthesized and contributed as ligands for coordination to gold(I). The immoblisation of the gold(I) complexes of hydroxy functionalized phosphinines on NP-TiO$_2$ was tested under standard conditons. ^{31}P CP MAS NMR of the immobilised material revealed that phosphinine moiety was changed structurally during immobilisation process. Further silica was also used as a carrier material for anchoring phosphinine derivatives by covalent tethering method and spectral studies revealed that nearly 25% of the ligand retained its identity on the surface of silica.

5. Phosphinine stabilized gold nanoparticles

5.1 Gold nanoparticles

Gold is the subject of ancient themes of investigation in the field of science. Gold has been now applied in the context of emerging nanoscience and nanotechnology with nanoparticles with self assembled monolayers (SAMs)[125]. Gold nanoparticles called Au NPs are the most stable metal nanoparticles[126] and are considered to be a key material in the 21st century[127]. In 1857 the formation of a deep red solution of colloidal gold was reported by Faraday by reduction of an aqueous solution of chloroaurate (AuCl$_4$)$^-$ with phosphorus in CS$_2$. Faraday studied the optical properties of thin films made from colloidal solutions and noticed reversible color changes of the films upon mechanical compression (from bluish-purple to green upon pressurizing)[128]. In the middle ages colloidal gold was used in medicine for the diagonosis of syphilis[129,130,131,132] and its use in medicine was continued in 20th century also. In the 20th century different methods for gold colloidal preparation were demonstrated. In the last few decades colloidal gold have considered as the subject of several reviews[133] especially after the breakthrough of Schmid[134,135,136] and Brust et al[137].

The synthesis of Au NPs by reducing gold(III) derivatives introduced by Turkevitch in 1951[138] was the most popular one for a very long time. This method involves citrate reduction of HAuCl$_4$ in water and produces Au NPs of ca. 20 nm diameter. Schmid reported the gold phosphine cluster (Au$_{55}$(PPh$_3$)$_{12}$Cl$_6$) in 1981, which remained unique due to its narrow dispersity (1.4 nm)[139]. Phosphine stabilized nanoparticles are also good precursors

[125] A. Mocanu, I. Cernica, G. Tomoaia, L. D Bobos, O. Horovitz and M. T. Cotisel, *Colloids and surfaces A . Physico chem, Eng Asp*. **2009**, *338*, 93-101.

[126] M. A Hayat, Colloidal Gold , Principles, method and application, Academic Press, San Diego, **1991**.

[127] R. C. Elder et al. *J. Am. Chem. Soc*. **1985**, *107*, 5024.

[128] M. Faraday, *Philos. Trans*, **1857**, *147*, 145-181.

[129] R. L. Kahn, Serum diagnosis for syphilis. In colloid chemistry, Alexander. J. Ed, The chemical catalog co, New York. **1928**, *11*, 757.

[130] Hauser and E. A. A. Potabile, *J. Chem. Educ*. **1952**, 456-458.

[131] D. H. Brown and W. E Smith., *Chem. Soc. Rev*. **1980**, *9*, 217-240.

[132] A. D Hyatt and B. T. Eaton, Immuno gold electron microscopy in virus diagnosis and research, Eds. CRC press, Boca Raton, FL, **1993**.

[133] G. Schmid, In nanoscale materials in Klabunde. K. J. Ed Wiley, New York. **2001**.

[134] G. Schmid and L. F. Chi, *Adv Mater*. **1998**, *10*, 515-527.

[135] G. Schmid, Clusters and colloids, Ed, VCH, weinheim. **1994**.

[136] G. Schmid, *Chem Rev*. **1992**, *92*, 1709-1727.

[137] M. Brust and C. J. Kiely, *Colloids and Surfaces A. Physico Chem. Eng. Asp*. **2002**, *202*, 119-126.

[138] J. Turkevitch, P. C. Stevenson and J. Hillier, *Discuss. Faraday Soc*. **1951**, *11*, 55-75.

[139] G. Schimd, R. Pfell., R. Boese, F. Bandermann, S. Meyer, G. H. M. Calis and J. van der Velden, *Chem. Ber*, **1981**, *114*, 3634 - 3642.

for other functionalized nanoparticle building blocks with well defined metallic cores[140]. The possibility of using alkane thiols of different chain lengths for the stabilization of Au NPs and their analysis was reported by Mulvaney and Giersig in 1993[141]. The colloidal particles form monolayers, and the core to core interparticle spacing is determined by the size of the alkane chains on the stabilizers used in the preparation of sols. Later the Brust-Schiffrin method[142] of Au NPs synthesis had a significant impact because it allows the facile synthesis of thermally and air stable NPs of reduced dispersity and controlled size. The synthesis is carried out in a two phase system and uses the thiol ligands that strongly bind gold due to soft character of both gold and sulfur. These particles can be redissolved in commonly used organic solvents without suffering decomposition and irreversible aggregation. These NPs can also be functionalized like stable organic compounds. The Brust method was applied to improve the synthesis of Schmids cluster ($Au_{55}(PPh_3)_{12}Cl_6$) using $HAuCl_4.3H_2O$ and $N(C_8H_{15})Br$ in a water - toluene mixture to which PPh_3 and then $NaBH_4$ were added. It was found that the cluster formed in this method has the formula ($Au_{101}(PPh_3)_{21}Cl_5$). Hutchison et al[143] described a safer, more convenient, and more versatile synthesis of phosphine stabilized nanoparticles analogous to those originally reported by Schmid. The synthesis eliminated the use of boranes, could be carried out at ambient temperature, permitted the use of a variety of passivating phosphine ligands, and provided control over particle core size.

The general formula of gold phosphinine clusters is $[Au_aL_b]^{n+}[X]^-_n$, where L is a ligand bonded to the peripheral gold atoms of the cluster[135]. In most cases, gold clusters are cationic, so they require counter ions X^- ($n \neq 0$). Solvent molecules from the mother liquor are often involved in the stabilisation of the cluster. A thorough study of the composition of Au NPs involves the knowledge of stoichiometry, the structure of the gold skeleton and the connectivity with the ligand. Elemental analyses for the determination of chemical composition is considered to be a first approach of the characterization of such clusters. However, the large molecular mass and inaccuracy of the data do not allow unambiguous determination of their stoichiometry. Other physical measurements which include conductivity analysis and osmometric measurements are often also unable to give clearly interpretable results. In determining the exact molecular structure of gold clusters X-ray

[140] G. Schön and U. Simon. *Colloid. Polym. Sci.* **1995**, *273*, 101.
[141] L. Bronstein, D. Chernyshov, P. Valetsky, N. Tkachenko, H. Lemmetyinen, J. Hartmann and S. Forster, *Langmuir.* **1999**, *15*, 83-91.
[142] M. Brust, M. Walker, D. Bethell, D. J Schiffrin and R. J. Whyman, *J. Chem. Soc. Chem. Commun.* **1995**, 1655-1656.
[143] W. W. Walter, Scott, M. Reed, Marvin, G. Warner and E. Hutshison, *J. Am. Chem. Soc*, **2000**, 12890-12891.

analyses are thus indispensable although their application is hampered by difficulties inherent in the nature of cluster compounds. For cluster anaysis by X-ray, a cluster contains a heavy atom surrounded by a pool of inert light atoms (ligands). To require a stable packing, the inclusion of counter ions or solvent molecules at cavities of clusters is necessary. As the solvents being volatile and also due to the rotational freedom of counter ions, the crystals are of poor quality. The absence of rotational freedom of the ligands together with the strong intercluster interactions is the relevant cause for the rigorous attachment to the crystallographic symmetry.

The chemical properties of large ligand stabilized transition metals are limited. This is due to their enhanced tendency to decompose in solution[144]. The partial dissociation of ligands leads to fast aggregation processes through free surface atoms and finally to the precipitation of the metal[144]. Therefore chemical reactions are limited to fast reactions in the ligand sphere. ^{31}P NMR investigations on phosphine stabilized clusters in solution have shown that phosphines are highly fluxional[145]. Due to the high fluxionality of phosphine ligands only one sharp ^{31}P NMR signal is observed for $Au_{55}(PPh_3)_{12}Cl_6$ at room temperature although ^{197}Au-^{31}P couplings are to be expected. The fluxional behaviour is thought to result from facile skeltal rearrangement, and is common to all types of clusters. The studies showed that there were differences between spectra in solution and in the solid state which could be related to fluxional behaviour[145]. Thus if fluxional processes that occur in solution are frozen out in the solid, the solid state ^{31}P NMR spectra would reveal more directly than those of the solutions the phosphine environments and hence the structure of the cluster.

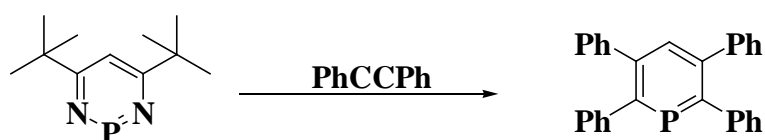## 5.2 Synthesis of phosphinine stabilized gold nanoparticles

Classical tertiary phosphines with sp^3 hybridized phosphorus atom have been well explored in the size controlled synthesis of gold nanoparticles and their applications in catalysis for the past few decades[144]. Recently phosphinines have been investigated for the stabilization of gold nanoparticles. The products were characterized by large angle XRD, TGA and IR spectra thereby suggesting that phosphinine was grafted on the surface gold metal[91]. However, these analytical methods have not been yet given precise structural information of how the

---

[144] M. C. Dainie. *Chem. Rev*. **2004**, *104*, 293-346.

[145] F. A. Vollenbroek, P. C. Bouten, J. M. Trooster, J. P. van der Berg and J. J. Bour, *Inorg. Chem.* **1980**, *19*, 2685-2698.

phosphinines interact with the gold surface. Although coordination in molecular phosphinine - gold complex is only known to occur in η^1 mode, phosphinines may bind to other to transition metals in η^1, η^2 or η^6 mode to a single metal atom; in clusters also bridging interaction of a phosphinine with two or three metal atoms is known. Hoping that the solid state NMR spectroscopy could be likely to gather information based on the mode of interactions of phosphinines on gold surface, gold nanoparticles of 2,3,5,6-tetraphenyl phosphinines in two different ratios - Au NPs P- 0.2 (Au : P - 1 : 0.2) and Au NPs P- 0.5 (Au : P - 1 : 0.5) were prepared according to the reported procedure[91] and were then characterized by solid state NMR.
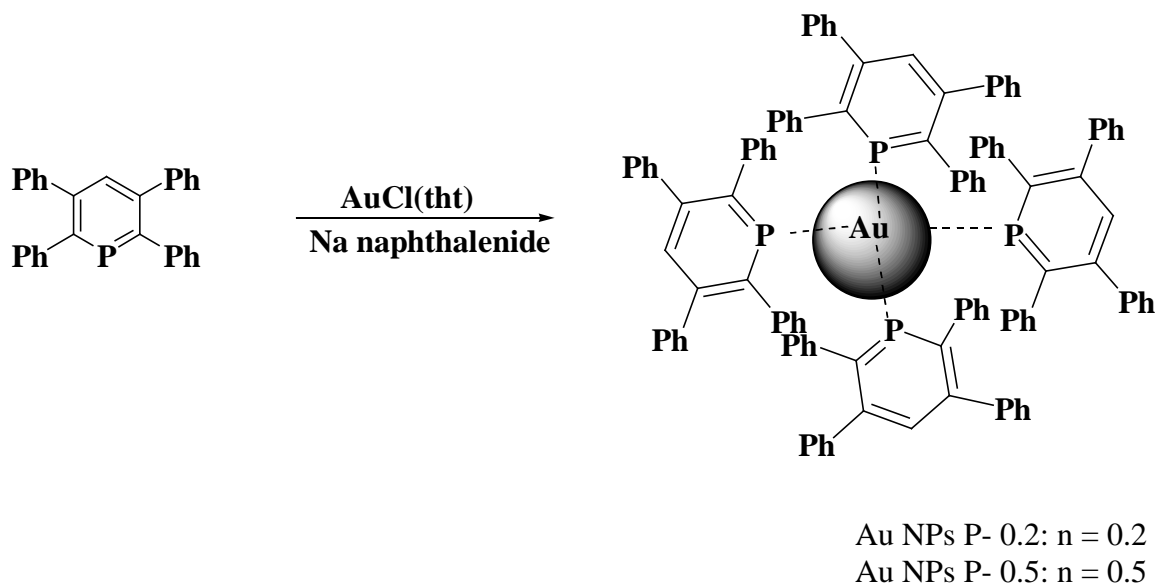
To begin with, 2,3,5,6-tetraphenyl phosphinine was prepared by reacting 4,6- di-tert-butyl-1,3,2-diazaphosphinine with excess of diphenyl acetylene at high temperature using the previously described [4+2] cycloaddition - cycloreversion route[44] (**scheme 30**). The ligand was isolated as white powder from the crude mixture by flash chromatography with hexane : toluene (8 : 2). The compound displayed a $^{31}P\{^1H\}$ signal at 210 ppm. ^1H and ^{13}C NMR data were identical with those reported in the literature[146].

scheme 30: Synthesis of 2,3,5,6-tetra phenyl phosphinine

The syntheses of phosphinine stabilized gold NPs proceeded via the reduction of AuCl(tht) in the presence of the phosphinine. The reduction process was carried out as described at room temperature in thf by dropwise addition of sodium naphthalenide solution to a mixture of the complex and n molar equivalents of phosphinine (n = 0.2, 0.5) (**scheme 31**). The resulting purple colored solution was stirred at room temperature for six hrs. The purple solid obtained after evapoartion of the solvent was washed several times with thf and hexanes to remove both naphthalene and sodium salts.

[146] M. Doux, L. Ricard, F. Mathey, P. Le. Floch and N. Mezailles, *Eur. J. Inorg. Chem.* **2003**, 687-698.

Ph—⬡—Ph
Ph—⬡(P)—Ph   →[AuCl(tht) / Na naphthalenide]→   (Au NPs structure with phosphinine ligands)

Au NPs P- 0.2: n = 0.2
Au NPs P- 0.5: n = 0.5

scheme 31: synthesis of Au NPs stabilized by 2,3,5,6- tetraphenyl phosphinines

5.3 The study of phosphinine - gold surface environment by ^{31}P CP MAS NMR

In order to establish the chemical environment of the phosphinine stabilized nanoparticles, the materials with different phosphinines in gold ratio were charcterized by ^{31}P CP MAS NMR spectroscopy **(Fig 24** and **25)**. The solid state ^{31}P NMR spectra recorded at 400 M Hz showed several spinning side band manifolds with isotopic chemical shifts of 178, 63.9, 35.7 and 17.5 ppm for Au NPs P-0.2 and 174, 63.9, 35.1 and 19.4 ppm for Au NPs P-0.5 **(Table 4)**. All lines were either broad (Au NPs P-0.2) or showed fine structure (Au NPs P-0.5) attributable to scalar and residual dipolar couplings of P with [197]Au (I = 3/2). Such splittings have been previously described[145,147]. Although simulation is in principle feasible[148] it is not possible to further analyze them due to lack on sufficient information of efg tensors. The isotropic shift $\delta_{iso} = 178 /176$ ppm with large intensity in the two Au NPs is similar as the values observed in solution spectra of molecular Au(I) phosphinine complexes with s-coordinated ligands. This suggests the presence of same coordination mode in the Au NPs. The line widths of the isotropic shifts at $\delta = 176$ (for Au NPs P-0.2) and 178 ppm (for Au NPs P-0.5) in the solid state spectra were 2.2 and 2.7 k Hz respectively. These values are much greater than those observed in the solution spectra of gold(I) phosphinines. One obvious reason for increase in the line width in the solid state is dipolar broadening due to [197]Au nuclei, which is absent in the solution. Spinning of the probe at magic angle could not be able to remove the entire

[147] E. N. de Silva, G. A. Bowmaker and P. C.Healy, *J. Mol. Str.* **2000**, *516*, 263-272.
[148] P. D. Boyle, B. J. Johnson, A. Buehler and L. H. Pignolet, *Inorg. Chem.* **1986**, *25*, 7-9.

dipolar broadening as the quadrupolar interaction of the gold is comparable in magnitude with the Zeeman interaction[149]. The failure to observe unusual chemical shifts or extremely short relaxation times that may be attributed to interactions of the nuclear spins with paramagnetic electron spins indicates that Au NPs are diamagnetic and not metallic.
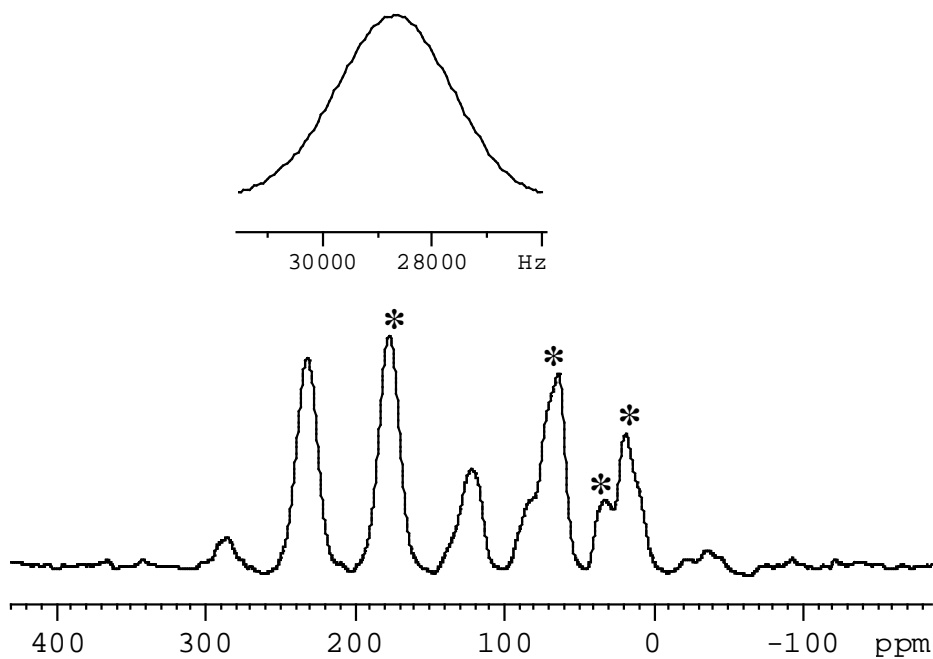

Fig 24: ^{31}P CP MAS NMR spectrum of Au NPs P- 0.2, υ_{rot}: 8.6 kHz, ns: 256, contact time: 1 ms, pulse delay: 3 s recorded at 400 M Hz.

[149] J. G. Hexem, M. H. Frey and S. J. Opella, *J. Am. Chem. Soc.* **1981**, *103*, 224.
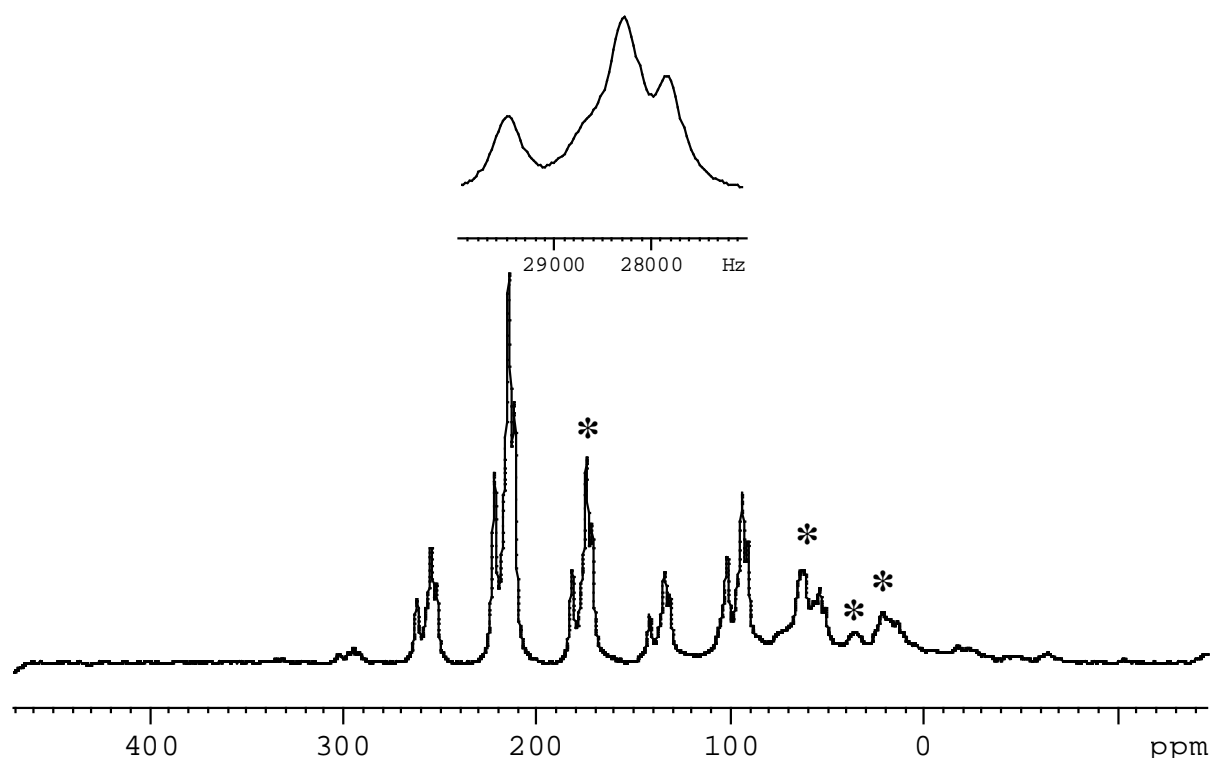
Fig 25: ^{31}P CP MAS NMR spectrum of Au NPs P- 0.5, υ_{rot}: 10 k Hz, ns: 256, contact time: 1 ms, pulse delay: 4 s recorded at 400 M Hz.

In order to corroborate the assignment of the most intense signals to s-coordinated phosphinine ligands on Au(I), the molecular complex **14** was prepared for comparison purpose. The reaction was carried out by stirring equivalent amounts of phosphinine and AuCl(tht) in thf at RT for 15 min. The completion of the reaction was checked by ^{31}P NMR spectroscopy. The solution was concentrated and a pale yellow solid precipitated out by the addition of excess hexane was characterized by routine solution NMR technique **(scheme 32)**. As encountered in other gold(I) phosphinines a coordination shift of $\Delta\delta$ = -35 ppm was observed.
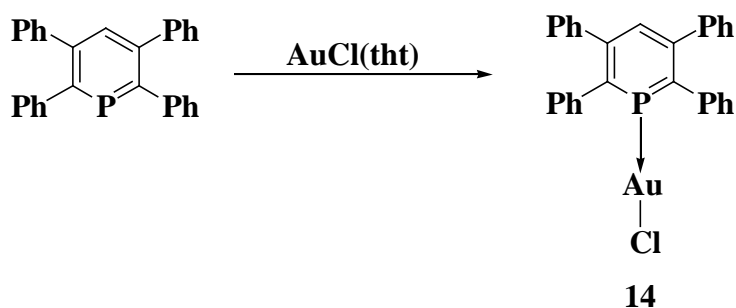
scheme 32: Synthesis of 2,3,5,6-tetra phenyl phosphinine gold(I) chloride **14**.

An isotropic line at roughly the same chemical shift of 175 ppm along with the side bands was noticed in the ^{31}P CP MAS NMR spectrum of a solid sample **(Fig 26)**. The observed asymmetrical splitting of lines into four peaks is attributed to scalar and residual dipolar coupling of the phosphorus with the Au (I =3/2); similar patterns have been observed for Au(I)-phosphine complexes[150]. Attempts to simulation of the observed splitting to determine scalar and dipolar coupling constants remained unfeasible. The overall width of the isotropic signal of complex **14** is found to be 1.9 k Hz which is comparable to the line widths of Au NPs P- 0.2 and Au NPs P- 0.5 **(Fig 24** and **Fig 25)**. The observed similarities between spectra of **14** and Au NP support initial assignment that ligands are η^1 coordinated to one Au atom; the close analogy suggests that Au atom is also Au(I).
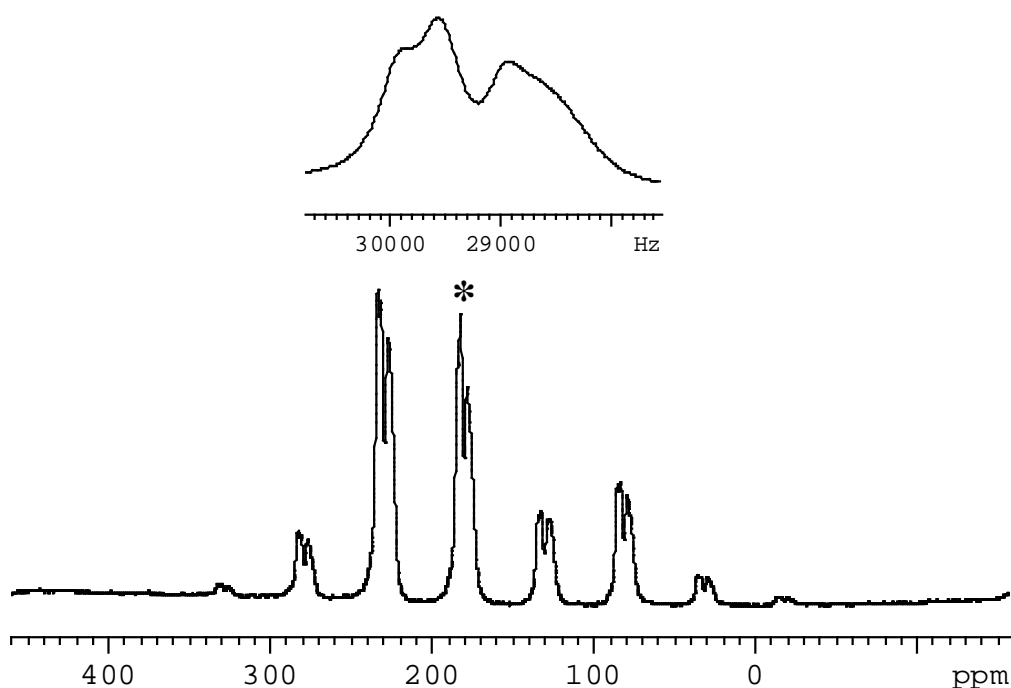

Fig 26: ^{31}P CP MAS NMR spectrum of **14**, υ_{rot}: 8 kHz, ns: 512, contact time: 1 ms, pulse delay: 6 s recorded at 400 M Hz.

[150] J. W. Diesveld, E. M. Menger, H. T. Edzes and W. S. Veeman, *J. Am. Chem. Soc*. **1980**, *102*, 7935-7936.

Table 4. ^{31}P CP MAS NMR chemical shifts of Au NPs and parent complex:

Compound	δ_{iso} [ppm]
Au NPs P- 0.2	176, 63.9, 35.7 and 17.5
Au NPs P- 0.5	178, 63.9, 35.1 and 19.4
14	175

To confirm that the asymmetric splitting pattern result from the interactions between ^{31}P and quadrupolar [197]Au nuclei, ^{31}P CP MAS NMR spectra of Au NPs P- 0.5 and **14** were recorded at 300 M Hz, expansions of isotropic lines in the spectra of **14** and Au NPs P- 0.5 are presented in the **Fig 27**. The spectra were run at different field strengths because quadrupolar induced splitting in contrast to scalar splitting are field dependent. A decrease in line width was noticed for both the samples (1.9 to 1.7 k Hz for **14**, 2.7 to 2.5 k Hz for Au NPs P- 0.5) with decreasing field strength. The resolution of the signals of **14** and Au NPs P- 0.5 measured at 400 M Hz become less apparent at 300 M Hz. As the line separation and line width are slightly field dependent, this decrease in line widths confirms the assignment to quadrupole induced splittings.
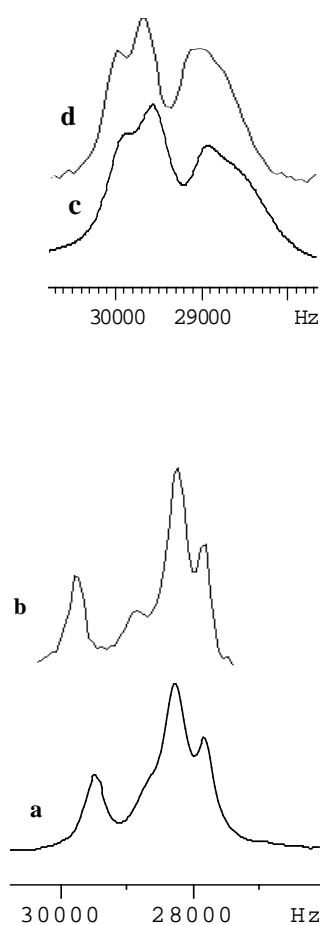
Fig 27: The enlarged portions of the isotropic chemical shift of ^{31}P CP MAS NMR of Au NPs P-0.5: recorded at **a)** 400 MHz, υ_{rot}: 4 kHz , **b)** 300 MHz, υ_{rot}: 4 k Hz and **14**: recorded at **c)** 400 MHz, υ_{rot}: 9 kHz , **d)** 300 MHz, 8 kHz.

For further analysis of the composition of Au NPs, the ^{13}C CP MAS NMR spectrum of Au NP P-0.5 was run and it displayed peaks at 126, 127 and 134 ppm characterestics of napthalene carbons in addition to the peaks corresponding to phenyl carbons **(Fig 28)**. This shows that residual amount of naphthalene is also incorporated in the Au NPs.
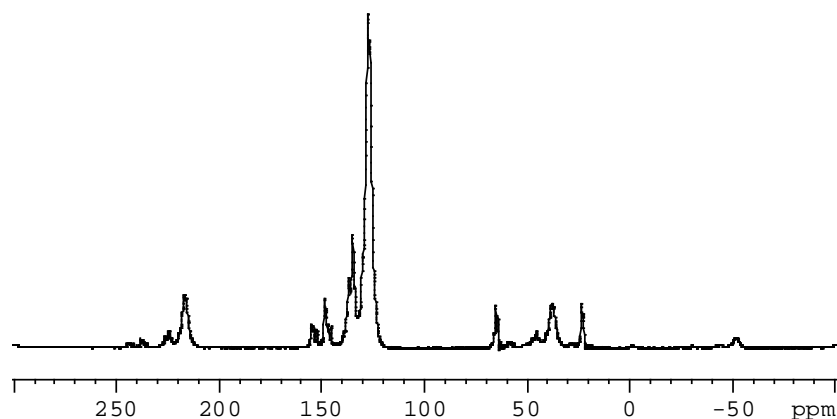
.

Fig 28: ^{13}C CP MAS NMR spectrum of Au NP-0.5, υ_{rot}: 9 k Hz, ns: 8192, contact time: 3 ms, pulse delay: 5 s.

The assigned η^1 coordinated phosphinine ligands that are bonded to Au(I) would require presence of appropriate counter ions. To clear this, XPS measurement of Au NPs were made and gave the evidence for the existence of Cl^{-} ions in the samples. This finding confirmed independently that these Au NPs appear likewise to be in the form of cationic clusters with chloride as the counter ion. The spectra recorded at different field strengths in the case of **14** are field dependent indicating the assignment to quadrupolar induced splitting. For Au NP P-0.5 the lines are field independent. This suggests that efg is presumably much larger ie the Au is in a less symmetrical environment[151]. The observation of splitting in Au NP P-0.5 confirms that phosphinines remain persumably bound to a single Au. The observation of broad lines without fine structure for Au NP-0.2 point to be a more heterogenous environment which induces additional line broadening.

To summarize, Au NPs of phosphinines with different gold - phosphorus ratios were prepared according to a previously published procedure and characterized by ^{31}P CP MAS NMR spectroscopy. The comparison of the spectral data with those of authentic Au-phosphinine complexes and also with XPS measurements suggested that gold nanoparticles appeared to be in the form of cationic clusters with the Cl^{-} as the counter ion and contained terminal P coordinated phosphinine ligands together with decomposition products.

---

[151] C. Olivieri Alejandro, *Solid State Magnetic Resonance*. **1992**, *1*, 345-353.
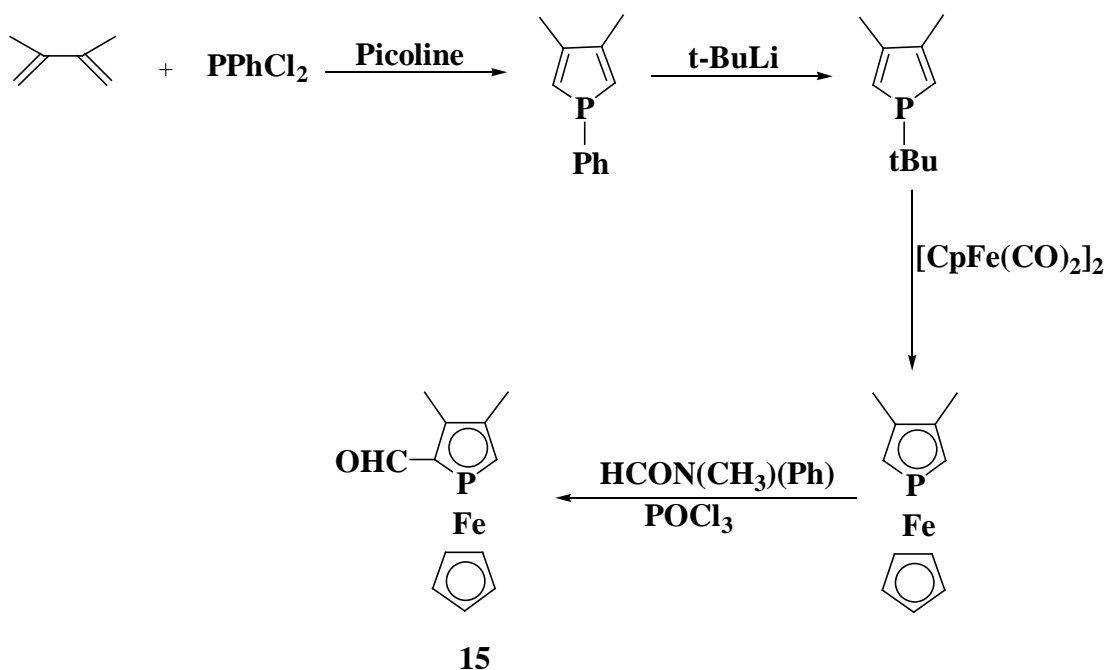
6. Immobilisation of monophosphaferrocene

6.1 Anchoring of monophoshaferrocene onto HMS

There is a continuing interest in the chemistry of phosphaferrocenes because of their use as ligands in homogenous catalysts. Many reports have dealt with the unique combination between their π acceptor properties, which makes them potential ligands for soft catalytic centres, and the planar chiral type structures provided by ferrocene backbone[64,67]. The chemical reactivity of phosphaferrocenes allows aromatic electrophilic substitution[67] which enables to introduce additional functional groups into the phospholyl ring, thereby rendering phosphaferrocene a planar chirality. In view of their potential use for homogenous catalysis and in regard of the fact that phosphaferrocenes exhibit reasonable stability and can tolerate a wide range of experimental conditions, it seemed worth while to study the heterogenization of monophosphaferrocene and study the immobilised materials by solid state NMR.

The popular, non-toxic and chemically resistant silica was proposed to apply for heterogenising monophosphaferrocene by covalent tethering. Immobilisation can be achieved by introducing a suitable functionality onto the monophosphaferrocene and modifying the silica support. For this purpose, 3,4-dimethyl monophosphaferrocene and hexagonal mesoporous silica (HMS) were selected. The synthesis of this monophosphaferrocene is quite straight forward as described in the literature[64] **(scheme 33)**. 3,4-dimethyl-1-phenyl phosphole[152] is first synthesized from 2,3-dimethyl-1,3-butadiene and dichlorophenylphosphine, upon treatment with t-BuLi yields 1-tert-butyl-3,4-dimethylphosphole[153]. This product on heating with Fe[Cp(CO)$_2$]$_2$ in xylene at 160$^\mathrm{o}$C forms the corresponding monophosphaferrocene which was then functionalized with a formyl group at the ortho position of phosphole ring by reacting it with POCl$_3$ and N-methyl-N-phenylformamide (Vilsmeyer reaction) in dichloromethane. Spectroscopic data of 2-formyl-3,4-dimethylmonophosphaferrocene **15** were identical with those reported in the literature[67].

---

[152] A. Breque, F. Mathey and P. Savignac, *Synthesis*. **1981**, 983-985.
[153] F. Mathey, *Tetrahedron*. **1972**, *28*, 4171-4181.

scheme 33: Synthesis of 2-formyl-3,4-dimethylmonophosphaferrocene **15**

Functionalization of HMS with 3-amino propyl tialkoxy silane

Calcined HMS was functionalized with 3-aminopropyltrialkoxysilane according to the literature report[154] **(scheme 34)**. HMS was refluxed with 3-aminopropyl trialkoxy silane in toluene for 24hrs. It was then filtered, washed with toluene in several portions and dried under vacuum. Organic loading of the materials was calculated from the results obtained from the elemantal analyses as 23 x 10^{-4} mol/g^{-1} and 22.6 x 10^{-4} mol/g^{-1} of the materials for APTESi-HMS and APTMS-HMS respectively. The surface areas of the materials were determined by measuring nitrogen isotherm at 77K. Calcined HMS has a BET surface area of 812 m^{2}g^{-1}. Upon surface functionalization of HMS with APTESi, a decrease in the HMS surface area to about 537 m^{2}g^{-1} was observed as expected[154]. The materials APTESi-HMS and APTMSi-HMS were further characterized by ^{13}C CP MAS NMR and ^{29}Si CP MAS/MAS NMR.

---

[154] A. R. Silva, K. Wilson, A. C. Whitwood, J. H. Clark and C. Freire, *Eur. J. Inorg. Chem.* **2006**, 1275-1283.
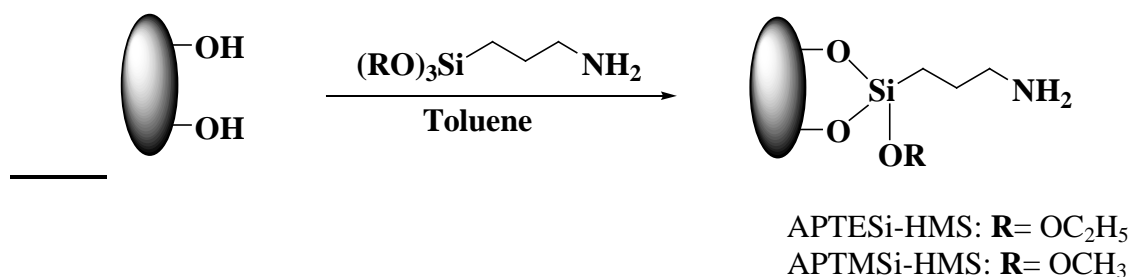
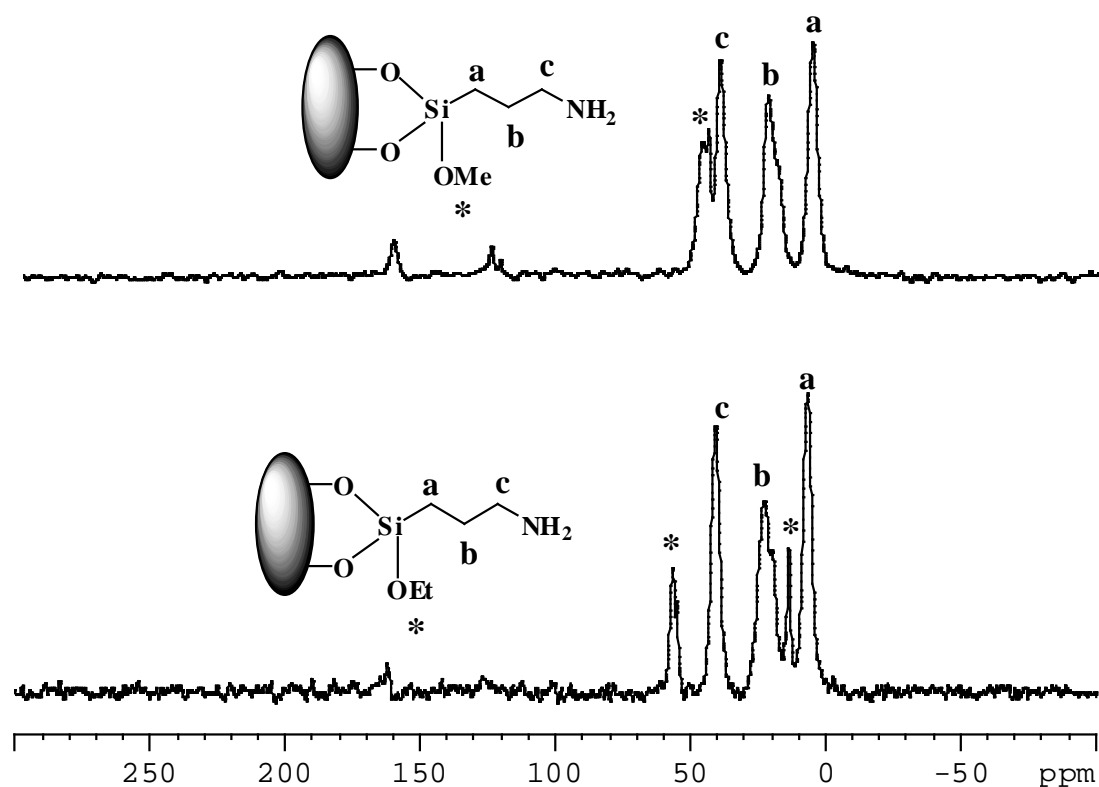**scheme 34:** Functionalization of HMS with 3-amino propyl trialkoxysilane

Fig 29: ^{13}C CP MAS NMR spectrum of APTESi-HMS, υ_{rot}: 8 kHz, ns: 4096, contact time: 1.8 ms, pulse delay: 5 s (bottom trace), APTMSi-HMS υ_{rot}: 8 k Hz, ns: 4096, contact time: 3 ms, pulse delay: 5 s (top trace); **a**, **b**, **c** and ✳ represent carbon atoms of n-propyl group and methoxy / ethoxy group respectively.

^{13}C CP MAS NMR spectrum of APTESi-HMS (**Fig 29**) showed resonances at 6.5, 22.8 and 40.7 ppm, which were attributed to -*CH$_2$*Si, (-CH$_2$)$_2$*CH$_2$* and -*CH$_2$*NH$_2$ carbon atoms of the aminopropyl group respectively. In addition, signals observed at 13.5 and 56.6 ppm were assigned to the ethoxy group bound to the silicon atom in the tether. ^{13}C CP MAS NMR (**Fig 29**) of APTMSi-HMS displayed chemical shifts at 8.1, 24.4 and 41.5 ppm for the three carbon atoms -*CH$_2$*Si, (-CH$_2$)$_2$*CH$_2$* and -*CH$_2$*NH$_2$ in the propyl chain. The signal at 48.4 ppm was assigned to the methoxy carbon attached to silicon in the tether. A less intense signal at 162 ppm in APTESi-HMS and APTMSi-HMS was corresponded to the carbonate salts on the silica surface. The relative signal intensities suggest that the products are best described by the structures shown in **Fig 29** which is formed by condensing two of the three alkoxy groups with surface –OH functions and represents the most frequently formed structural motif for immobilised trialkoxy silanes[155].

^{29}Si CP-MAS NMR (**Fig 30,** middle trace, **Table 5**) of APTESi-HMS gave resonances at –111 and –102 ppm which are assigned to Q^4 and Q^3 species of the silica framework

---

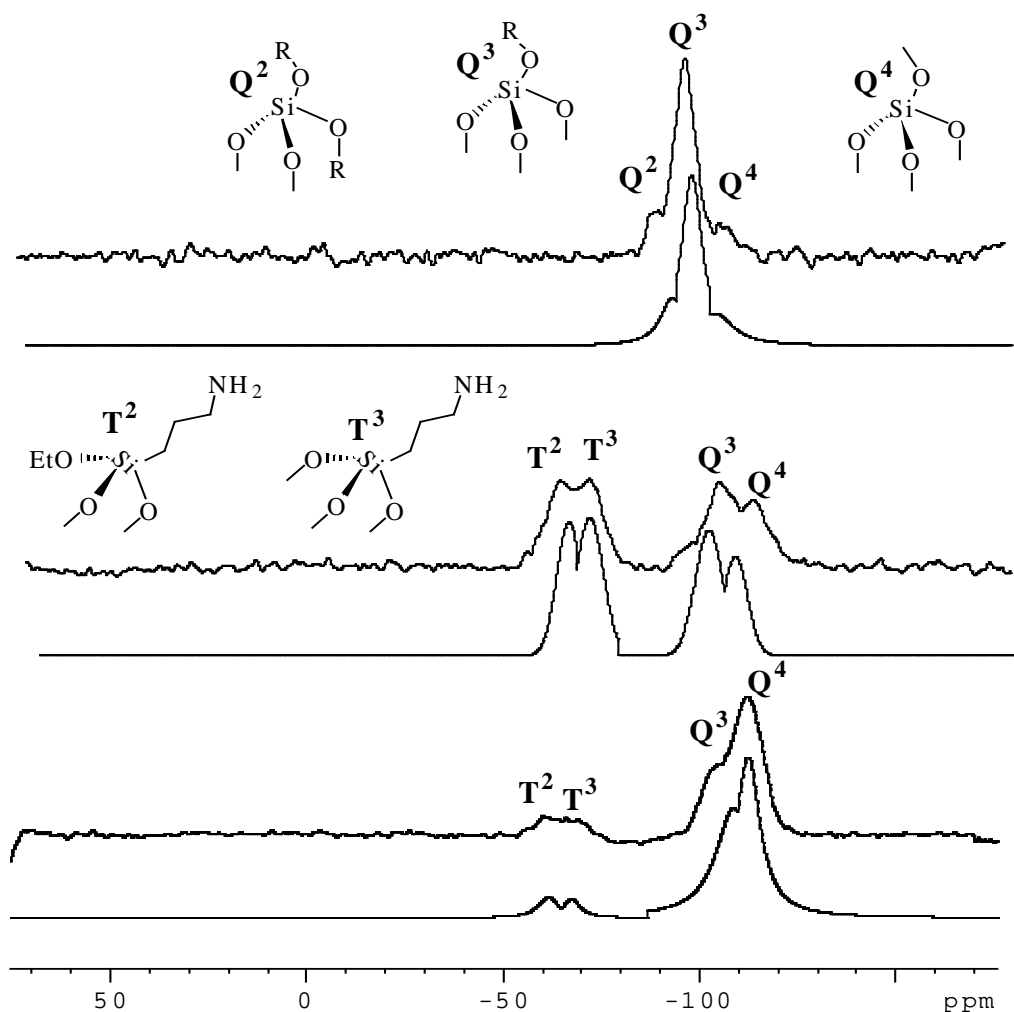[155] A. Tarafdar and P. Pramanik, *Microporus and mesoporous materials*. **2006**, 91, 221-224.

Fig 30: ^{29}Si MAS NMR spectra, υ_{rot}: 8 kHz, ns: 1536, pulse delay: 120 s (bottom trace) and CP MAS NMR, υ_{rot}: 8 kHz, ns: 3072, contact time: 0.8 ms, pulse delay: 7.5 s (middle trace) of APTESi-HMS and CP MAS NMR spectra, υ_{rot}: 9 kHz, ns: 3072, contact time: 1.4 ms, pulse delay: 7.5 s (top trace) of HMS.

$[Q^n=Si(OSi)_n(OH)_{4-n}]^{[155]}$. Q^4 sites correspond to bulk silicon nuclei with $Si(OSi)_4$ group and Q^3 sites are those associated with single Si-OH group that includes both free and hydrogen bonded silinols. Both type of silanes must be spatially close to the aminopropyl functions or remaining surface OH-groups. ^{29}Si CP MAS NMR of the unmodified HMS showed an additional weak signal attributable to Q^2 site besides the Q^4 and Q^3 sites, with Q^3 sites making the major contribution **(Fig 30,** top trace). Two additional bands as T^3 and T^2 observed at –69 and –60 ppm in ^{29}Si CP-MAS NMR of APTESi-HMS were attributed to grafted organosilane species $[T^m = RSi(OSi)_m(OEt)_{3-m}]$. A similar behaviour is normally observed in the organo functionalized MCM-41[123].

In ^{29}Si MAS NMR, connectivity between protons of propyl tether and any of the silicon nuclei in the bulk material was diminished. A ^{29}Si MAS NMR of APTESi-HMS showed increased relative intensities of Q^4 and Q^3 resonances of the silica frame-work as compared to the T^3 and T^2 bands (**Fig 30,** middle trace). However Q^4 and Q^3 have also different relative intensities with respect to each other. Crosspolarisation amplifies signals of Si close to hydrogen. The Si atoms in the bulk are not accessible to crosspolarisation as they are too remote. The real quantification is further not feasible due to the unknown influence of T_1. In the case of ^{13}C CP MAS of APTESi-HMS only one environment for propyl functionality was observed, while for ^{29}Si CP MAS NMR two environments are feasible. The reason could be that ^{13}C nuclei are more remote from framework Si atom in different environment, so δ ^{13}C is less sensitive to changes.

In APTMSi-HMS the bulk ^{29}Si CP MAS signals were observed at about –113 and –103 ppm (Q^4 and Q^3). The relative intensity of Q^4 is slightly larger than Q^3, while silane resonances in the tether being found at –67 and -61 ppm (T^3 and T^2) with T^2 has the major contribution (**Fig 31**, middle trace, **Table 5**). Increased intensity of T^2 sites could indicate that mostly only two of the three methoxy groups attached to the silicon atom in the tether have been consumed for bonding with the surface -OH functions.
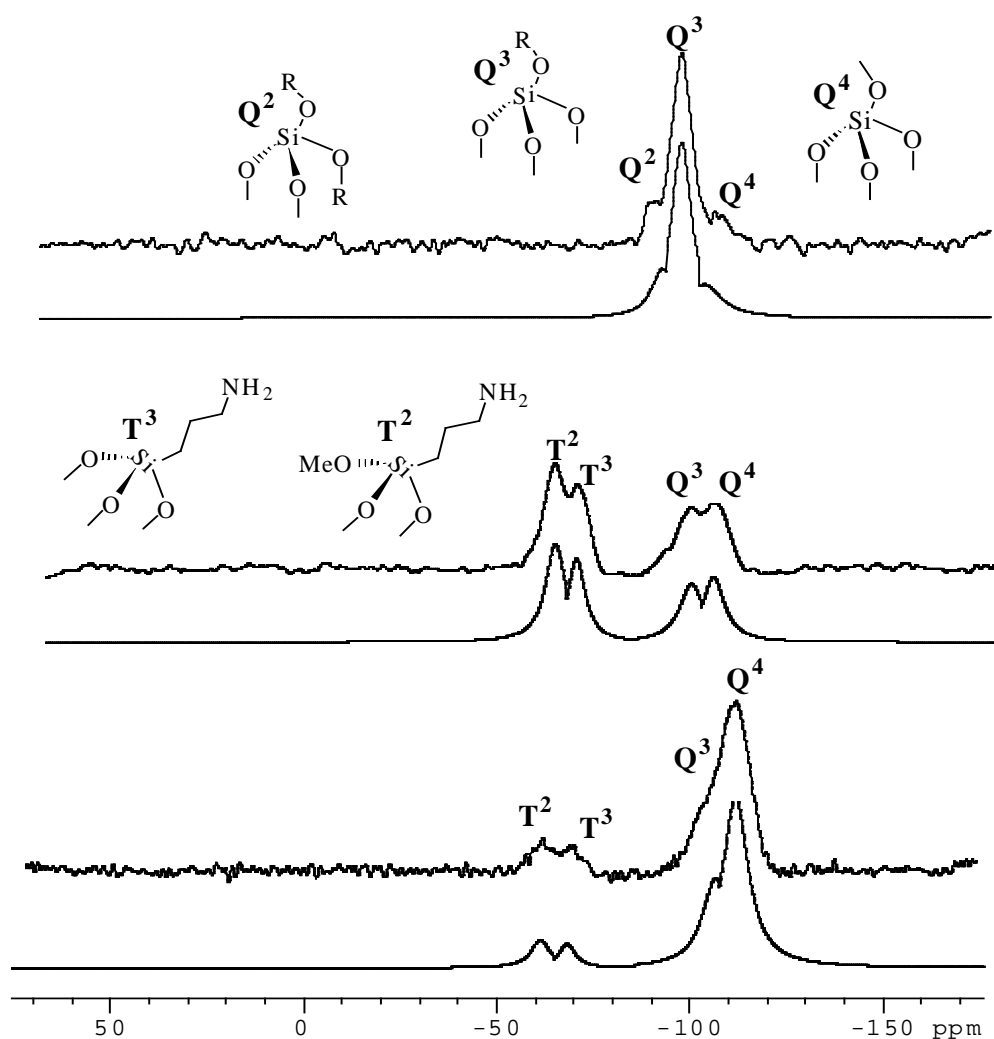
Fig 31: ^{29}Si MAS NMR , υ_{rot}: 8 kHz, ns: 2048, pulse delay: 120 s (bottom trace) and CP MAS NMR, υ_{rot}: 8 kHz, ns: 768, contact time: 1.8 ms, pulse delay: 7.5 s (middle trace) of APTMSi-HMS and CP MAS NMR spectra, υ_{rot}: 9 kHz, ns: 3072, contact time: 1.4 ms, pulse delay: 7.5 s (top trace) of HMS.

Table 5. ^{29}Si CP MAS NMR chemical shifts [ppm] of silica supports

Compound	Q^4	Q^3	Q^2	T^3	T^2
HMS	-110	-102	-93		
APTESi-HMS	-111	-102	-	-69	-60
APTMSi-HMS	-113	-103	-	-67	-61

Anchoring of monophosphaferrocene by Schiff condensation

The anchoring process of **15** onto APTESi-HMS was carried out by Schiff condensation between the free amino group, covalently attached to the HMS surface, with the carbonyl group of the ligand **15** in methanol. The anchored material obtained after filtering off the supernatant liquid was washed with methanol in several portions and dried under vacuum. ^{31}P CP MAS NMR spectrum recorded for the material at different rotational frequencies gave very weak signals. However, the ^{31}P HP Dec NMR showed a strong spinning side band manifold around an isotropic line at $\delta = -76$ ppm. ^{13}C CP MAS NMR analysis of the immobilised material has not given an adequate information to elucidate the structure of the immobilised species. Thus it was proposed to synthesise a relative homogenous compound by Schiff condensation with n-propylamine. For this purpose equivalent amount of **15** and n-propylamine was heated in methanol for 5 hrs **(scheme 35)**.
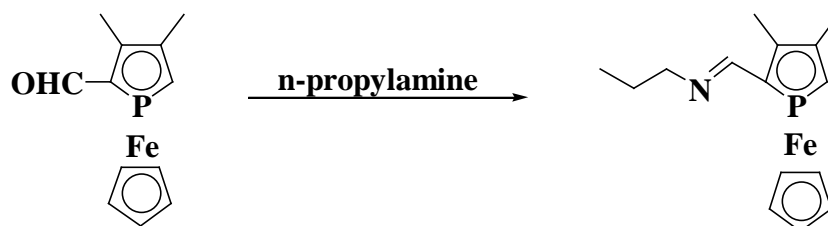

scheme 35: Schiff condensation of **15** with n-propylamine.

The reaction mixture gave only one ^{31}P NMR signal at -75 ppm. The structure of the product from the reaction mixture was confirmed by ^{1}H NMR analysis. The ^{1}H NMR spectrum of the compound displayed two distinct doublets at 8.17 ppm ($^{3}J_{HP} = 8.8$ Hz) and 3.95 ppm ($^{2}J_{HP} = 37.4$ Hz) corresponding to the protons of imino carbon and CH of phosphole ring. Cp protons observed as a singlet at 4.2 ppm. The two methyl groups of phosphole ring resonated at 2.21 and 2.31 ppm. Propyl protons were resonated at 0.89, 1.57 and 3.12 ppm respectively. All attempts to isolate the compound by column chromatography were not successful and led to the decomposition products along with the starting material.

Anchoring of monophosphaferrocene by one step reductive amination

As the anchoring of monophosphaferrocene by Schiff condensation has not come up with the expectation, it was proposed to carry out the anchoring of **15** onto APTESi-HMS and

APTMSi-HMS by one-step reductive amination between the free amino group on the silica surface and the formyl group of the ligand **15** with excess of mild reducing agent NaBH$_3$CN in methanol. The anchored materials [CpFePNH]/APTESi-HMS and [CpFePNH]/APTMSi-HMS obtained after filtering off the supernatant liquid, were washed with methanol in several portions and dried under vacuum (**scheme 36**).

[CpFePNH]/APTESi-HMS: R = OEt

[CpFePNH]/APTMSi-HMS: R = OMe
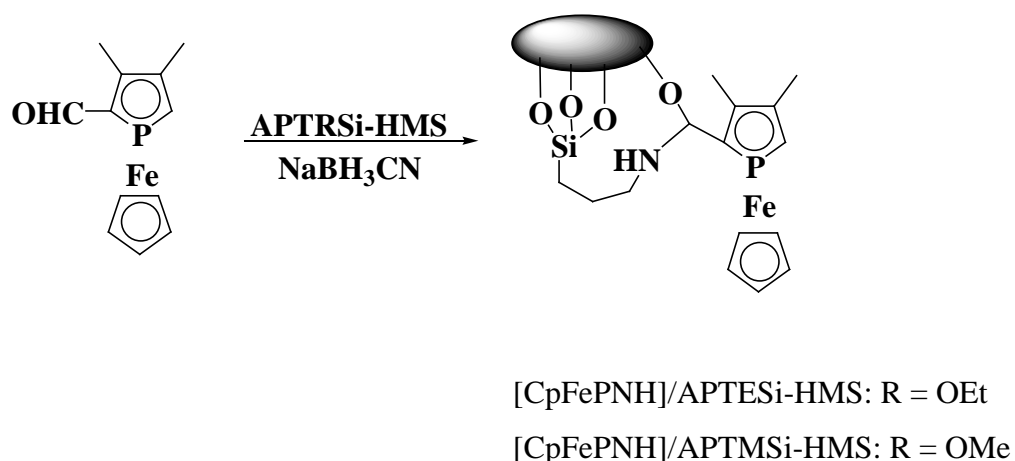
scheme 36: Anchoring of **15** onto APTESi-HMS/APTMSi by one step reductive amination.

Organic loading of the materials was calculated from the results obtained from the elemantal analyses as 25 x 10^{-4} mol/g^{-1} and 24 x 10^{-4} mol/g^{-1} of the materials for [CpFePNH]/APTESi-HMS. A further decrease was observed in BET surface area to 397 m^{2}g^{-1} in [CpFePNH]/APTESi-HMS as compared to that of APTESi-HMS and HMS having 537 and 812 m^{2}g^{-1}, respectively. A similar profile was also reported in the [Cu(acac)$_2$] immobilisation upon functionalized HMS structure[154]. To compare the immobilised monophosphaferrocene with homogenous system, one step reductive amination of **15** with 3-aminopropyl triethoxy silane was carried out in a similar condition as applied for immobilised monophosphaferrocene. ^{31}P{^{1}H} NMR spectrum of the reaction mixture displayed signals at -75.4 ppm and a less intense one at -76.1 ppm. All the attempts to isolate the compound was not successful. Thus it was adopted to develop the P/$\lor$N functionalized monophosphaferrocenes which lacks the trialkoxysilyl groups that may hamper the purification of the desired one. In this respect, benzylamine was selected which upon reductive amination with **15**, followed by hydrolysis yielded the respective P/$\lor$N ligand, **17** (**scheme 37**) in moderately good yield, which was characterized by routine analytical

techniques. $^{31}P\{^1H\}$ NMR spectrum displayed a single resonance at -76.5 ppm. ^1H NMR spectrum of the compound displayed two singlets at

16: R = $(CH_2)_3Si(OEt)_3$
17: R = $CH_2C_6H_5$
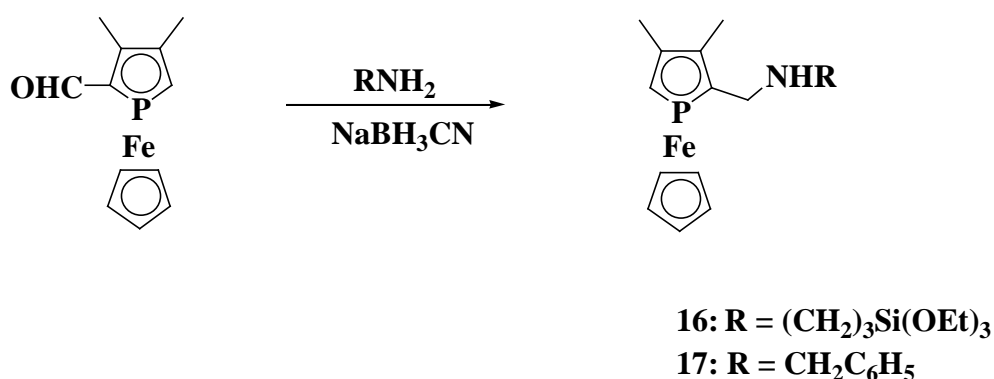
scheme 37: Synthesis of P/\/N derivatives of monophosphaferrocene

2.10 ppm and 2.17 ppm corresponding to two methyl groups of phospholyl ring. Doublet of doublet observed at 3.16 ppm ($^3J_{HP}$ = 13.5 Hz) was assigned to methylene protons. The peak at 3.63 ppm observed as a doublet ($^2J_{HP}$ = 37 Hz) was attributed to alpha proton with respect to phosphorus of phosphole ring. Cp protons were resonated as singlet at 4.06 ppm with the account of five protons. Protons of phenyl group were observed as multiplet at 7.21 - 7.35 ppm. In ^{13}C NMR spectrum, the doublets at 76.7 ($^1J_{CP}$ = 58.3 Hz) and 96.6 ppm ($^1J_{CP}$ = 58.9 Hz) were assigned for α-Cs and the doublets at 94.64 ($^2J_{CP}$ = 4.9 Hz) and 97.43 ppm ($^2J_{CP}$ = 6.8 Hz) were assigned for β-Cs with respect to phosphorus of phosphole ring. Cp carbons and methyl carbons were resonated as singlets at 73.01 ppm, and 13.8 and 17.3 ppm respectively. Further the structure of the compound was confirmed by mass spectrum. Electron ionization mass spectrum of the compound gave peak at m/e = 351 (M^+) corresponding to the molecular ion.

The ^{31}P HP Dec NMR **(Fig 32)** of [CpFePNH]/APTESi-HMS showed, a strong signal at –76 ppm with sideband manifolds.
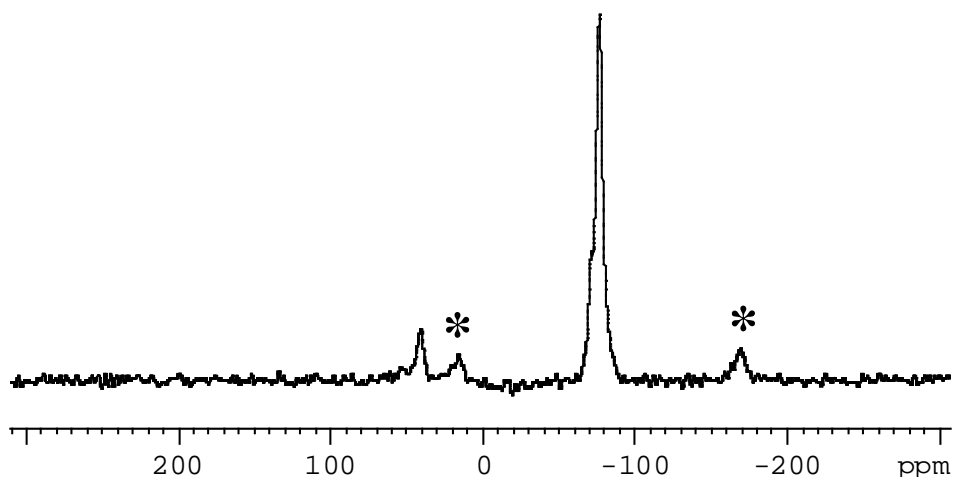
Fig 32: ^{31}P HP Dec MAS NMR spectrum of [CpFePNH]/APTESi-HMS, υ_{rot}: 15 kHz, ns: 1024, pulse delay: 5 s.

The isotropic line displayed a shoulder at the low field side indicating the presence of two different species with slightly different chemical environment. Deconvolution allowed to determine the chemical shifts of both sites as –76 and –72 ppm (relative intensity 12 : 3). Besides these signals a signal of less intensity centered around 40 ppm was also visible as in the case of the Schiff condensation. The signals at –76 ppm was attributed to immobilised monophosphaferrocene. As observed earlier there is an increase in half width of the signal upon immobilisation. The half width of [CpFePNH]/APTESi-HMS is found to be 2.7 k Hz while that of monophosphaferrocene is 0.9 k Hz.

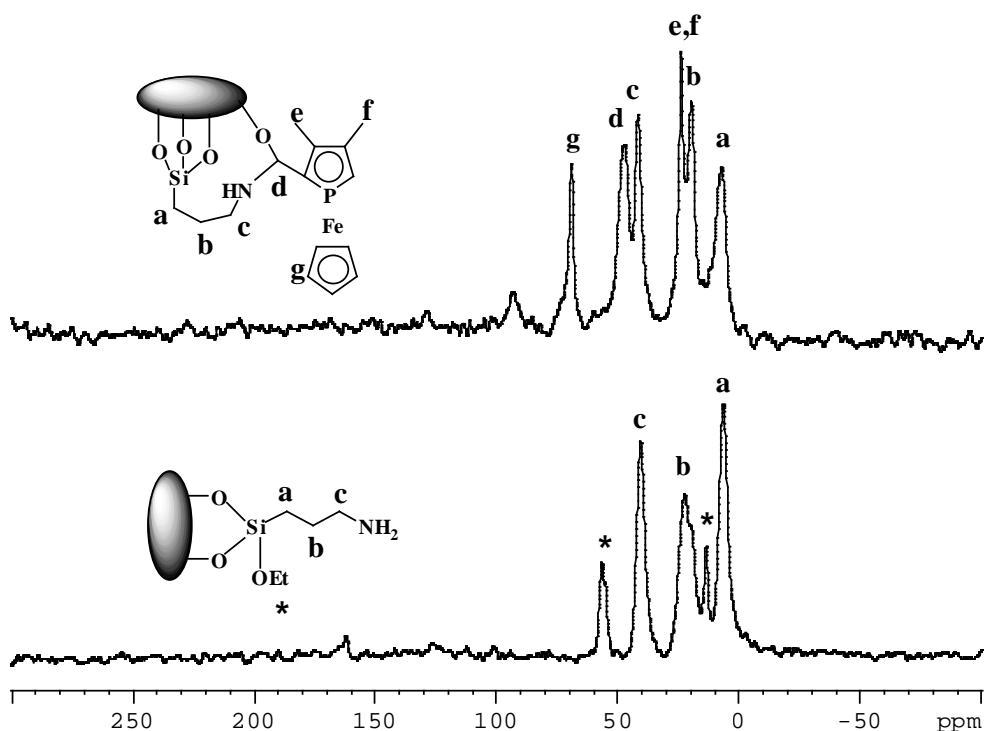**Fig 33:** ^{13}C CP MAS NMR spectra of APTESi-HMS, υ_{rot}: 8 kHz, ns: 4096, contact time: 1.8 ms, pulse delay: 5 s (bottom trace), [CpFePNH]/APTESi-HMS, υ_{rot}: 8 kHz, ns: 8192, contact time: 3 ms, pulse delay: 5 s (top trace); **a**, **b**, **c** and **✶** represent carbon atoms of n-propyl group and ethoxy group respectively; **d**, **e**, **f**, **g** represent carbon atoms of phosphaferrocene moeity.

The ^{13}C CP MAS NMR spectrum of [CpFePNH]/APTESi-HMS gave signals at 7.3, 19.9 and 42.3 ppm which were assigned to the carbon atoms of the propyl tether **(Fig 33).** A signal at 24.0 ppm were attributed to the methyl groups of phosphole ring. The signals at 69.6 and 93.6 ppm were assigned to the Cp ring carbons, and quaternery carbons and CH carbons of the phosphole ring respectively. While comparing with APTESi-HMS, signals of SiOEt groups are absent in [CpFePNH]/APTESi-HMS. But an additional strong signal was observed at 47.2 ppm. The appearance of this signal could be explained in a way that SiOEt groups had been cleaved during the reductive coupling reaction and thereby rendering two diastereomers. The possible mechanism of the reaction which is depicted in the **scheme 38** involves the nucleophilic attack of surface siloxide anion formed via the proton removal from the surface –OH group by BH_3CN^- at the silicon atom of SiOEt groups. Likewise the surface siloxide anion so formed could also undergo the nucleophilic attack at the electron defficient imino carbon formed during condensation giving rise to the chiral centre at the amino carbon atom.
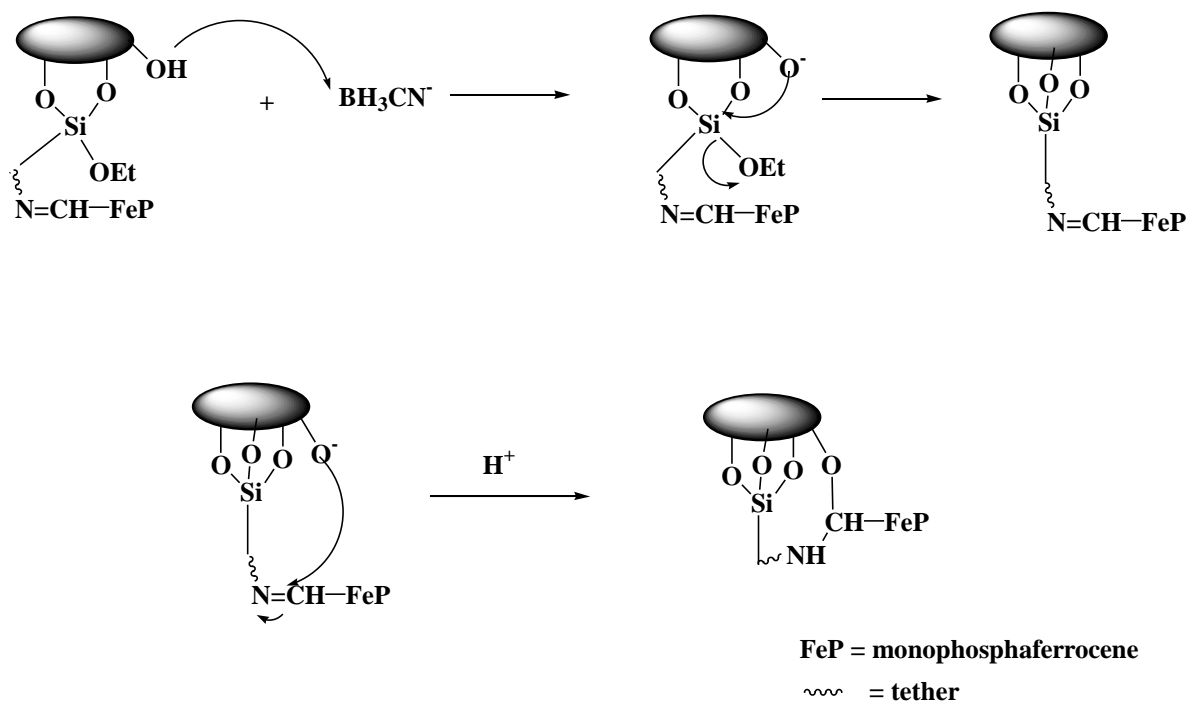
scheme 38: proposed mechanism for the immobilised monophosphaferrocene formation.

This could give an explanation for the observence of an additional ^{31}P signal with a shift of −72 ppm near to the major signal. Thus the two ^{31}P signals (with one minor and the other major) correspond to two diastreomeric forms of immobilised monophosphaferrocenes.

^{29}Si MAS NMR of the [CpFePNH]/APTESi-HMS gave broad Q^4 and Q^3 resonances at −113 and −104 ppm respectively accounting for the bulk silica framework. T^3 and T^2 bands resonated at −69 ppm and −62 ppm were assigned to phosphaferrocene grafted silane species with T^3 resonance contributing major system **(Fig 34)**. As observed in the case of APTESi-HMS the signal intensities of the bulk resonances (Q^4 and Q^3) in ^{29}Si CP MAS NMR of the
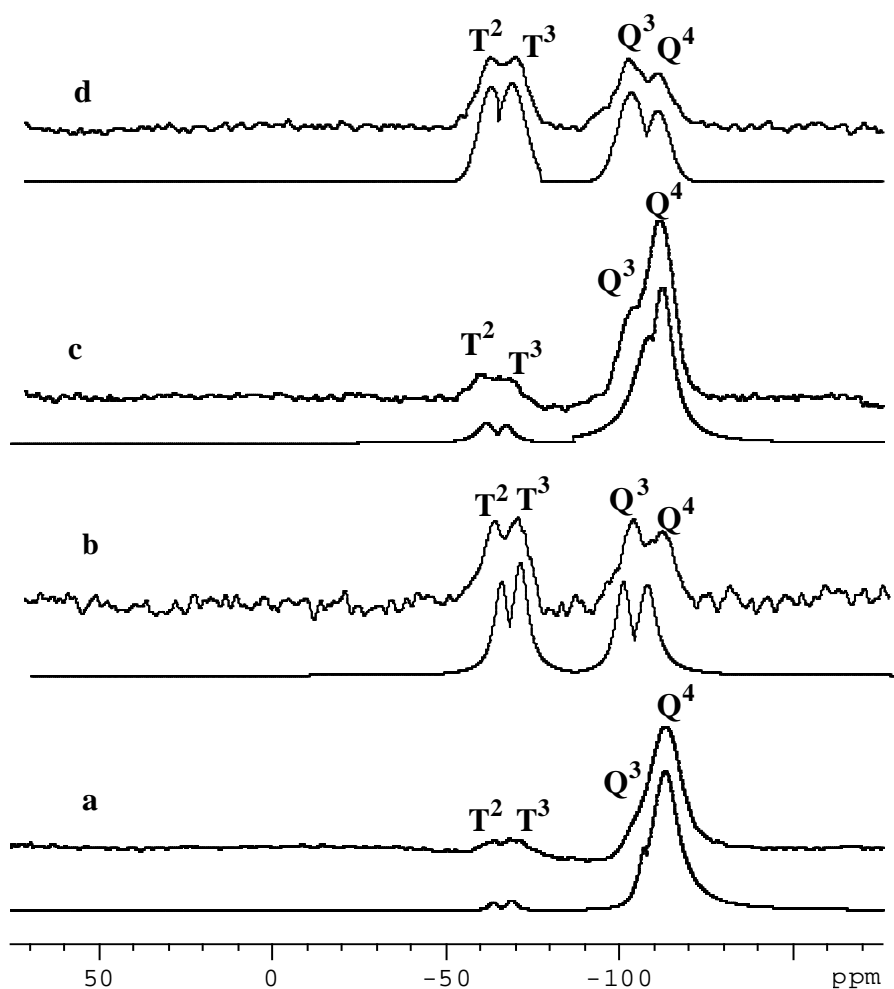
Fig 34: ^{29}Si MAS, υ_{rot}: 8 kHz, ns: 1536, pulse delay: 120 s and CP MAS NMR spectra, υ_{rot}: 8 kHz, ns: 3072, contact time: 0.8 ms, pulse delay: 7.5 s of APTESi-HMS, (**c** and **d**), **:** ^{29}Si MAS, υ_{rot}: 8 kHz, ns: 1536, pulse delay: 120 s and CP MAS NMR spectra, υ_{rot}: 8 kHz, ns: 2048, contact time: 1.8 ms, pulse delay: 7.5 s of [CpFePNH]/APTESi-HMS (**a** and **b**).

[CpFePNH]/APTESi-HMS were diminished with respect to the intensities of grafted silane resonances (T^3 and T^2) for the same reason as had been previously discussed. The similar values of resonances are also observed in MCM-41 functionalized 3-triethoxysilyl propyl ligands[156]. In contrast to the earlier observation, unexpectedly ^{31}P HP Dec NMR of monophosphaferrocene anchored APTMSi-HMS ([CpFePNH]/APTMSi-HMS) displayed a very strong resonance at 40 ppm corresponding to surface side product (major contribution) associated with weak signal at –78 ppm of the anchored monophosphaferrocene. This finding is corroborated with the view that the nature of alkoxy groups on the silane tether is persumably responsible for the unknown surface side product.

---

[156] G.Fan, S. Cheng, M. Zhu and X. Gao, *Appl. Organometal. Chem.* **2007**, *21*, 670-675.

6.2 Anchoring of monophosphaferrocene onto capped HMS

Monophosphaferrocene was also examined for anchoring onto capped HMS. In this contest, APTESi-HMS was first subjected to end capping with silylating agent[157,158] in order to remove the residual silanol groups on the surface of HMS. In addition, trimethylsilylation may also render the surface more hydrophobic and improve stability against moisture and mechanical compression.

Capping was done by treating APTESi-HMS with hexamethyldisilazane in toluene for 24hrs. After filtering off the supernatant liquid, the material was rinsed with toluene in several portions to get rid of any residual trace of hexamethyldisilazine **(scheme 39)**. The capping of residual silanol groups was monitored by ^{13}C CP MAS and ^{29}Si CP MAS NMR spectroscopy.
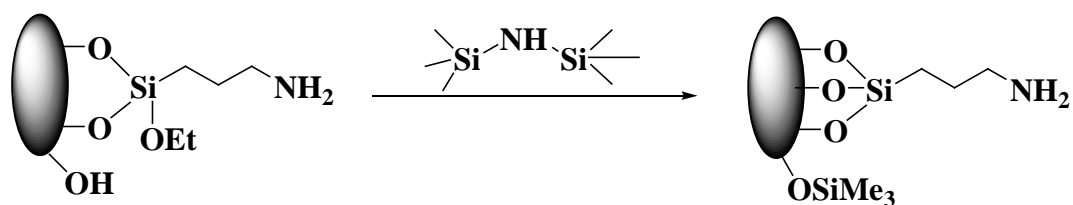
scheme 39: Capping of APTESi-HMS

^{13}C CP MAS NMR displayed a strong resonance at -2.4 ppm, which corresponds to capping trimethylsilyl groups **(Fig 35)**. The resonances at 7.7, 23.7 and 42.3 ppm corresponding to the carbon atoms of propyl tether indicated that functionality on the silica surface remained unchanged. These values are nearly similar to those found in APTESi-HMS. The signals of very low intensity at 13.8 and 56.2 ppm were corresponded to the ethoxy group which is bound to the silicon atom in the tether. The relative signal intensities suggest that the capped product is best described by a structure shown in **(Fig 35,** bottom trace**)** which is formed by condensing the three alkoxy groups with surface –OH functions and represents the most frequently formed structural motif for immobilised capped trialkoxy silanes[159].

[157] J. C. Hicks, R. Dabestani, A. C. Buchanan III and C. W. Jones, *Inorganic Chimia Acta*. **2008**, *361*, 3024-3032.
[158] M. W. McKittrick and C. W. Jones, *J. Am. Chem. Soc.* **2004**, *126*, 3052-3053.
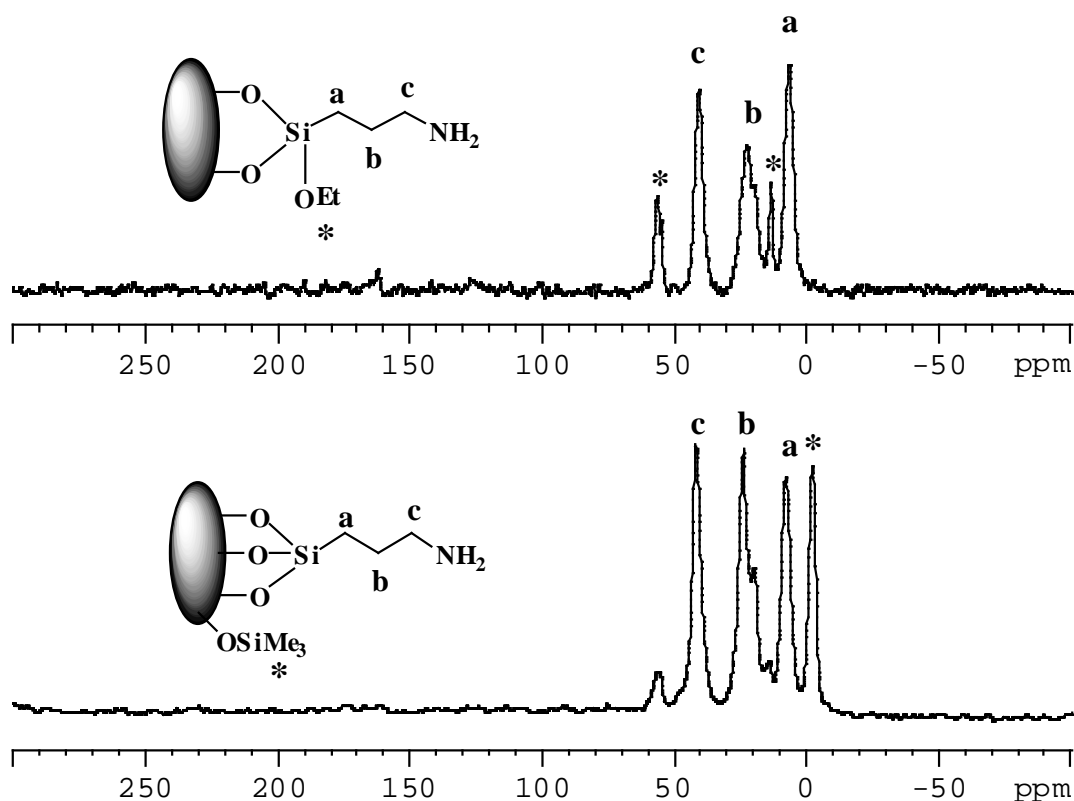[159] B. Buszweski , *Chromatographia*. **1989**, 28, 574-578.

Fig 35: ^{13}C CP MAS NMR spectra of capped APTESi-HMS, υ_{rot}: 5 kHz, ns: 8192, contact time: 1.8 ms, pulse delay: 5 s (bottom trace), APTESi-HMS, υ_{rot}: 8 kHz, ns: 4096, contact time: 1.8 ms, pulse delay: 5 s (top trace); **a**, **b**, **c** and ✷ represent carbon atoms of n-propyl group and ethoxy / trimethyl siloxy group respectively.

Capping of silanol group was further revealed by examining ^{29}Si CP MAS spectrum which exhibits a resonance at 8 ppm corresponding to trimethyl silyl group. The two signals were observed for the SiO_2 framework at -112 and -102 ppm, respectively corresponding to Q^4 and Q^3 sites with Q^4 species in slightly larger contribution. As compared to APTESi-HMS, the intensity of Q^3 sites get reduced **(Fig 36)**. This is in accordance with the partial $SiMe_3$ capping of silanol groups (Q^3 species)[159]. The ^{29}Si CP MAS NMR spectrum also showed signals attributable to T^3 and T^2 sites at -69 and -61 ppm, respectively. The intensity of the T^3 signal is found to be greater than that in APTESi-HMS. The increased intensity of T^3 sites upon capping is in accord with the fact that residual ethoxy groups attached to silicon atom in the tether has been consumed for forming bonds with the surface -OH functions.
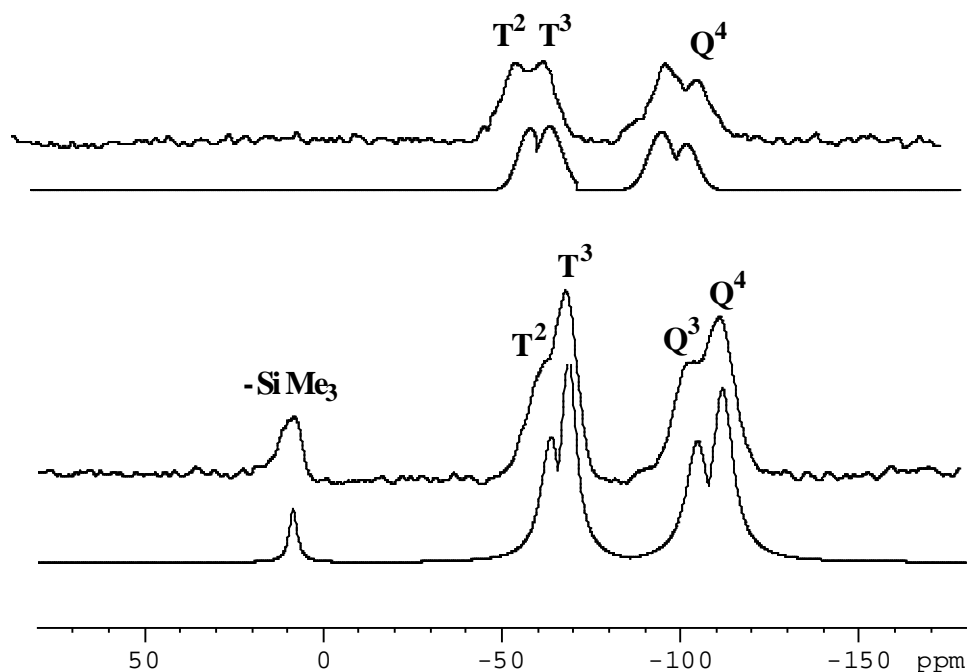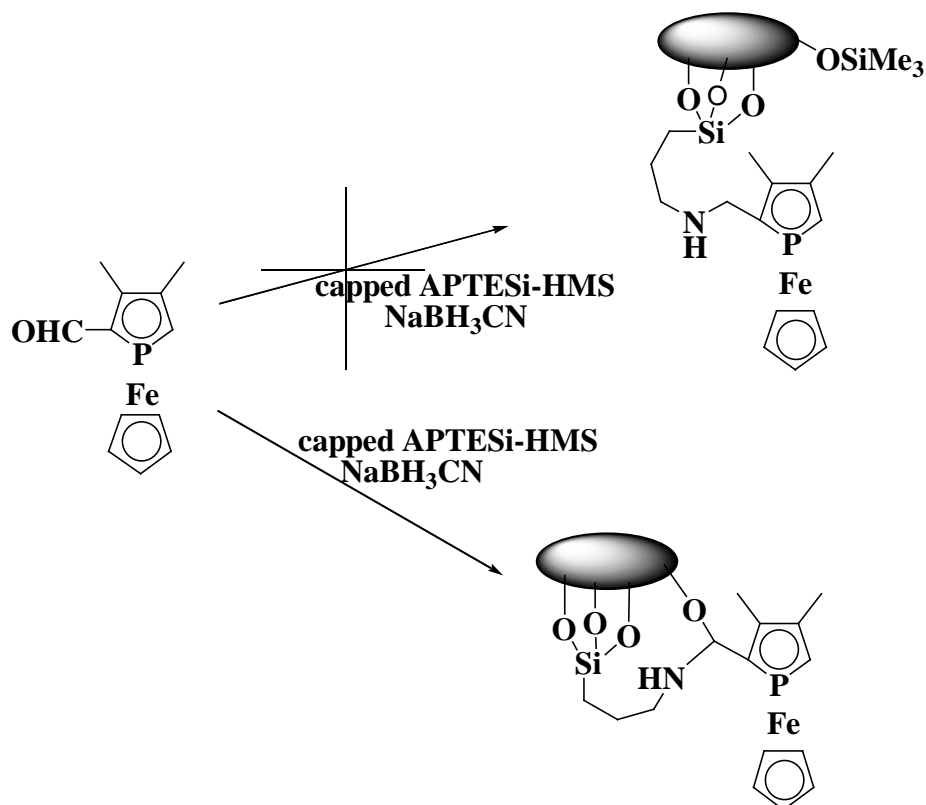
Fig 36: ^{29}Si CP MAS NMR spectra of capped APTESi-HMS, υ_{rot}: 8 kHz, ns: 3072, contact time: 4 ms, pulse delay: 7.5 s (bottom trace), APTESi-HMS, υ_{rot}: 8 kHz, ns: 3072, contact time: 0.8 ms, pulse delay: 7.5 s (top trace).

.

The capped APTESi-HMS was then subjected for anchoring monophosphaferrocene by single step reductive amination procedure **(scheme 40)**.

scheme 40: Anchoring of **15** onto capped APTESi-HMS by one step reductive amination.

The anchored material ([CpFePNH]/cappedAPTESi-HMS) was monitored by ^{31}P NMR, which displayed the same pair of signals at -76 and –72 ppm, as had been described before **(Fig 37)**.
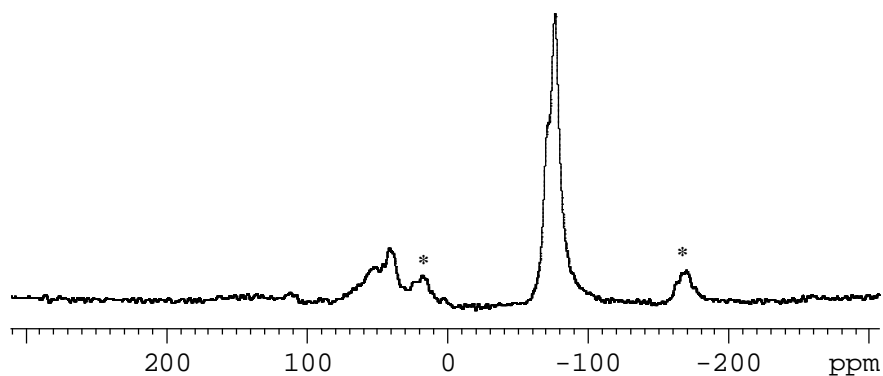

Fig 37: ^{31}P HP Dec MAS NMR of anchored monophosphaferrocene onto capped APTESi-HMS, υ_{rot}: 15 kHz, ns: 1024, pulse delay: 5 s.

A reduced intense side product centered around 40 ppm was seen here also. The half width of ^{31}P NMR signal of the major isomer is nearly the same as found in [CpFePNH]/ APTESi-HMS. Eventhough the spectroscopic characterization by ^{31}P NMR helped in revealing the anchoring of phosphaferrocene onto capped APTESi-HMS, it proved to be impossible to gather information whether the capping had remained intact during the immobilisation process or not. The ^{13}C CP MAS NMR of the material was measured and compared with that of [CpFePNH]/ APTESi-HMS **(Fig 38)**.
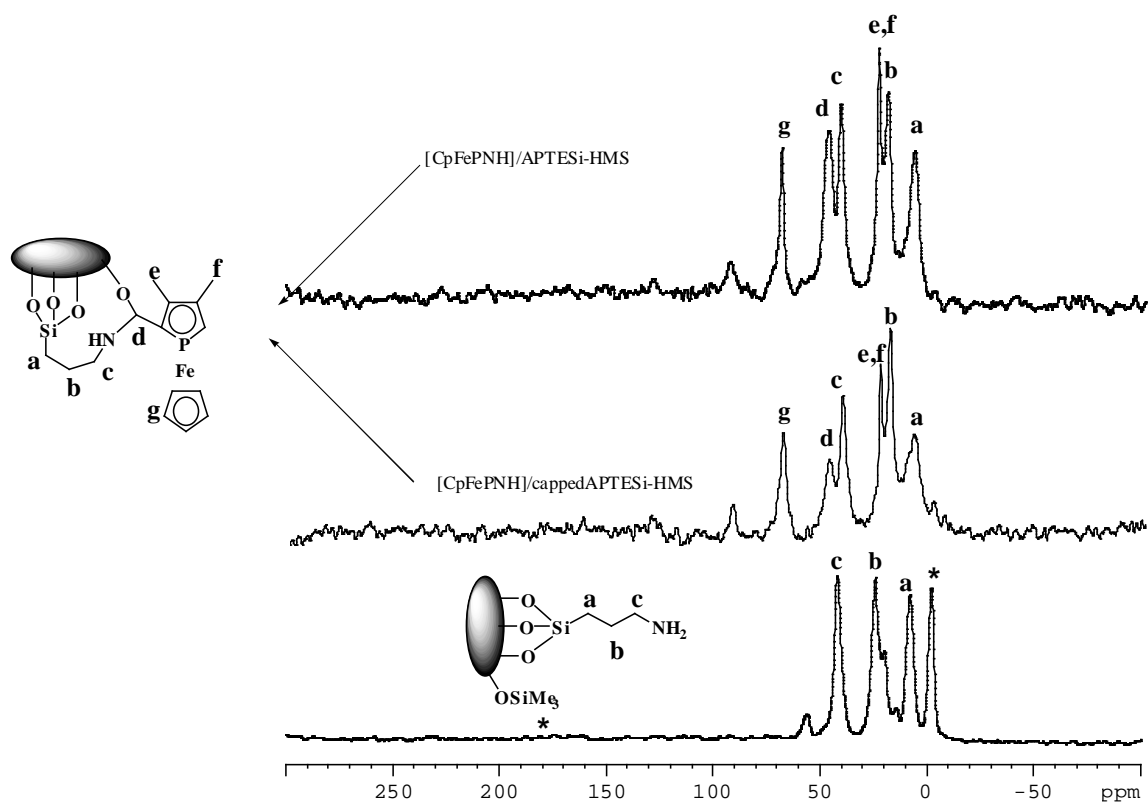
Fig 38: ^{13}C CP MAS NMR spectra of capped APTESi-HMS, υ_{rot}: 5 kHz, ns: 8192, contact time: 1.8 ms, pulse delay: 5 s (bottom trace), [CpFePNH]/ capped APTESi-HMS, υ_{rot}: 15 k Hz, ns: 12288, contact time: 3 ms, pulse delay (middle trace: 5 s [CpFePNH]/APTESi-HMS, υ_{rot}: 8 kHz, ns: 8192, contact time: 3 ms, pulse delay: 5 s (top trace); **a**, **b**, **c** and ✱ represent carbon atoms of n-propyl group and trimethyl silyloxy group respectively; **d**, **e**, **f**, **g** represent carbon atoms of phosphaferrocene moeity.

The absence of a signal corresponding to trimethyl silyl group in [CpFePNH]/cappedAPTESi-HMS revealed that end capping with trimethylsilyl group was no longer persisted in the immobilised material. The signals at 6.8, 19.5 and 41.5 ppm were assigned to the propyl chain. The signal at 47.6 ppm was assigned to the amino carbon. The resonance at 24.1 ppm was attributed to the methyl groups of phosphole ring. Cp ring and, quaternary and CH carbons were observed at 69.8 and 92.6 ppm respectively. Based on these results the anchored monophosphaferrocene is best described by the structure as shown in **(scheme 40).**

To conclude, monophosphaferrocene was attempted to immobilise via covalent tethering onto amino functionalized HMS materials by Schiff condensation. Solid state NMR studies have not given a satisfactory explanation for the anchoring process of the title compound. Thus the immobilisation of monophosphaferrocene onto modified HMS by reductive amination was carried out and, anchored material so obtained was studied and compared with the soluble

100

molecular reference compounds by NMR methods. The study revealed that monophosphaferrocene which was immobilised onto the silica surface exists in two diastereomeric forms. Further the anchoring process of monophosphaferrocene onto capped amino functionalized HMS was also investigated by solid state NMR methods and showed that here also gave a product with same characterestics as uncapped material and that the capping was removed during the immobilisation process.

7. Experimentals

7.1 General remarks

All manipulations were carried out under argon atmosphere and solvents were dried by standard procedures unless otherwise mentioned.

Chemicals

The following chemicals were synthesized according to the reported procedure:

Tris(trimethylsilyl) phosphine[160], Bis{[(3-diphenylphosphanyl)-methyl]-benzene-1,2-diol}palladiumdichloride **2**[97], Bis{[(3-diphenylphosphanyl)-methyl]-benzene-3,4-diol} palladiumdichloride **3**[97], AuCl(tht)[161], 1-Triethoxysilyl-3-chlorodimethylsilylpropane[107], 3,4-dimethyl-1-phenylphosphole[152], benzylideneacetophenone[108], 1-ter-butyl-3,4-dimethylphosphole[153], 3,4-dimethylmonophosphaferrocene[64], 2-formyl-3,4-dimethylmonophosphaferrocene[67], 4,5-dit-butyl-1,3,2-diazaphosphinine[44], 2,3,5,6-tetraphenyl phosphinine[44], hexagonal mesoporous silica[122].

All other chemicals were commercially available and purchased from Acros, Aldrich, Fluka, Merck, Strem.

Nuclear Magnetic Resonance Spectroscopy: Solution NMR spectra were recorded with a Bruker AV 250 spectrometer (^{1}H: 250.1 MHz, ^{13}C: 62.8 MHz, ^{31}P: 101.2 MHz, ^{29}Si: 79.49 MHz) or AV 400 spectrometer (^{13}C: 100.5 MHz, ^{31}P: 161.9 MHz, ^{29}Si: 79.49 MHz) at 303K. NMR spectra of solids or suspensions were recorded with a Bruker Avance 400 spectrometer (^{13}C: 100.5 MHz, ^{31}P: 161.9 MHz, ^{29}Si: 79.49 MHz) equipped with a 4 mm MAS probe. Solid samples were prepared in standard ZrO_2 rotors and suspensions in HR MAS rotors equipped with an additional tight PTFE spacer to prevent extrusion of the liquids. MAS experiments were carried out by using spinning speeds between 3 and 5 k Hz (solids) or 1.5 to 6 k Hz (suspensions). Cross-polarisation was applied using a ramp-shaped contact pulse

[160] G. Becker, H. Schimdt, G. Uhl, M. Regitz, W. Rösch and U. J. Vogelbacher, *Inorg. Synth.* **1990**, *27*, 243-253.
[161] R. Uson, A. Laguna and M. Laguna, *Inorg. Synth*, **1989**, *26*, 85.

and a mixing time between 3 and 5 ms if required. Measurements on nonspinning solid samples aiming at the observation of powder lineshape were made with a Hahn-echo pulse sequence. Experiments aiming at the selective observation of mobile species were carried out with the standard pulse sequence used to record $X\{^1H\}$ spectra in solution. It was found that superior line shapes were in these cases obtained if decoupling of ^1H was accomplished by using a WALTZ-sequence rather tha the high power CW – decoupling scheme normally applied for solid samples. Chemical shifts are referenced to ext. TMS (^1H, ^{13}C) or 85% H_3PO_4 ($\varXi$= 40.480747 MHz, ^{31}P).

Elemental Analysis: The C, H, N analyses were recorded on a Perkin-Elmer 240 CHSN/O.

EI- Mass Spectrometry: Varian MAT 711, EI, 70 eV

**ESI- Mass Spectrometry:** Bruker Daltonics-micrOTOF-Q.

Melting point: Melting points were recorded with a Buchi B-545 melting point apparatus.

Single Crystal X ray measurements: The Diffractometer Nonius Kappa CCD and Siemens P4 were used and the structure solutions and refinements were carried out using SHELXS, SHELXL, SHELXTL programmes.

BET measurements: The measurements were carried out with Micromeritics ASAP 2000 particle size analyzer.

7.2 Analytical data

1-Phenylacetenyldimethylsilyl-3-triethoxysilylpropane

$$C_6H_5 \equiv\!\!-\!\!\underset{|}{\overset{|}{Si}}\diagdown\diagup\diagdown Si(OEt)_3$$
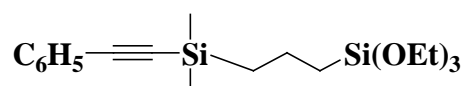
n-BuLi (2.3 mL, 5.8 mmol, 2.5 M solution in hexane) was added dropwise to a stirred solution of phenyl acetylene (0.63 mL, 5.77 mmol) in thf at –78°C. Phenyl lithium acetylide so formed was added dropwise to the solution of 1-triethoxysilyl-3-chlorodimethylsilylpropane (1.5 mL, 5.775 mmol) at –78°C. After addition the resulting mixture was allowed to stir at room temperature for 16 hrs. The solvent was then evacuated in vacuum. Dichloromethane (15 mL) was added, stirred and filtered to remove the precipitated lithium chloride. The mixture was concentrated to obtain a brownish yelow oil which was used for subsequent reactions without further purification.

Yield: 1.6 g, 78%.

^{1}H NMR (CDCl$_3$): δ (ppm) = 0.01 (s, 6H, Si(CH$_3$)$_2$), 0.65 (m, 4H, Me$_2$Si*CH$_2$*CH$_2$*CH$_2$*Si(OEt)$_3$), 1.15 (t, ^{3}J$_{HH}$ = 7.2 Hz , 9H, Si(OCH$_2$*CH$_3$*)$_3$), 1.6(m, 2H, Me$_2$SiCH$_2$*CH$_2$*CH$_2$Si(OEt)$_3$), 3.7 (q, ^{3}J$_{HH}$ = 8.1 Hz , 6H, Si(O*CH$_2$*CH$_3$)$_3$), 7.15 - 7.2 (m, 2H, Arom-H), 7.35 - 7.41(m, 3H, Arom-H).

^{13}C NMR (CDCl$_3$): δ (ppm) = 1.2 (2C, Me$_2$Si), 14.89 (Me$_2$Si*CH$_2$*CH$_2$CH$_2$Si(OEt)$_3$), 17.85 (Me$_2$SiCH$_2$*CH$_2$*CH$_2$Si(OEt)$_3$), 18.65 (3C, Si(OCH$_2$*CH$_3$*)$_3$), 20.58 (Me$_2$SiCH$_2$CH$_2$*CH$_2$*Si(OEt)$_3$), 58.65 (3C, Si(O*CH$_2$*CH$_3$)$_3$), 93.75 (PhC*C*Si), 106.03 (Ph*C*CSi), 123.59 (arom-C), 128.50 (2C, arom-C)), 132.29 (arom-C).

MS (EI =70eV): *m/e* (%) = 364.2 (M$^+$).

## 3,5-Diphenyl-2-dimethyl (3'-triethoxysilyl propyl) silyl phosphinine
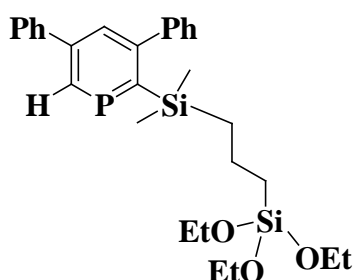
A solution of 4,5-dit-butyl-1,3,2-diazaphosphinine (0.54 mmol) and 1-phenylacetenyl dimethylsilyl-3-triethoxysilylpropane (0.2 g, 0.54 mmol) in toluene (5 mL) was heated at 100°C for four hrs. The reaction was monitored by ^{31}P NMR spectroscopy. After the solution was cooled to room temperature, phenyl acetylene (0.2 g, 2 mmol) was added and the reaction mixture was heated further at 100°C for 4 hrs. The completion of the reaction was checked by ^{31}P NMR. After the evaporation of the solvent, the yellow oil so obtained was subjected to flash column chromatography on silica using hexane: toluene (2 : 8) mixture to give a mixture of isomers.

^{31}P{^{1}H} NMR (C$_6$D$_6$): δ (ppm) = 240 (major isomer), 232, 208 and 201 (minor isomers).

^{1}H NMR (C$_6$D$_6$) of major isomer: 0.15 (m, CH_2Si(CH$_3$)$_2$), 0.23 (d, J$_{HH}$ = 1.4Hz, Si(CH_3)$_2$), 0.84 (t, Si(OCH$_2$$CH_3$)$_3$), 1.7 (m, CH$_2$$CH_2CH_2$Si(OCH$_2CH_3$)$_3$), 1.73 (m, CH_2Si(OCH$_2CH_3$)$_3$), 3.81 (q, Si(OCH_2CH$_3$)$_3$), 7.10 - 7.24 (m, 6H, arom H), 7.28 - 7.41 (m, 4H, arom H), 7.56 (m, 1H, arom H), 8.86 (dd, ^{2}J$_{HP}$ = 37.5 Hz, ^{4}J$_{HH}$ = 1.5 Hz, 1H, arom H).

^{29}Si{^{1}H} NMR (C$_6$D$_6$) of major isomer: -2.5 (Si(CH$_3$)$_2$), -46.5 (Si(OCH$_2$CH$_3$)$_3$.

Benzylidene-3,4-dimethoxyacetophenone
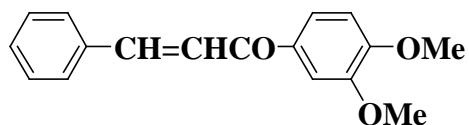
2.2 g of sodium hydroxide was dissolved in 20 mL of water. To this, 12 mL of EtOH was added. 7.2 g (0.04 mol) of 3,4-dimethoxyacetophenone, followed by 4.16 g (0.04 mol) of benzaldehyde was added at 0°C. The reaction mixture was stirred at RT for 4hrs. It was then poured into petroleum ether (50 mL) with vigorous stirring. The yellow solid separated out was washed with water until neutrality and dried. The crude product was used for further reaction.

Yield: 8.8g, 82%; m.p: 72°C.

Elemental Analysis: calcd (%) for $C_{17}H_{16}O_3$ (268.32): C 76.11, H 5.97; found C 75.85, H 6.05.

^{1}H NMR (CDCl$_3$): δ (ppm) = 3.94 (s, 3H, -OCH$_3$), 3.95 (s, 3H, -OCH$_3$), 6.89 (d, $^3J_{HH}$ = 8.3 Hz, 1H, arom-H), 7.37-7.41 (m, 3H, arom-H), 7.49 (d, $^3J_{HH}$ = 15.6Hz, 1H, =CHPh), 7.60-7.68 (m, 4H, arom-H), 7.75 (d, $^3J_{HH}$ = 15.7Hz, 1H, =CHCO).

^{13}C{^{1}H} NMR (CDCl$_3$): δ(ppm) = 56.02 (-OCH$_3$), 56.05 (-OCH$_3$), 109.98, 110.91, 121.72, 122.97, 128.31, 128.88, 130.30, 131.28, 135.17, 143.94, 149.30, 153.30 (arom-C, Vinyl-C), 188.57 (-CO).

MS (ESI): *m/e* **(%)** = 268.1 (100) [M]$^+$.

2,3-Dimethoxybenzylidene acetophenone
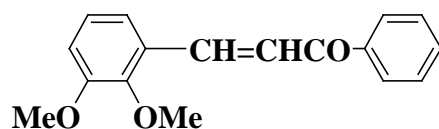
3.3 g of sodium hydroxide was dissolved in 30 mL of water. To this 18.3 mL of EtOH was added. 7.2 g (0.04 mol) of acetophenone, followed by 8.28 g (0.04 mol) of 2,3-dimethoxy benzaldehyde was added to the reaction mixture at 0°C. The reaction mixture was stirred at RT for 4 hrs. It was then poured into petroleum ether (50 mL) with vigorous stirring. The yellow oil separated out was washed with water until neutrality and dried. The crude product was used for further reaction.

Yield: 9.0 g, 84%.

^{1}H NMR (CDCl$_3$): δ (ppm) = 3.82 (s, 3H, -OCH$_3$), 3.84 (s, 3H, -OCH$_3$), 6.90 (d, $^3J_{HH}$ = 7.9 Hz, 1H, =CHPh), 7.04 (t, 1H, arom-H), 7.22 (d, $^3J_{HH}$ = 7.9 Hz, 1H, =CHCO-), 7.41-7.59 (m, 4H, arom-H), 7.97-8.11 (m, 3H, arom-H).

$^{13}C\{^1H\}$ NMR (CDCl$_3$): δ (ppm) = 56.00 (-OCH$_3$), 61.60 (-OCH$_3$), 114.70, 119.59, 123.52, 124.16, 128.23, 128.48, 128.54, 129.07, 132.65, 138.28, 139.59, 148.95, 153.19 (arom-C, vinyl-C), 190.71 (-CO).

MS (ESI): *m/e* (%) = 268.1 (10) [M$^+$], 237.1(100) [M-2Me]$^+$.

General Procedure for the synthesis of aryl pyrylium salts[34]

Tetrafluroboric acid (52% ethereal solution, 2.2 equiv) was added dropwise at 70°C to a solution of corresponding chalcone derivative (2.2 eqiv) and acetyl derivative (1 eqiv) in 1,2-dichloroethane (50 mL). The reaction mixture was refluxed for 6 hrs, it was then allowed to cool to RT; followed by the addition of a threefold amount of ether. The solid which was seperated out was washed with diethyl ether and dried under vacuum.

2-(3',4'-Dimethoxyphenyl)-4,6-diphenyltetrafluroborate
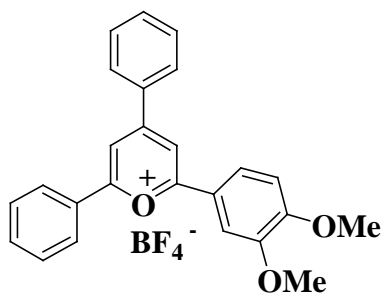
The pyrylium salt was obtained as orange solid from benzylidene acetophenone (12.96 g, 62.3 mmol), 3,4-dimethoxyacetophenone (5.61 g, 31.15 mmol) and tetrafluroboric acid(52% ethereal solution, 8.3 mL, 62.30 mmol).

Yield: 8.2 g , 58%; **m.p:** 248°C.

Elemental Analysis: calcd (%) for C$_{25}$H$_{21}$O$_3$B$_1$F$_4$ (456.25): C 65.81, H 4.64; found C 65.81, H 4.32.

^{1}H NMR (CD$_3$COCD$_3$): δ (ppm) = 4.03 (s, -OCH$_3$, 3H), 4.04 (s, -OCH$_3$, 3H), 7.35 (d, J$_{HH}$ = 8.7 Hz, 1H), 7.72-7.86 (m, 6H), 8.06 (d, J$_{HH}$ = 2.1 Hz, 1H), 8.32 (dd, J$_{HH}$ = 8.5 Hz, 2.3 Hz,

1H), 8.44-8.48 (m, 2H), 8.54-8.58 (m, 2H), 8.97 (d, J_{HH} = 1.6 Hz, 1H), 9.00 (d, J_{HH} = 1.6 Hz, 1H).

^{13}C{^{1}H} NMR (CD$_3$COCD$_3$): δ (ppm) = 56.76 (-OCH$_3$), 56.81 (-OCH$_3$), 111.91, 113.37, 115.03, 115.62, 122.29, 125.45, 129.34 (2C), 130.40 (2C), 130.43, 130.82 (2C), 130.85 (2C), 134.20, 135.59 (2C), 151.35, 157.39, 166.12, 170.53, 172.19.

MS (ESI): *m/e* (%) = 369.15 (100) [M-BF$_4$]$^+$.

2,6-Di(3',4'-dimethoxy phenyl)-4-phenyl pyrylium tetrafluroborate
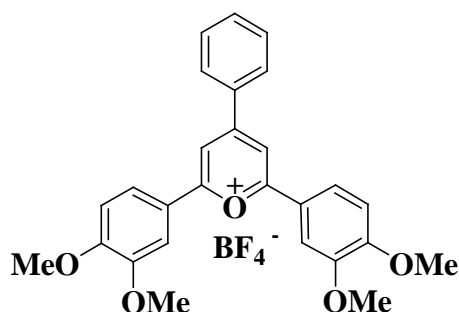
The pyrylium salt was obtained as red solid from benzylidene-3,4-dimethoxyacetophenone (9.18 g, 34.24 mmol), 3,4-dimethoxyacetophenone (3.08 g, 17.12 mmol) and tetrafluroboric acid (52% ethereal solution, 4.6 mL, 34.24 mmol).

Yield: 4.27 g, 47%; **m.p:** 185.2^{o}C.

Elemental Analysis: calcd (%) for C$_{27}$H$_{25}$O$_5$B$_1$F$_4$ (516.31): C 62.81, H 4.88; found C 62.73, H 4.48.

^{1}H NMR (CD$_3$COCD$_3$): δ (ppm) = 4.03 (s, 6H, 2 x -OCH$_3$), 4.04 (s, 6H, 2 x -OCH$_3$), 7.34 (d, J_{HH} = 8.7 Hz, 2H), 7.70 - 7.86 (m, 3H), 8.03 (d, J_{HH} = 2.2 Hz, 2H), 8.24 (dd, $J_{H,H}$ = 8.6 Hz, $J_{H,H}$ = 2.2 Hz, 2H), 8.35 - 8.39 (m, 2H), 8.86 (s, 2H).

^{13}C{^{1}H} NMR (CD$_3$COCD$_3$): δ (ppm) = 55.72 (2 x -OCH$_3$), 55.85 (2 x -OCH$_3$), 110.58, 112.40, 113.31, 120.92, 121.54, 123.90, 125.81, 126.58, 127.04, 127.04 127.42, 127.80, 127.86, 128.55, 128.77, 129.01, 129.33, 129.86, 134.29, 150.36, 155.96, 164.21, 169.90.

MS(ESI): *m/e* **(%)** = 429.17 (100) [M-BF$_4$]$^+$.

4-(2',3'-Dimethoxyphenyl)-2,6-diphenyl pyrylium tetrafluroborate
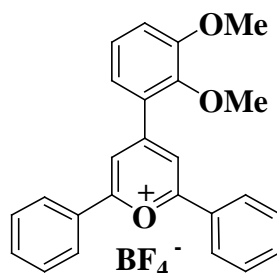
The pyrylium salt was obtained as dark orange solid from 2,3-dimethoxy benzylidene acetophenone (10.53 g, 38.8 mmol), acetophenone (2.16 mL, 19.4 mmol) and tetrafluroboric acid (52% ethereal solution, 5.3 mL, 38.8 mmol).

Yield: 4.9 g, 56%; **m.p:** 183°C.

Elemental Analysis: calcd (%) for C$_{25}$H$_{21}$O$_3$B$_1$F$_4$ (456.25): C 65.81, H 4.64; found C 64.42, H 4.52.

^{1}H NMR (CD$_3$C0CD$_3$): δ (ppm) = 3.95 (s, -OCH$_3$), 4.02 (s, -OCH$_3$), 7.40 (d, J$_{HH}$ = 8.0 Hz, 1H), 7.49 (dd, J$_{HH}$ = 8.1 Hz, 1.4 Hz, 1H), 7.62 (dd, J$_{HH}$ = 7.8 Hz, 1.6 Hz, 1H), 7.78 - 7.93 (m, 7H), 8.56 - 8.61 (m, 5H).

^{13}C{^{1}H} NMR (CD$_3$COCD$_3$): δ(ppm) = 56.90 (-OCH$_3$), 62.3 (-OCH$_3$), 119.51 (2C), 119.54 (2C), 123.40, 126.10, 129.09, 129.61 (4C), 130.28, 131.01 (4C), 136.10 (2C), 149.74, 154.47, 166.98, 171.65 (2C).

MS(EI = 70eV): *m/e* **(%)** = 369.1 (100) [M-BF$_4$]$^+$.

2-(3'-Methoxyphenyl)-4,6-diphenyl pyrylium tetrafluroborate
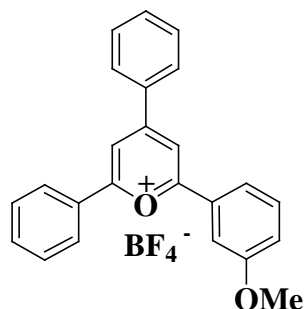
The pyrylium salt was obtained as dark orange solid from benzylidene acetophenone (9.09 g, 43.69 mmol), 3-methoxy acetophenone (3.27 g, 21.84 mmol) and tetrafluroboric acid (52% ethereal solution, 5.9 mL, 43.69 mmol).

Yield: 4.6 g, 60%**; m.p:** 182°C.

Elemental Analysis: calcd (%) for $C_{24}H_{19}O_2B_1F_4$ (426.23): C 67.63, H 4.49; found C 66.52, H 4.41.

Spectral data are identical with those reported in the litetraure[48].

General procedure for the synthesis of methoxy functionalized phosphinines:

The corresponding pyrylium salt (1 equiv) was dissolved in acetonitrile, and tris(trimethylsilyl)phosphine (2.5 equiv) was added dropwise at RT. The resulting black colored solution was heated at 80°C for 5 hrs. The formation of product was confirmed by ^{31}P NMR spectroscopy. After cooling to room temperature, the solvent was removed under vacuum. The residue was dissolved in CH_2Cl_2 and an appropriate amount of silica gel was added. The solvent was evaporated, followed by flash chromatography with petroleum ether\ethyl acetate (18.5:1.5) to give the corresponding phosphinine as pale yellow - yellow solid.

2-(3',4'-Dimethoxyphenyl)-4,6-diphenyl phosphinine
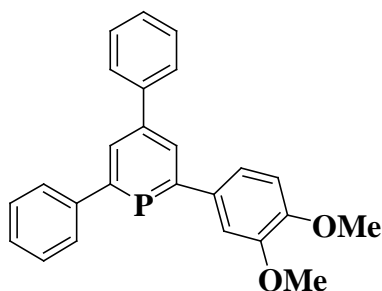
Phosphinine was obtained as yellow solid from corresponding pyrylium salt (3.38 g, 7.2 mmol) and tris(trimethylsilyl)phosphine (4.42 g, 18.09 mmol) in acetonitrile (25 mL).

Yield: 0.87g (32%); **m.p:** 147°C.

Elemental Analysis: calcd (%) for $C_{25}H_{21}O_2P_1$ (384.41): calcd. C 78.11, H 5.51; found. C 78.11, H 5.62.

^{31}**P{^{1}H} NMR (C$_6$D$_6$):** δ = 182.3 ppm.

^{1}**H NMR (C$_6$D$_6$):** δ (ppm) = 3.41 (s, -OCH$_3$, 3H), 3.44 (s, -OCH$_3$, 3H), 6.6 (d, $^3J_{HH}$ = 8.2 Hz, 1H), 7.18 - 7.36 (m, 8H), 7.45 - 7.50 (m, 2H), 7.71 - 7.74 (m, 2H), 8.11 (dd, $^3J_{HP}$ = 5.9 Hz, $^4J_{HH}$ = 1.1 Hz, 1H), 8.21 (dd, $^3J_{HP}$ = 5.8 Hz, $^4J_{HH}$ = 1.2 Hz, 1H).

^{13}**C{^{1}H} NMR (C$_6$D$_6$):** δ (ppm) = 55.47 (-OCH$_3$), 55.50 (-OCH$_3$), 111.97 (d, $^3J_{CP}$ = 13.4 Hz), 112.64, 120.11 (d, $^3J_{CP}$ = 13.4 Hz), 125.48, 127.94, 127.97, 128.05, 128.13, 128.34, 129.02 (2C), 129.05 (2C), 129.11, 131.39 (d, $^2J_{CP}$ = 11.4 Hz, C3/5), 131.63 (d, $^2J_{CP}$ = 11.3 Hz, C3/5), 136.50 (d, $^2J_{CP}$ = 24.7 Hz, C-α of Ph), 142.65 (d, $^3J_{CP}$ = 3.2 Hz, C4), 143.69 (d, $^2J_{CP}$ = 24.5 Hz, C-α of Ph), 144.33 (d, $^3J_{CP}$ = 13.9 Hz), 150.51, 171.91 (d, $^1J_{CP}$ = 52.5 Hz, C2/C6), 172.14 (d, $^1J_{CP}$ = 52.1, C2/C6).

MS (EI = 70eV): *m/e* **(%)** = 384.1 (100) [M]$^+$.

2,6-Di(3',4'-dimethoxy phenyl)-4-phenylphosphinine
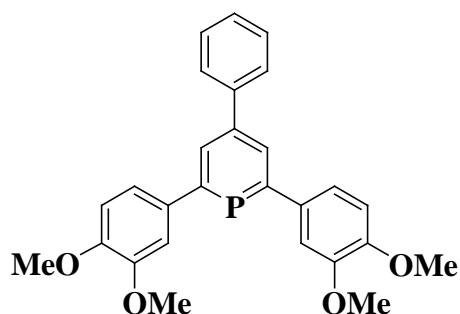
Phosphinine was obtained as yellow solid from corresponding pyrylium salt (2.09 g, 4.05 mmol) and tris(trimethylsilyl)phosphane (1.98 g, 8.116 mmol) in acetonitrile (15 mL).

Yield: 0.40 g, 22%; **m.p:** 125°C.

Elemental Analysis: calcd (%) for $C_{27}H_{25}O_4P_1$ (444.47): C 72.96, H 5.67; found C 72.96, H 5.67.

^{31}P{^{1}H} NMR (C$_6$D$_6$): δ (ppm) = 181.0.

^{1}H NMR (C$_6$D$_6$): δ (ppm) = 3.42 (s, 6H, 2 x -OCH$_3$), 3.45 (s, 6H, 2 x -OCH$_3$), 6.68 (d, $^3J_{HP}$ = 8.2 Hz, 2H), 7.18 - 7.27 (m, 3H), 7.35 - 7.41 (m, 4H), 7.53 - 7.57 (m, 2H), 8.24 (d, $^4J_{HP}$ = 5.9 Hz, 2H).

^{13}C{^{1}H} NMR (C$_6$D$_6$): δ (ppm) = 55.49 (2 x -OCH$_3$), 55.51 (2 x -OCH$_3$), 112.00 (d, $^2J_{CP}$ = 13.3 Hz, C3/5, 2C), 112.67 (2C), 120.14 (d, $^2J_{CP}$ = 12.9 Hz, 2C), 127.96 (2C), 127.98 (2C), 129.11 (2C), 131.43 (d, $^3J_{CP}$ = 11.9 Hz, 2C), 136.62 (d, $^2J_{CP}$ = 24.6 Hz, C-α of Ph, 2C), 142.83 (d, $^3J_{CP}$ = 3.5 Hz, C4), 144.42 (d, $^3J_{CP}$ = 13.6 Hz, 2C), 150.52 (2C), 172.13 (d, $^1J_{CP}$ = 52.1 Hz, C2/C6, 2C).

MS(EI = 70eV): *m/e* (%) = 444.2 (100) [M]$^+$.

4-(2',3'-Dimethoxyphenyl)-2,6-diphenylphosphinine
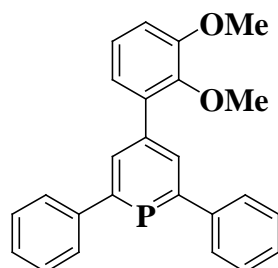
Phosphinine was obtained as yellow solid from corresponding pyrylium salt (4.98 g, 10.92 mmol) and tris(trimethylsilyl)phosphine (6.19 mL, 21.84 mmol) in acetonitrile (30 mL).

Yield: 0.9g, 22% **; m.p:** 112°C.

Elemental Analysis calcd (%) for $C_{25}H_{21}O_2P_1$ (384.41): C 78.11, H 5.51; found C 77.12, H 5.76.

$^{31}P\{^1H\}$ NMR (C_6D_6): δ (ppm) = 184.3.

^1H NMR (C_6D_6): δ (ppm) = 3.36 (s, 3H, -OCH$_3$), 3.53 (s, 3H, -OCH$_3$), 6.61 (m, 1H), 6.97 (d, J_{HH} = 5.0 Hz, 2H), 7.10 - 7.24 (m, 6H), 7.71 - 7.73 (m, 4H), 8.25 (d, $^3J_{HP}$ = 5.9 Hz, 2H).

$^{13}C\{^1H\}$ (C_6D_6): δ (ppm) = 55.60 (-OCH$_3$), 60.10 (-OCH$_3$), 112.82, 122.96 (d, $^4J_{CP}$ = 2.04), 124.10, 127.68, 127.96, 128.01 (3C), 128.13, 129.00 (4C), 133.70 (d, $^2J_{CP}$ = 12.1 Hz, C3/C5, 2C), 137.14 (d, $^3J_{CP}$ = 2.7 Hz, C4), 141.4 (d, $^3J_{CP}$ = 14.3 Hz), 143.62 (d, $^2J_{CP}$ = 24.3 Hz, C-α of Ph, 2C), 147.41 (d, $^4J_{CP}$ = 1.6 Hz), 153.68, 170.95 (d, $^1J_{CP}$ = 52.4 Hz, C2/C6, 2C).

MS(EI = 70eV): m/e (%) = 384.1 (100) [M] $^+$.

2-(3'-Methoxy phenyl)-4,6-diphenylphosphinine
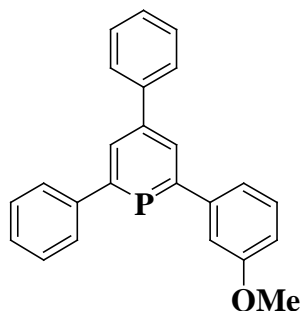
Yield: 1.2g, 36%; **m.p:** 121°C

Elemental Analysis: calcd (%) for $C_{24}H_{19}O_1P_1$ (354.39): C 81.34, H 5.40; found C 81.43, H 5.50

Spectral data are identical with those reported in the literature[48].

General procedure for the synthesis of hydroxy functionalized phosphinines

The corresponding methoxy functionalized phosphinine (1 eqiv) was dissolved in dichloromethane. To this BBr_3 (10 eqiv) in CH_2Cl_2 was added dropwise at $-78°C$. The reaction mixture was warmed to room temperature and allowed to stir for about 24 hrs. It was then poured into cooled degassed water and stirred for 30 min. The dichloromethane layer was separated and dried over $MgSO_4$. The crude mixture was then flash column chromatographed with silica gel using hexane : dichloromethane (50 : 50) to obtain the title product.

2-(3',4'-Dihydroxyphenyl)-4,6-diphenyl phosphinine
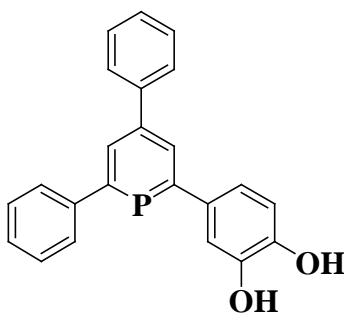
2-(3',4'-dihydroxyphenyl)-4,6-diphenylphosphinine was obtained from 2-(3',4'-dimethoxyphenyl)-4,6-diphenylphosphinine (0.84 g, 2.2 mmol) and BBr$_3$ in CH$_2$Cl$_2$ (1M) (11 mL, 11 mmol).

Yield: 0.5 g (63%); **m.p:** 192°C.

Elemental Analysis calcd (%) for C$_{23}$H$_{17}$O$_2$P$_1$ (356.36): calcd. C 77.52, H 4.81; found. C 77.70, H 5.55.

^{31}P {^{1}H} NMR (CD$_2$Cl$_2$): δ (ppm) = 181.1.

^{1}H NMR (CD$_2$Cl$_2$): δ (ppm) = 5.41 (s, br, 2 x -OH, 2H), 6.90 (d, J_{HH} = 8.3 Hz, 1H), 7.21 (m, 1H), 7.32 (m, 1H), 7.44 - 7.56 (m, 6H), 7.71 - 7.78 (m, 4H), 8.16 (dd, $^4J_{HH}$ = 1.2 Hz, $^3J_{HP}$ = 9.1 Hz, 1H), 8.02 (m, 1H).

^{13}C{^{1}H} NMR (CD$_2$Cl$_2$): δ (ppm) = 114.88 (d, $^3J_{CP}$ = 13.1 Hz), 116.16 (2C), 120.53 (d, $^3J_{CP}$ = 13.1 Hz), 127.91, 128.11 (2C), 128.14, 128.32, 129.29 (2C), 129.36, 131.38 (d, $^2J_{CP}$ = 11.9 Hz, C3/C5), 131.63 (d, $^2J_{CP}$ = 12.2 Hz, C3/C5), 136.72 (d, $^2J_{CP}$ = 24.8 Hz, C-α of Ph), 142.51 (d, $^3J_{CP}$ = 3.3 Hz, C4), 143.61 (d, $^2J_{CP}$ = 24.4 Hz, C-α of Ph), 144.37, 144.59 (2C), 144.76 (d, $^4J_{CP}$ = 2.1 Hz), 171.21 (d, $^1J_{CP}$ = 51.7 Hz, C2/C6), 171.55 (d, $^1J_{CP}$ = 51.2 Hz, C2/C6).

MS(EI = 70eV): *m/e* (%) = 356.1 (100) [M]$^+$.

4-(2',3'-Dihydroxyphenyl)-2,6-diphenyl phosphinine
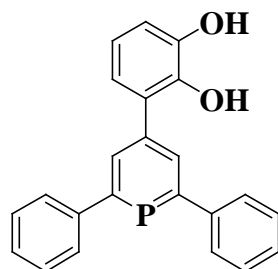
4-(2',3'-dihydroxy)phenyl-2,6-diphenylphosphinine was obtained from 4-(2',3'-dimethoxyphenyl)-4,6-diphenylphosphinine (0.7 g, 1.8 mmol) and BBr_3 (1M) (9 mL, 9 mmol) in CH_2Cl_2.

Yield: 0.4 g (62.4%); **m.p.** 165°C.

Elemental Analysis calcd (%) for $C_{23}H_{17}O_2P_1$ (356.36) with ethylacetate: C 72.96, H 5.67; found C 72.43, H 5.00.

^{31}P {^{1}H} NMR (CD$_2$Cl$_2$): δ (ppm) = 185.3.

^{1}H NMR (CD$_2$Cl$_2$): δ (ppm) = 4.85 (s, br, 2 x -OH, 2H), 6.58 - 6.81 (m, 4H), 7.18 - 7.23 (m, 5H), 7.65 - 7.68 (m, 4H), 8.08 (d, $^3J_{HP}$ = 5.7 Hz, 2H).

^{13}C{^{1}H} NMR (CD$_2$Cl$_2$): δ (ppm) = 115.05, 121.00 (2C), 122.42, 127.49 (2C), 127.89 (2C), 128.14 (2C), 128.68, 129.18 (2C), 133.42 (d, $^3J_{CP}$ = 12.1 Hz, C3/C5, 2C), 140.25 (d, $^3J_{CP}$ = 13.9 Hz), 141.53 (d, $^3J_{CP}$ = 1.8 Hz, C4), 143.62 (d, $^2J_{CP}$ = 24.1 Hz, C-α of Ph, 2C), 144.73 (2C), 171.87 (d, $^1J_{CP}$ = 52.8, C2/C6, 2C).

MS(EI = 70eV): *m/e* **(%)** = 356.1 (100) [M] $^+$.

2-(3'-Hydroxyphenyl)-4,6-diphenylphosphinine
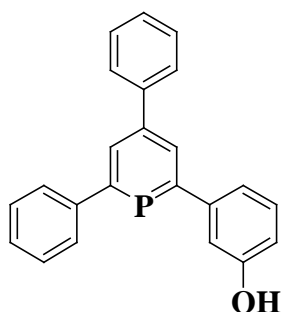
2-(3'-hydroxyphenyl)-4,6-diphenylphosphinine was obtained from 2-(3'-methoxyphenyl)-4,6-diphenylphosphinine (0.7 g, 1.97 mmol) and BBr_3 in CH_2Cl_2 (1M) (9.9 mL, 9.85 mmol).

Yield: 0.41g (61.3%); **m.p:** 183°C

Elemental Analysis calcd (%) for $C_{23}H_{17}O_1P_1$ (340.36): cald. C 81.17, H 5.46; found. C 81.33, H 5.32.

^{31}P {^1H} NMR (CD$_2$Cl$_2$): δ (ppm) = 184.2.

^1H NMR (CD$_2$Cl$_2$): δ (ppm) = 3.96 (s, br, -OH, 1H), 6.56 - 6.61 (m, 1H), 6.97 - 6.99 (m, 1H), 7.03 (m, 1H), 7.12 - 7.28 (m, 7H), 7.39 (m, 2H), 7.64 - 7.69 (m, 2H), 8.08 (d, $^3J_{HP}$ = 5.8 Hz, 2H).

^{13}C{^1H} NMR (CD$_2$Cl$_2$): δ (ppm) = 114.69 (d, $^3J_{CP}$ = 12.7 Hz), 115.03 (d, $^4J_{CP}$ = 2.1 Hz), 120.06 (d, $^3J_{CP}$ = 13.3 Hz), 127.91, 127.94, 128.04 (2C), 128.13, 129.01 (4C), 130.02, 131.83 (d, $^3J_{CP}$ = 10.2 Hz, C3/C5), 132.00 (d, $^3J_{CP}$ = 10.2 Hz, C3/C5), 142.40 (d, $^3J_{CP}$ = 3.2 Hz, C4), 143.59 (d, $^2J_{CP}$ = 24.0 Hz, C-α of Ph), 144.21 (d, $^3J_{CP}$ = 13.5 Hz), 145.02 (d, $^2J_{CP}$ = 24.6 Hz, C-α of Ph), 156.74 (2C), 171.55 (d, $^1J_{CP}$ = 52.3 Hz, C2/C6), 171.87 (d, $^1J_{CP}$ = 52.5 Hz, C2/C6).

MS(EI = 70eV): *m/e* (%) = 339.09 (100) [M-H]$^+$.

General procedure for the synthesis of gold(I) complexes of functionalized phosphinines

The corresponding functionalized phosphinine (1 equiv) and AuCl(tht) (1 equiv) were weighed inside a glove box. Freshly distilled CH$_2$Cl$_2$ or thf was then added and the mixture allowed to stir at RT for about 15min. The completion of reaction was checked by ^{31}P NMR spectroscopy. Reduction of volume, followed by hexane precipitation afforded the corresponding gold(I) complex as pale yellow - yellow solid.

2-(3',4'-Dimethoxyphenyl)-4,6-diphenylphosphinine gold(I) chloride
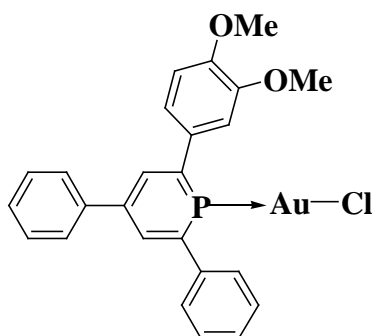
The title complex was obtained as yellow solid from 2-(3',4'-dimethoxyphenyl)-4,6-diphenylphosphinine (0.14 g, 0.355 mmol) and AuCl(tht) (0.11 g, 0.355 mmol) in CH_2Cl_2 (5 mL).

Yield: 0.21g (96%); **m.p:** 142°C.

Elemental Analysis calcd (%) for $C_{25}H_{21}O_2P_1Cl_1Au_1$ (616.83): calcd. C 48.70, H 3.44; found. C 47.75, H 3.34.

^{31}P{^{1}H} NMR (CD$_2$Cl$_2$): δ (ppm) = 152.39.

^{1}H NMR (CD$_2$Cl$_2$): δ (ppm) = 3.93 (s, -OCH$_3$, 3H), 3.99 (s, -OCH$_3$, 3H), 7.05 (d, $^4J_{HP}$ = 8.0 Hz, 1H), 7.36 (dt, $^4J_{HP}$ = 8.2 Hz, $^3J_{HH}$ = 2.1 Hz, 1H), 7.41 - 7.42 (m, 1H), 7.49 - 7.59 (m, 6H), 7.70 - 7.74 (m, 2H), 7.78 - 7.83(m, 2H), 8.40 (dd, $^3J_{HP}$ = 22.7 Hz, $^4J_{HH}$ = 1.7 Hz, H at C3/C5, 1H), 8.49 (dd, $^3J_{HP}$ = 22.7 Hz, $^4J_{HH}$ = 1.6 Hz, H at C3/C5, 1H).

^{13}C{^{1}H} NMR (CD$_2$Cl$_2$): δ (ppm) = 55.09 (s, -OCH$_3$), 55.29 (s, -OCH$_3$), 111.07, 111.10, 111.13, 120.06 (d, $^3J_{CP}$ = 12.7 Hz), 126.93 (d, $^4J_{CP}$ = 3.3 Hz), 127.63 (d, $^3J_{CP}$ = 11.6 Hz), 128.03 (d, $^4J_{CP}$ = 1.1 Hz), 128.40 (4C), 128.54 (d, $^4J_{CP}$ = 2.1 Hz), 130.38 (d, $^3J_{CP}$ = 12.3 Hz), 134.97 (d, $^2J_{CP}$ = 10.1 Hz, C3/C5), 135.18 (d, $^2J_{CP}$ = 10.6 Hz, C3/C5), 138.01 (d, $^2J_{CP}$ = 12.0 Hz), 139.75 (d, $^2J_{CP}$ = 5.7 Hz), 142.82 (d, $^3J_{CP}$ = 26.2 Hz, C4), 148.97, 149.92 (d, $^4J_{CP}$ = 2.2 Hz), 158.83 (d, $^1J_{CP}$ = 36.1 Hz, C2/C6), 158.84 (d, $^1J_{CP}$ = 36.1 Hz, C2/C6).

MS (EI = 70eV): *m/e* **(%)** = 616.0 (100) [M]$^+$, 384.1 (50) [M-AuCl]$^+$.

2,6-Di (3',4'-dimethoxy phenyl)-4-phenylphosphinine gold(I) chloride
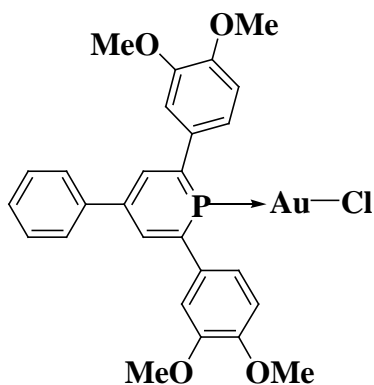
The title complex was obtained as a pale yellow solid from 2,6-di(3',4'-dimethoxy) phenyl-4-phenylphosphinine (0.05 g, 0.112 mmol) and AuCl(tht) (0.036 g, 0.112 mmol) in CH$_2$Cl$_2$ (5 mL).

Yield: 0.07g (94%); **m.p:** 145°C.

Elemental Analysis: calcd (%) for C$_{27}$H$_{25}$O$_4$P$_1$Cl$_1$Au$_1$ (676.89) with CH$_2$Cl$_2$: C 44.15, H 3.57; found C 44.39, H 3.88

^{31}P{^{1}H} NMR (CD$_2$Cl$_2$): δ (ppm) = 150.40.

^{1}H NMR (CD$_2$Cl$_2$): δ (ppm) = 3.95 (s, 2 x -OCH$_3$, 6H), 3.99 (s, 2 x -OCH$_3$, 6H), 7.04 (d, ^{4}J$_{HP}$ = 9.3 Hz, 2H), 7.34 - 7.42 (m, 4H), 7.49 - 7.60 (m, 3H), 7.70 - 7.74 (m, 2H), 8.39 (d, ^{3}J$_{HP}$ = 22.7 Hz, H at C3/C5, 2H).

MS(EI = 70eV): *m/e* **(%)** = 676.1 (100) [M]$^+$, 444.1(75) [M-AuCl]$^+$.

4-(2',3'-Dimethoxyphenyl)-2,6-diphenylphosphinine gold(I) chloride
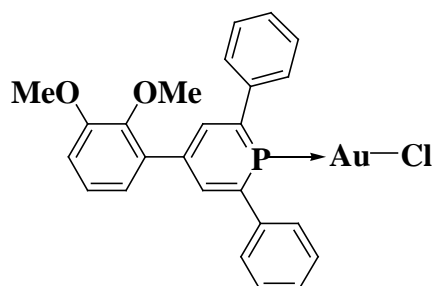
The title complex was obtained as white solid from 4-(2',3'-dimethoxy)phenyl-2,6-diphenylphosphinine (0.07 g, 0.182 mmol) and AuCl(tht) (0.058 g, 0.182 mmol) in CH_2Cl_2 (5 mL).

Yield: 0.11 g (98%); **m.p:** 147°C.

Elemental Analysis: calcd (%) for $C_{25}H_{21}O_2P_1Cl_1Au_1$ (616.83) with CH_2Cl_2: C 44.50, H 3.30; found C 44.47, H 3.21.

$^{31}P\{^1H\}$ NMR (CD_2Cl_2): δ (ppm) = 153.10.

^1H NMR (CD_2Cl_2): δ (ppm) = 3.75 (s, -OCH$_3$, 3H), 3.95 (s, -OCH$_3$, 3H), 7.02 - 7.09 (m, 2H), 7.17 - 7.24 (m, 1H), 7.53 - 7.61 (m, 6H), 7.79 - 7.84 (m, 4H), 8.41 (d, $^3J_{HP}$ = 22.9 Hz, H at C3/C5, 2H).

$^{13}C\{^1H\}$ NMR (CD_2Cl_2): δ (ppm) = 56.3 (s, -OCH$_3$), 61.1 (s, -OCH$_3$), 113.74, 122.44 (d, $^4J_{CP}$ = 3.4 Hz), 124.86, 128.89 (d, $^3J_{CP}$ = 12.0 Hz, 4C), 129.63(3C), 129.65 (2C), 129.72(d, $^4J_{CP}$ = 2.4 Hz, 2C), 135.11(d, $^2J_{CP}$ = 5.3 Hz), 138.87 (d, $^2J_{CP}$ = 10.7 Hz, C3/C5), 139.10 (d, $^2J_{CP}$ = 11.9 Hz, C3/C5), 140.97 (d, $^3J_{CP}$ = 27.9 Hz, C4), 146.83 (d, $^4J_{CP}$ = 2.9 Hz), 153.75, 153.77, 158.87 (d, $^1J_{CP}$ = 38.5 Hz, C2/C6, 2C).

MS(ESI): *m/e* **(%)** = 670.07 (100) [M + CH$_3$O + Na]$^+$.

2,3,5,6-Tetraphenylphosphinine gold(I) chloride
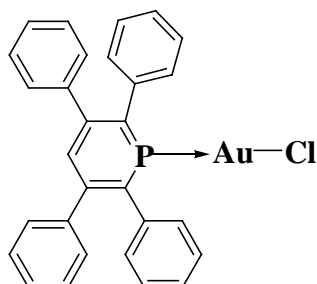
The title complex was obtained as a pale yellow solid from 2,3,5,6-tetraphenyl phosphinine (0.15 g, 0.355 mmol) and AuCl(tht) (0.11 g, 0.355 mmol) in thf (5 mL).

Yield: 0.21 g (95%); **m.p:** 177.3°C.

Elemental Analysis: calcd (%) for $C_{29}H_{21}P_1Cl_1Au_1$ (632.88): C 55.04, H 3.34; found C 53.52, H 3.46.

$^{31}P\{^1H\}$ NMR (CD$_2$Cl$_2$): δ (ppm) = 175.

^1H NMR (CD$_2$Cl$_2$): δ (ppm) = 7.20 - 7.31 (m, 2 x C_6H_5, 10H), 7.34 (br s, 2 x C_6H_5, 10H), 7.72 (d, $^4J_{HP}$ = 7.11 Hz, 1H, H at C4).

$^{13}C\{^1H\}$ NMR (CD$_2$Cl$_2$): δ (ppm) = 128.31 (2C), 128.57 (4C), 128.77 (d, $^4J_{CP}$ = 1.42 Hz, 4C), 128.83 (2C), 129.88 (d, $^4J_{CP}$ = 1.2 Hz, 4C), 130.89 (d, $^3J_{CP}$ = 11.5 Hz, 4C), 135.79 (d, $^3J_{CP}$ = 26.2 Hz, C4), 136.99 (d, $^2J_{CP}$ = 12.2 Hz, 2C), 140.38 (d, $^3J_{CP}$ = 8.9 Hz, 2C), 150.39 (d, $^2J_{CP}$ = 8.2 Hz, C3/C5, 2C), 156.27 (d, $^1J_{CP}$ = 34.2 Hz, C2/C6, 2C).

MS (EI = 70eV): *m/z* (%) = 632.1 (100) [M] $^+$, 400.2 (75) [M-AuCl] $^+$.

2-(3',4'-Dihydroxyphenyl)-4,6-diphenylphosphinine gold(I) chloride
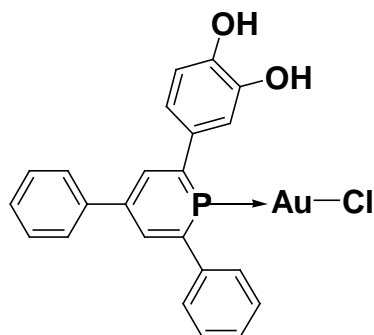
The title complex was obtained as yellow solid from 2-(3',4'-dihydroxyphenyl)-4,6-diphenylphosphinine (0.1 g, 0.28 mmol) and AuCl(tht) (0.09 g, 0.28 mmol) in thf (5 mL).

Yield: 0.15 g (90%); **m.p:** 202°C

Elemental Analysis: calcd (%) for $C_{23}H_{17}O_2P_1Cl_1Au_1$ (588.78): C 46.92, H 2.91; found C 47.84, H 3.53

$^{31}P\{^1H\}$ NMR (CD$_2$Cl$_2$): δ (ppm) = 152.40.

^{1}H NMR (CD$_2$Cl$_2$): δ (ppm) = 6.88 (dd, $^3J_{HH}$ = 0.8 Hz, $^4J_{HP}$ = 8.2 Hz, 1H), 7.18 (dt, $^4J_{HH}$ = 2.2 Hz, $^3J_{HP}$ = 8.1 Hz, 1H), 7.28 (m, 1H), 7.41 - 7.57 (m, 6H), 7.77 - 7.88 (m, 4H), 8.44 (dd, $^4J_{HH}$ = 1.6 Hz, $^3J_{HP}$ = 22.4 Hz, 1H, H at C3/C5), 8.52 (dd, $^4J_{HH}$ = 1.6 Hz, $^3J_{HP}$ = 22.4 Hz, 1H, H at C3/C5).

4-(2',3'-Dihydroxyphenyl)-2,6-diphenylphosphinine gold(I) chloride

The title complex was obtained as yellow solid from 4-(2',3'-dihydroxyphenyl-2,6-diphenylphosphinine (0.1g, 0.28 mmol) and AuCl(tht) (0.09 g, 0.28 mmol) in thf (5 mL).
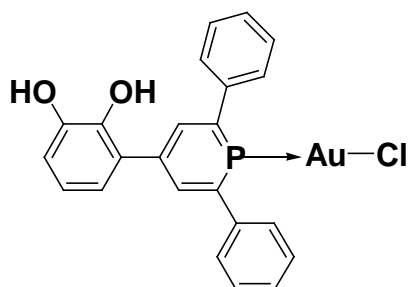
.

Yield: 0.16g, (97%); **m.p:** 208°C.

Elemental Analysis: calcd (%) for $C_{23}H_{17}O_2P_1Cl_1Au_1$ (588.78): C 46.92, H 2.91; found C 47.97, H 3.43.

$^{31}P\{^1H\}$ NMR (CD$_2$Cl$_2$): δ (ppm) = 153.17.

^1H NMR (CD$_2$Cl$_2$): δ (ppm) = 6.74 - 6.86 (m, 2H), 6.93 (dd, $^3J_{HH}$ = 1.6 Hz, $^4J_{HP}$ = 7.2 Hz, 1H), 7.45 - 7.57 (m, 6H), 7.84 - 7.88 (m, 4H), 8.57 (d, $^3J_{HP}$ = 22.7 Hz, 2H, H at C3/C5).

MS (ESI): *m/e* **(%)** = 587.02 (100)[M-H]$^+$.

Bis(2-(3',4'-dimethoxy)phenyl)-4,6-diphenylphosphinine gold(I) triflate
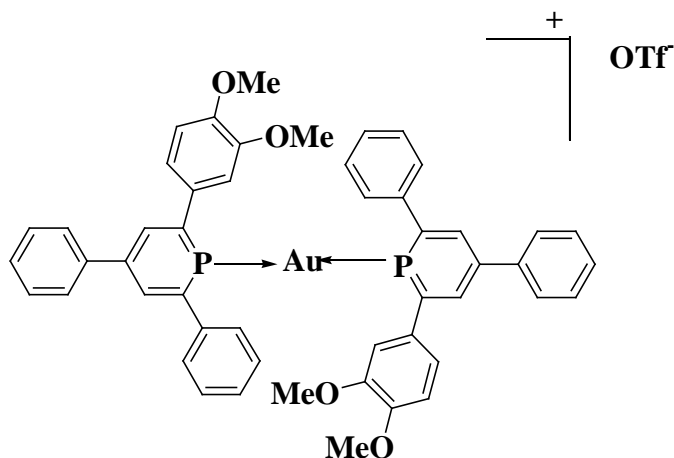
2-(3',4'-dimethoxyphenyl)-4,6-diphenyl phosphinine (0.096 g, 0.2.5 mmol) and AuCl(tht) (0.04 g, 0.125 mmol) were stirred in DCM (5 mL) for 15 mts at RT. The solution of silver triflate (0.03 g, 0.125 mmol) in DCM was added dropwise to the reaction mixture at –78°C. The mixture was warmed to RT and stirred. The completion of reaction was checked by ^{31}P NMR spectroscopy. Reduction of volume, followed by precipitation and filtration yielded the title complex.

Yield: 0.12 g, (86%); **m.p:** 242°C.

^{31}P NMR (CD$_2$Cl$_2$): δ (ppm) = 169.9.

^{1}H NMR (CD$_2$Cl$_2$): δ (ppm) = 3.89 (s, 2 x -OCH$_3$, 6H), 3.91 (s, 2 x -OCH$_3$, 6H), 6.96 - 7.00 (m, 2H), 7.27 - 7.31 (m, 4H), 7.48 - 7.59 (m, 12H), 7.70 - 7.75 (m, 8H), 8.27 (dd, ^{4}J$_{HH}$ = 1.4 Hz, ^{3}J$_{HP}$ = 13.6 Hz, 2H), 8.29 (dd, ^{4}J$_{HH}$ = 1.3 Hz, ^{3}J$_{HP}$ = 13.8 Hz, 2H).

MS (ESI): *m/e* **(%)** = 996.24 [M - CF$_3$SO$_3$ + CH$_3$OH]$^+$.

General procedure for the immobilisation of hydroxy functionalized phosphinine gold(I) chloride on TiO$_2$

η^1Gold(I) complex of hydroxy functionalized phosphinine (0.25 mmol) dissolved in THF (20 mL) was added to TiO$_2$ (1 g) (preheated at 60°C for 4hrs). The suspension was stirred at RT for about 24 hrs. It was then filtered, washed with thf (3 x 20 mL) and dried under vacuum for 8 hrs.

2-(3',4'-Dihydroxyphenyl)-4,6-diphenyl phosphinine gold(I) chloride on TiO$_2$

Immobilised material was obtained from 2-(3',4'-dihydroxyphenyl)-4,6-diphenyl phosphinine gold(I) chloride 0.15 g (0.25 mmol) and TiO$_2$ (1 g).

Elemental Analysis: found (%) C : 1.29, H : -

^{31}P{^{1}H} CP MAS: δ (ppm) = 27.
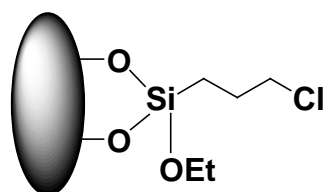
4-(2',3'-Dihydroxyphenyl)-2,6-diphenyl phosphinine gold(I) chloride on TiO$_2$

Immobilised material was obtained from 4-(2',3'-dihydroxyphenyl)-2,6-diphenyl phosphinine gold(I) chloride 0.15 g (0.25 mmol) and TiO$_2$ (1 g).

Elemental Analysis: found (%) C : 1.27, H : -

^{31}P{^{1}H} CP MAS: δ (ppm) = 25.

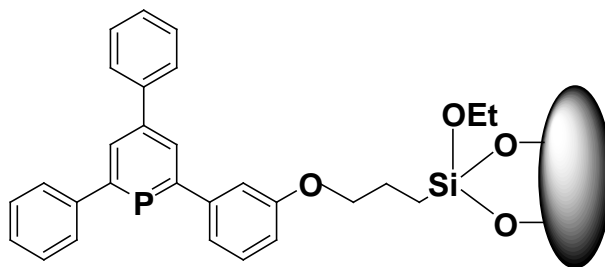## 3-Chloropropyl triethoxy functionalized HMS (ClPTESi-HMS)

A mixture of calcined HMS (3.00 g) in dry toluene (50 mL) and (3-chloropropyl)triethoxysilane (2.16 g, 9.00 mmol) was refluxed for 24 hrs. The material was filtered, washed with toluene (3 x 50 mL), and dried under vacuum at 80°C for 8 hrs.

Elemental Analysis: found (%) C: 17.91, H: 2.93.

^{29}Si{^{1}H}, CP MAS NMR: δ (ppm) = -53 (T^2), -90 (Q^2), -101 (Q^3), -109 (Q^4).

^{13}C{^{1}H}, CP MAS NMR: δ (ppm) = 8.1 (-SiCH_2CH$_2$CH$_2$Cl), 15.0 (-SiOCH$_2$$CH_3$), 23.6 (-SiCH$_2$$CH_2CH_2$Cl), 43.9 (SiCH$_2CH_2$$CH_2$Cl), 57.6 (-Si$OCH_2CH_3$).

Immobilisation of 2-(3'-hydroxyphenyl)-4,6-diphenylphosphinine onto ClPTESi- HMS

Triethylamine (0.89 g, 8.8 mmol) was added to the suspension of ClPTESi-HMS (0.85 g) in toluene (7 mL). To this 2-(3-hydroxy)phenyl-4,6-diphenylphosphinine (0.3 g, 0.88 mmol) in CH$_2$Cl$_2$ (5 mL) was added dropwise at -78°C. The suspension was then warmed to room temperature and allowed to stir at RT for 24 hrs. It was then filtered, washed successively with toluene (3 x 20 mL) and DCM (3 x 20 mL) and dried under vacuum for about 8 hrs.

Elemental Analysis: found (%) C: 17.91, H 2.93.

^{31}P HP-Dec(MAS): δ (ppm) = 183.

General procedure for the synthesis of phosphinine stabilized gold nanoparticles

15 mL of sodium naphthalenide in thf (1 mmol in 10 mL of thf) was added dropwise to a solution of an appropriate amount of 2,3,5,6- tetraphenylphosphinine and AuCl(tht) in thf (20 mL). The dark purple solution was allowed to stir at RT for a couple of hrs. The dark purple solid obtained after the removal of solvent under vacuo, was washed with thf (2 x 15mL) and hexane (2 x 15 mL).

Au NPs P- 0.5

The dark purple solid was obtained from 2,3,5,6-tetraphenylphosphinine (0.31g, 0.78 mmol) and AuCl(tht) (0.48 g, 1.5 mmol).

Elemental Analysis: calcd (%) for $C_{29}H_{21}P_1$ over gold: C 86.98, H 5.9; found C 46.89, H 3.30.

.

$^{31}P\{^1H\}$ **CP MAS:** δ (ppm) = 178.

Au NPs P- 0.2

The dark purple solid was obtained from 2,3,5,6-tetraphenylphosphinine (0.12 g, 0.3 mmol) and AuCl(tht) (0.48 g, 1.5 mmol).
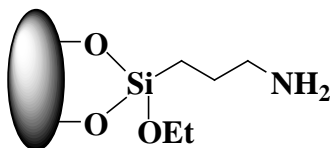
Elemental Analysis: calcd (%) for $C_{29}H_{21}P_1$ over gold: C 43.85, H 2.66; found C 24.22, H 1.76.

$^{31}P\{^1H\}$ CP MAS: δ (ppm) = 176.

General procedure for the preparation of 3-Amino propyl functionalized HMS

3-aminopropyltrialkoxysilane (9.0 mmol) was added to the calcined HMS (3.0 g) in 50mL toluene and was refluxed for 24hrs. It was then filtered, washed with toluene (3 x 50mL) and dried under vacuum.

a) APTESi-HMS

APTESi-HMS was obtained from 3-aminopropyltriethoxysilane (2.1 mL, 9.0 mmol) and HMS (3.0 g).

Elemental Analysis: found (%) C : 8.70, H : 2.39, N : 2.43.

$^{29}Si\{^1H\}$ CP MAS NMR: δ (ppm) = -111 (Q^4), -102 (Q^3), -69 (T^3), -60 (T^2).

$^{13}C\{^1H\}$ CP MAS NMR: δ (ppm) = 6.5 (-SiCH_2CH$_2$CH$_2$NH$_2$), 13.5 (-SiOCH$_2$$CH_3$), 22.8 (-SiCH$_2$$CH_2CH_2NH_2$), 40.7 (-SiCH$_2CH_2$$CH_2NH_2$), 56.6 (-Si$OCH_2CH_3$).
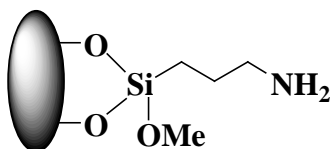
b) APTMSi-HMS

APTMSi-HMS was obtained from 3-aminopropyltrimethoxysilane (1.6 mL, 9.0 mmol) and HMS (3 g).

Elemental Analysis: found (%) C : 10.42, H : 2.81, N : 2.47.

^{29}Si{^{1}H} CP MAS NMR: δ (ppm) = -109 (Q^4), -101 (Q^3), -67 (T^3), -61 (T^2).

^{13}C{^{1}H} CP MAS NMR: δ (ppm) = 8.1 (-Si*CH$_2$*CH$_2$CH$_2$NH$_2$), 24.4 (SiCH$_2$*CH$_2$*CH$_2$NH$_2$), 41.5 (-SiCH$_2$CH$_2$*CH$_2$*NH$_2$), 48.4 (-Si*OCH$_3$*).

Capped APTESi-HMS
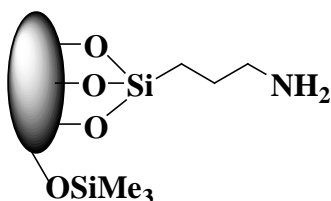
A mixture of 1,1,1,3,3,3-hexamethyldisilazane (5 g, 31 mmol) and APTESi-HMS (3 g) in toluene (20 mL) was stirred for 24 hrs at RT. It was then filtered, washed with toluene (3 x 50 mL) and dried under vacuum.

Elemental Analysis: found (%) C : 7.89, H : 2.30, N : 2.54.

^{29}Si{^{1}H} CP MAS NMR: δ (ppm) = -112 (Q^4), -102 (Q^3), -69 (T^3), -61 (T^2), 8 ((CH$_3$)$_3$Si).

¹³C{¹H} CP MAS NMR: δ (ppm) = -2.4 (*(CH₃)₃*Si-), 7.7 (-Si*CH₂*CH₂CH₂NH₂), 23.7 (SiCH₂*CH₂*CH₂NH₂), 42.3 (-SiCH₂CH₂*CH₂*NH₂).

Anchored monophosphaferrocene by Schiff condensation

2-formyl-3,4-dimethyl monophosphaferrocene (0.4 g, 1.52 mmol) was stirred with APTESi-HMS (2 g) in dry methanol (15 mL) at 55°C for 3days. The material was filtered, washed with methanol (3 x 50 mL) and dried under vacuum for 8 hrs.

Elemental Analysis: found (%) C: 13.49, H: 2.67, N: 2.22.

³¹P{¹H} HPDec MAS NMR: δ (ppm) = -76.

General procedure for the immobilisation of monophosphaferrocene onto HMS by reductive amination

2-formyl-3,4-dimethyl-1-phosphaferrocene (0.4 g, 1.52 mmol) was added to the functionalized HMS (2 g) in dry methanol. To this excess NaBH₃CN (5 equivalents) was added and the reaction mixture was heated at 50°C for about 3 days. The material was filtered, washed with methanol (3 x 50 mL) and vacuum dried for 8hrs.

a) [CpFePNH]/APTESi-HMS
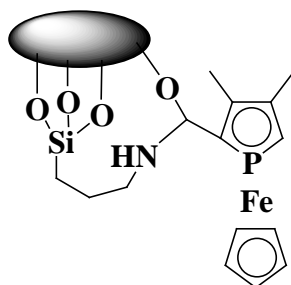
The anchored material was obtained from 2-formyl-3,4-dimethyl-1-phosphaferrocene (0.4 g, 1.52 mmol), APTESi-HMS (2 g) and NaBH₃CN (0.47 g, 7.6 mmol).

Elemental Analysis: found(%) C: 11.69, H: 2.94, N: 2.34

^{31}P{^{1}H} CP MAS NMR: δ (ppm) = -76 (major isomer), -72 (minor isomer)

^{29}Si{^{1}H} CP MAS NMR: δ (ppm) = -113 (Q^4), -104 (Q^3), -69 (T^3), -62 (T^2).

^{13}C{^{1}H} CP MAS NMR: δ (ppm) = 7.3 (-Si*CH$_2$*CH$_2$CH$_2$NHCH$_2$-), 19.9 (-SiCH$_2$*CH$_2$*CH$_2$NHCH$_2$-), 24.0 (2 x CH$_3$, methyl of phospholyl), 42.3 (-SiCH$_2$CH$_2$*CH$_2$*NHCH$_2$-), 47.2 (-SiCH$_2$CH$_2$CH$_2$NH*CH*-), 69.6 (C$_5$H$_5$), 93.6 (quaternery C, CH of phospholyl).

b) [CpFePNH]/APTMSi-HMS

The anchored material was obtained from 2-formyl-3,4-dimethyl-1-phosphaferrocene (0.4 g, 1.52 mmol), APTMSi-HMS (2 g) and NaBH$_3$CN (0.47 g, 7.6 mmol).

Elemental Analysis: found(%) C: 14.00, H: 2.55, N: 2.29.

^{31}P{^{1}H} CP MAS NMR: δ (ppm) = 40 (major product), -78 (minor product).
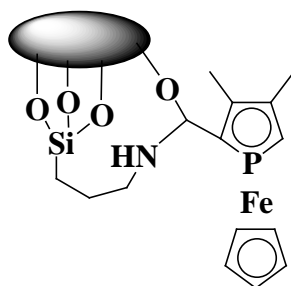
c) [CpFePNH] / capped APTESi-HMS

The anchored material was obtained from 2-formyl-3,4-dimethyl-1-phosphaferrocene (0.4 g, 1.52 mmol), capped APTESi-HMS (2 g) and NaBH$_3$CN (0.47 g, 7.6 mmol).

.

Elemental Analysis: found(%) C: 14.12, H: 2.65, N: 2.38.

^{31}P{^{1}H} CP MAS NMR: δ (ppm) = -76 (major isomer), -72 (minor isomer).

^{13}C{^{1}H} CP MAS NMR: δ (ppm) = 6.8 (-Si*CH$_2$*CH$_2$CH$_2$NHCH$_2$-), 19.5 (SiCH$_2$*CH$_2$*CH$_2$NHCH$_2$-), 24.1 (2 x CH$_3$, methyl of phospholyl), 41.5 (-SiCH$_2$CH$_2$*CH$_2$*NHCH$_2$-), 47.6 (-SiCH$_2$CH$_2$CH$_2$NH*CH$_2$*-), 69.8 (C$_5$H$_5$), 92.6 (quaternery C, CH of phospholyl).

3,4-dimethyl phosphaferrocenyl-2-(N-propyl)methylimine
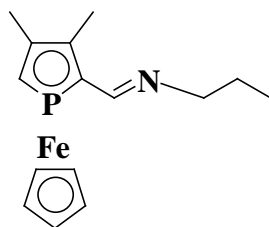
2-formyl-3,4-dimethylmonophosphaferrocene (0.1 g, 3.84 mmol) and n-propylamine (0.31 g, 3.846 mmol) were heated in methanol (15 mL) for 4 hrs.

Yield: 1.02 g, (86%).

^{31}P{^{1}H} NMR (CD$_3$OD): δ (ppm) = -75.

^{1}H NMR (CD$_3$OD): δ (ppm) = 0.89 (t, J_{HH} = 6.3 Hz, -CH$_2$CH$_2$*CH$_3$*), 1.57 (m, -CH$_2$*CH$_2$*CH$_3$), 2.21 (s, CH$_3$), 2.31 (s, CH$_3$), 3.12 (t, J_{HH} = 7.1 Hz, -*CH$_2$*CH$_2$CH$_3$), 3.95 (d, $^2J_{HP}$ = 37.4 Hz, CHP), 4.2 (s, C$_5$H$_5$), 8.17 (d, $^3J_{HP}$ = 8.8 Hz, CHN).

General procedure for the synthesis of amino functionalized monophosphaferrocene

The appropriate functionalized amine (1 equiv) was added to 2-formyl-3,4-dimethylmonophosphaferrocene (1 equiv) in methanol. An excess NaBH$_3$CN (10 equvalent)

was added, and the mixture was heated at 55°C for 5hrs. The mixture was then hydrolyzed with deoxygenated water. The organic phase was seperated and then passed through a short plug of neutral alumina. The solvent was removed under vacuum to obtain an orange oil.

3,4-dimethyl phosphaferrocenyl -2-(N-3'-triethoxysilylpropyl) methylamine
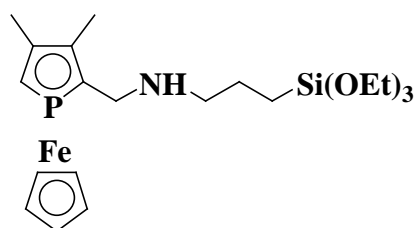
The title compound was prepared from 2-formyl-3,4-dimethylmonophosphaferrocene (0.72 g, 2.76 mmol), benzylamine (0.64 mL, 2.76 mmol), and excess NaBH$_3$CN (1.7 g, 27.6 mmol).

^{31}P{^{1}H} NMR (CD$_3$OD): δ (ppm) = -75.4 (major product) and 76.1(minor product).

3,4-dimethyl phosphaferrocenyl - 2-(N-benzyl) methylamine

The title compound was obtained from 2-formyl-3,4-dimethylmonophosphaferrocene (0.72 g, 2.76 mmol), benzylamine (0.15 g, 2.76 mmol), and excess NaBH$_3$CN (1.7 g, 27.6 mmol).

^{31}P{^{1}H} NMR (CD$_3$OD): δ (ppm) = -76.5.

^{1}H NMR (CD$_3$OD): δ (ppm) = 2.10 (s, CH$_3$, 3H), 2.17 (s, CH$_3$, 3H), 3.16 (dd, $^3J_{HP}$ = 13.52 Hz, CH$_2$NH, 2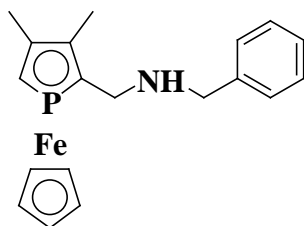H), 3.32 (s, CH$_2$ of benzyl, 2H), 3.63 (d, $^2J_{HP}$ = 37.01 Hz, α-H, 1H), 4.06 (s, Cp, 5H), 7.21 – 7.35 (m, C$_6$H$_5$, 5H).

^{13}C{^{1}H} NMR (CD$_3$OD): δ (ppm) = 13.8 (s, CH$_3$), 17.3 (s, CH$_3$), 53.73 (d, $^2J_{C,P}$ = 1.7 Hz, CH$_2$NH), 54.76 (s, CH$_2$ of benzyl), 73.01 (s, Cp), 76.70 (d, $^1J_{CP}$ = 58.3 Hz, α-C), 94.64 (d, $^2J_{CP}$ = 4.9 Hz, β-C), 96.26 (d, $^1J_{CP}$ = 58.9 Hz, α-C), 97.43 (d, $^2J_{CP}$ = 6.8 Hz, β-C), 123.75, 129.47, 130.72, 140.5 (Arom-C).

MS(EI = 70 eV): *m/e* (%) = 351.1 (100) [M]$^+$, 244.0 (44) [M - NHCH$_2$C$_6$H$_5$ + H]$^+$.

General procedure for the immobilisation of palladium catechol phosphines on TiO$_2$

Palladium catechol phosphines was stirred with TiO$_2$ in CH$_2$Cl$_2$ for one day at RT. It was then filtered, washed with CH$_2$Cl$_2$ and dried under vacuum.

Immobilisation of 2,3-dihydroxy palladium catechol phosphines on TiO$_2$
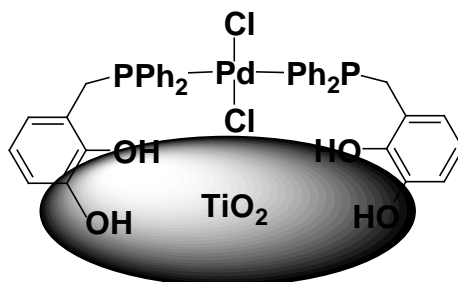
TiO$_2$ immobilised palladium catechol phosphines was obtained from 2,3-dihydroxy palladium catechol phosphine (0.28 g, 0.36 mmol) and neutral TiO$_2$ (3 g) in CH$_2$Cl$_2$ (25 mL).

^{31}P{^{1}H} CP MAS NMR: δ$_{iso}$ (ppm) = 20.8, δ$_{11}$= 97, δ$_{22}$ = 22, δ$_{33}$ = -38

Suspension of TiO$_2$ (neutral) immobilised palladium-2,3-dihydroxy catechol phosphines in CH$_2$Cl$_2$

^{31}P CP MAS NMR: δ$_{iso}$ (ppm) = 20.4, δ$_{11}$= 77, δ$_{22}$ = 28, δ$_{33}$ = -43.

Suspension of TiO$_2$ (neutral) immobilised palladium-2,3-dihydroxy catechol phosphines in DMF

^{31}P CP MAS NMR: δ_{iso} (ppm) = Nil

^{31}P{^{1}H} MAS NMR: δ (ppm) = 18.6 & 34.3 (1.5: 1), 26.6 & 79.4 (pairwise)

Suspension of TiO$_2$ (neutral) immobilised palladium-2,3-dihydroxy catechol phosphines in CH$_3$CN

^{31}P{^{1}H} CP MAS NMR: δ_{iso} (ppm) = 22.5, δ_{11} = 73, δ_{22} = 32, δ_{33} = -40.

^{31}P{^{1}H} MAS NMR: δ (ppm) = 18.3 & 32.0

Suspension of TiO$_2$ (neutral) immobilised palladium-2,3-dihydroxy catechol phosphines in DMF-NEt$_3$ (9:1)

^{31}P CP MAS NMR: δ_{iso} (ppm) = Nil

^{31}P{^{1}H} MAS NMR: δ (ppm) = 61.0

Suspension of TiO$_2$ (neutral) immobilised palladium-2,3-dihydroxy catechol phosphines in CH$_2$Cl$_2$ with 10 vol% NEt$_3$

^{31}P{^{1}H} CP MAS NMR: δ_{iso} (ppm) = Nil

^{31}P{^{1}H} MAS NMR: δ (ppm) = 61.0

Immobilisation of 3,4-dihydroxy palladium catechol phosphines on TiO_2
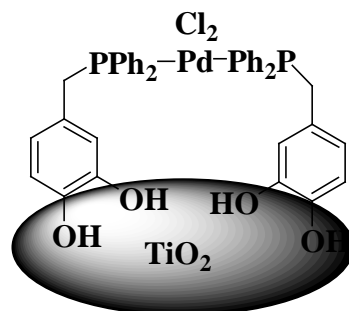
TiO_2 immobilised palladium catechol phosphines was obtained from 3,4-dihydroxy palladium catechol phosphine (0.28g, 0.36mmol)   and TiO_2 (3g) in CH_2Cl_2 (25ml).

Neutral TiO_2

$^{31}P\{^1H\}$ CP MAS NMR: δ_{iso} = 17.7 , δ_{11}= 82, δ_{22} = 19, δ_{33} = -50.

NP-TiO_2

$^{31}P\{^1H\}$ CP MAS NMR: δ_{iso} = 18.4

Suspension of TiO_2 immobilised palladium-3,4-dihydroxy catechol phosphines in CH_2Cl_2

Neutral TiO_2

$^{31}P\{^1H\}$ CP MAS NMR: δ_{iso} = 16.8, δ_{11}= 81, δ_{22} = 17, δ_{33} = -50.

 NP-TiO_2

$^{31}P\{^1H\}$ CP MAS NMR: δ_{iso} = 19.1

$^{31}P\{^1H\}$ MAS NMR: δ = Nil

Suspension of TiO$_2$ immobilised palladium-3,4-dihydroxy catechol phosphines in DMF

Neutral TiO$_2$

^{31}P{^{1}H} CP MAS NMR: δ_{iso} = Nil

^{31}P{^{1}H} MAS NMR: δ = 18.8 & 32.4 (0.7:1)

Suspension of TiO$_2$ immobilised palladium-3,4-dihydroxy catechol phosphines in CH$_3$CN

Neutral TiO$_2$

^{31}P{^{1}H} CP MAS NMR: δ_{iso} = Nil

^{31}P{^{1}H} MAS NMR: δ = 19.4 & 32.6

NP-TiO$_2$

^{31}P{^{1}H} CP MAS NMR: δ_{iso} = 18.4

Suspension of TiO$_2$ immobilised palladium-3,4-dihydroxy catechol phosphines in CH$_3$CN with 10 vol % NEt$_3$

NP-TiO$_2$

^{31}P{^{1}H} CP MAS NMR: δ_{iso} = 17.2

^{31}P{^{1}H} MAS NMR: δ = Nil

Sonogashira coupling of phenylacetylene with 4-Iodonitrobenzene catalyzed by 3,4-dihydroxypalladium catechol phosphines,[PdCl$_2$(L)$_2$] supported on NP-TiO$_2$
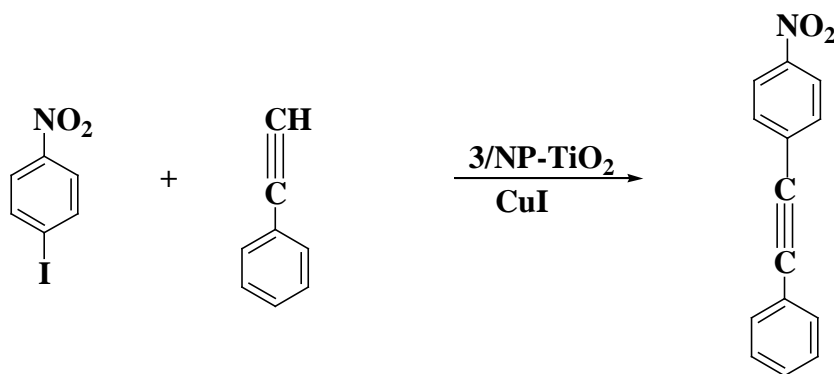
 Phenylacetylene (0.15 mL, 1.3 mmol), CuI (10 mg, 0.05 mmol) and [PdCl$_2$(L)$_2$]-TiO$_2$ (500 mg) were added to a solution of 4-iodonitrobenzene (80 mg, 0.32mmol) in triethyl amine (30 mL) and the suspension was stirred for one day at room temperature. It was then filtered, washed the solid residue with triethylamine (20 mL). Both the filtrate and washings were evacuated and, the resulting solid residue was chromatographed with short silica plug by using CH$_2$Cl$_2$: hexane (3:7) as eluant to obtain the pale yellow solid as the product - (4-nitrophenyl)phenylethyne (yield - 70%) after the solvent evaporation.

^{1}H, NMR (CDCl$_3$) δ (ppm) = 7.30-7.40 (m, 5H, Ph), 7.49-7.56 (m, 2H, C$_6$H$_4$NO$_2$), 7.61-7.67 (m, 2H, C$_6$H$_4$NO$_2$), 8.17-8.23 (m, 2H, C$_6$H$_4$NO$_2$).

NP-TiO$_2$ supported catalyst was reused for the second catalytic run which produced the yield of 68% of the coupling product while the third catalytic run dropped the yield of the coupling product to 10%.

7.3 BET data

a) HMS
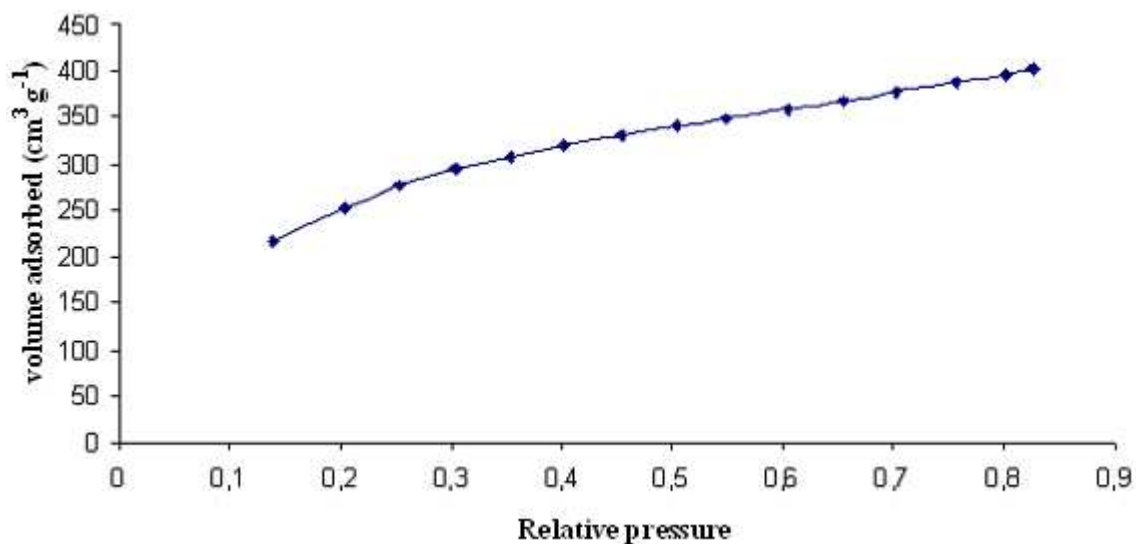
Area

Single Point Surface Area at P/Po 0.30 :	897 m²/g
BET Surface Area:	811m²/g
Langmuir Surface Area:	1755 m²/g
BJH Adsorption Cumulative Surface Area of pores between 8.50 and 1500.0 Å Radius:	671m²/g
BJH Desorption Cumulative Surface Area of pores between 8.50 and 1500.0 Å Radius:	944 m²/g

Volume

Single Point Total Pore Volume of pores less than 536.16 Å Radius at P/Po 0.981:	0.68 cm³/g

BJH Adsorption Cumulative Pore Volume of pores

between 8.50 and 1500.0 Å Radius: 0.52 cm³/g

BJH Desorption Cumulative Pore Volume of pores
    between 8.5 and 1500.0 Å Radius: 0.81 cm³/g

Pore Size

Average Pore Radius (2V/ Å by BET):   16.75 Å

BJH Adsorption Average Pore Radius (2V/ Å):   15.59 Å

BJH Desorption Average Pore Radius (2V/ Å):   17.20 Å

b) APTESi-HMS

Area

BET Surface Area: 536 m²/g

Pore Volume

Single Point Adsorption Total Pore Volume of pores less than
    2321.01 Å width at P/Po 0.99:   0.32 cm³/g

BJH Adsorption Cumulative Pore Volume of pores

    between 1.0 Å and 1000.0 Å width: 0.28 cm³/g

BJH Desorption Cumulative Pore Volume of pores

    between 1.0 Å and 1000.0 Å width: 0.27cm³/g

<div align="center">Pore Size</div>

Average pore width (4V/ Å by BET):   24.06 Å

BJH Adsorption average pore width (4V/ Å):   23.56 Å

BJH Desorption average pore width (4V/ Å):   23.85 Å

c) [CpFePNH]/APTESi-HMS

<div align="center">Area</div>

BET Surface Area: 397 m²/g

Pore Volume

Single Point Adsorption Total Pore Volume of pores less than
22167.73 Å width at P/Po 0.99:   0.25 cm³/g

BJH Adsorption Cumulative Pore Volume of pores
between 1.0 Å and 1000.0 Å width: 0.23 cm³/g

BJH Desorption Cumulative Pore Volume of pores
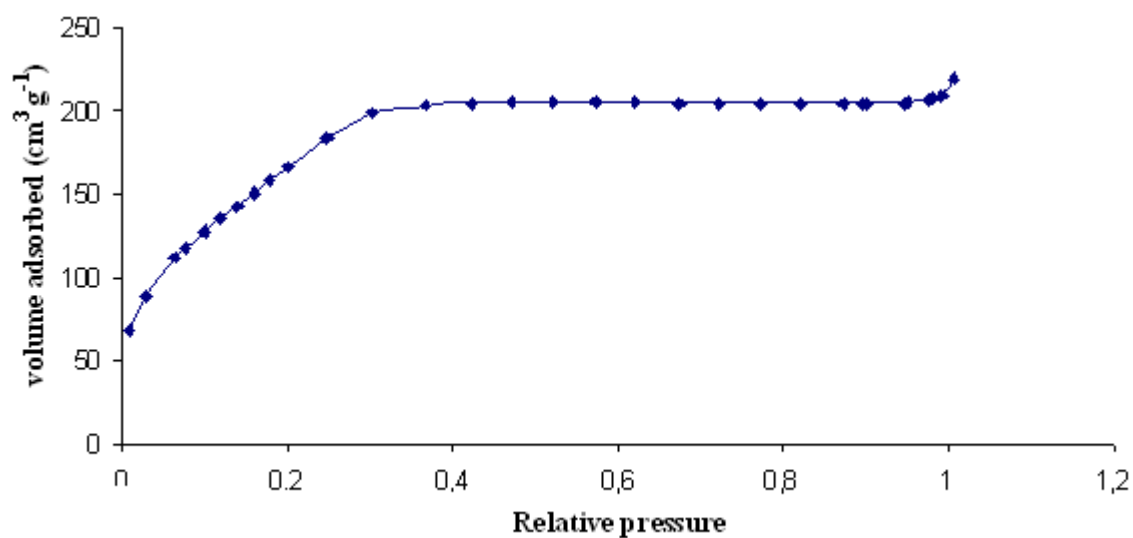between 1.0 Å and 1000.0 Å width: 0.23 cm³/g

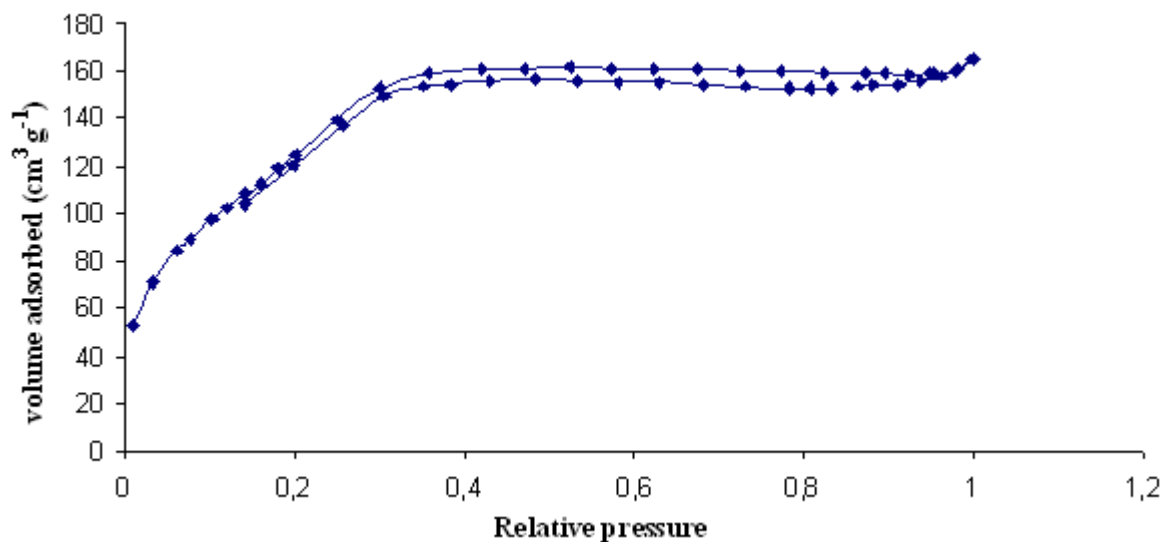## Pore Size

Average pore width (4V/ Å by BET):   25.75 Å

BJH Adsorption average pore width (4V/ Å):   24.4 Å

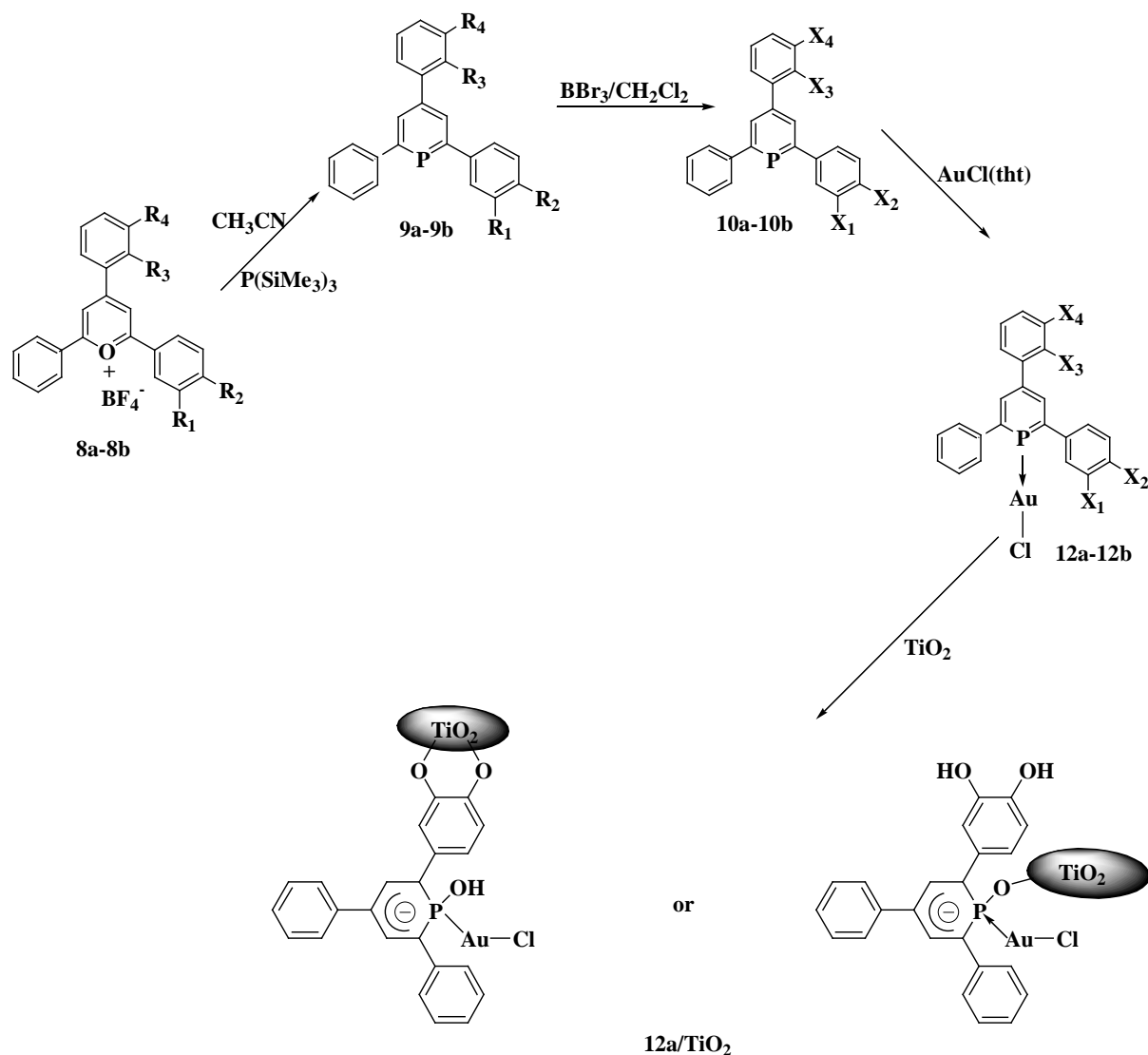BJH Desorption average pore width (4V/ Å):   24.55 Å

8. Summary and outlook

Summary

The present study aimed **(i)** to immobilise palladium catechol phosphines on TiO_2 and study the immobilised and remobilised species in various solvents by HR MAS NMR, **(ii)** to synthesise novel functionalized phosphinines and their complexes capable to anchor on a solid carrier, and to immobilise them on inorganic supports**, (iii)** to develop some novel gold(I) phosphinine complexes and phosphinine stabilized gold nanoparticles, and study the mode of ligand coordination on the gold surface by ^{31}P CP MAS NMR spectroscopy, **(iv)** to develop and anchor suitable functional derivatives of monophosphaferrocenes onto inorganic surface by covalent tethering method and study the anchoring process by CP MAS NMR spectroscopy.

For the first topic, two isomeric forms of palladium catechol phosphines were initially tested for immobilisation on different specimens of TiO_2, neutral TiO_2 and slightly acidic TiO_2 nanoparticles. Successful deposition of the complexes on both materials was monitored by ^{31}P CP MAS NMR. The study of both dry specimens and suspensions by ^{31}P HR MAS NMR experiments with and without cross polarization and magic angle spinning in combination cleared that the complexes immobilised on neutral TiO_2 redissolved in polar solvents, and that the mobility of those species was greatly effected by the ligand structure. The studies showed that immobilised complexes on slightly acidic TiO_2 nanoparticles are definitely more tightly bound and gave no evidence for either the occurrence of leaching or of any base induced reaction. However, eventhough the deposition of complexes on neutral titania is feasible they can be easily eluted by polar solvents. The use of the immobilised complex as catalyst in a carbon - carbon cross coupling reaction was also demonstrated in this context.
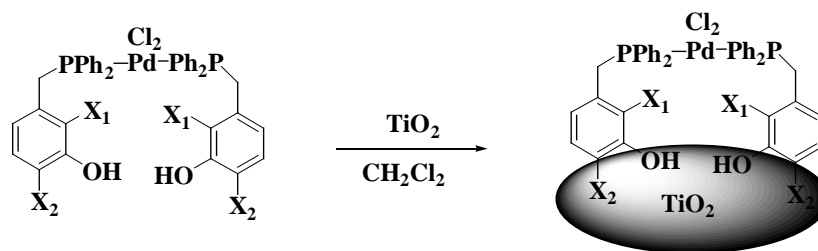
	X₁	X₂
2	OH	H
3	H	OH

The successful deposition of phosphine complexes on TiO₂ motivated to develop complexes of phosphinines having similar functionality on the aromatic moiety that could serve as a suitable candidate for the immobilisation on TiO₂. In this regard, two isomeric forms of novel phosphinines bearing OH- functionalities in the vicinal positions of the aromatic moiety were developed from the corresponding pyrylium salt by adopting the modular procedure of Vogt and Müller[35].

BBr$_3$/CH$_2$Cl$_2$

AuCl(tht)

CH$_3$CN

P(SiMe$_3$)$_3$

8a-8b   **9a-9b**   **10a-10b**   **12a-12b**

TiO$_2$

or

12a/TiO$_2$

	R$_1$	R$_2$	R$_3$	R$_4$		X$_1$	X$_2$	X$_3$	X$_4$
8a	OMe	OMe	H	H	**10a**	OH	OH	H	H
8b	H	H	OMe	OMe	**10b**	H	H	OH	OH
9a	OMe	OMe	H	H	**12a**	OH	OH	H	H
9b	H	H	OMe	OMe	**12b**	H	H	OH	OH

These species then served as ligands for the development of gold(I) complexes. The behavior of so formed gold(I) phosphinine upon attempts towards their immobilisation on TiO$_2$ surface was monitored by ^{31}P CP MAS NMR. Spectral studies revealed that the ligands were successfully deposited on TiO$_2$ surfaces, but modified structurally during the immobilisation process. The choice of silica as a solid carrier was also investigated; a functionalized phosphinine was synthesised and anchored onto a silica surface. The characterization of the supported material by ^{31}P MAS NMR revealed that nearly 25% of the ligand has retained its

identity on the carrier, but that the immobilisation was also accompanied by the formation of decomposition products on the surface.
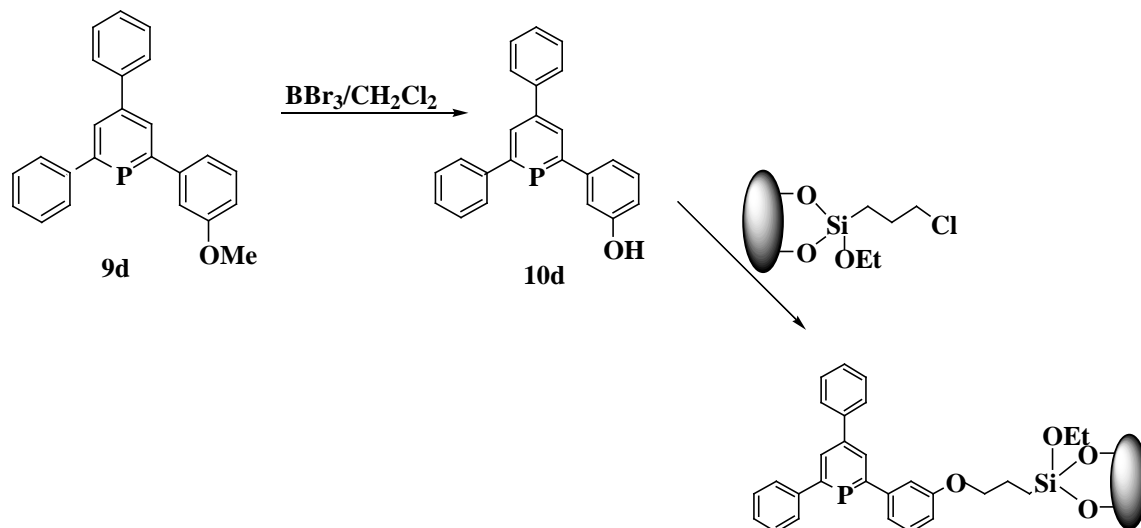
Au NPs of phosphinines with different gold - phosphorus ratios were prepared according to a previously reported procedure[91] and charaterized by ^{31}P CP MAS NMR spectroscopy. The comparison of the spectral data with those of authentic Au-phosphinine complexes and also with XPS measurements suggested that gold nanoparticles appeared to be in the form of cationic clusters with the Cl$^-$ as the counter ion and contained terminal P coordinated phosphinine ligands bound to Au(I) centres, together with decomposition products.

A monophosphaferrocene was prepared[59] and attempted to immobilise via covalent tethering onto amino functionalized HMS materials by Schiff condensation. However, spectral analysis of the immobilised material has not given an adequate information to eluicdate the structure of the immobilised species. Thus the immobilisation of monophosphaferrocene by reductive amination was carried out and, the anchored material so obtained was studied and compared with the relative soluble compounds by NMR methods. The solid state NMR studies revealed that monophosphaferrocene which was immobilised onto the silica surface exists in two diastereomeric forms. Further the anchoring process of monophosphaferrocene onto capped amino functionalized HMS was also investigated by solid state NMR methods and showed that here also anchored monophosphaferrocene exists in two diastereomeric forms but the capping was not persistant in the immobilised material.
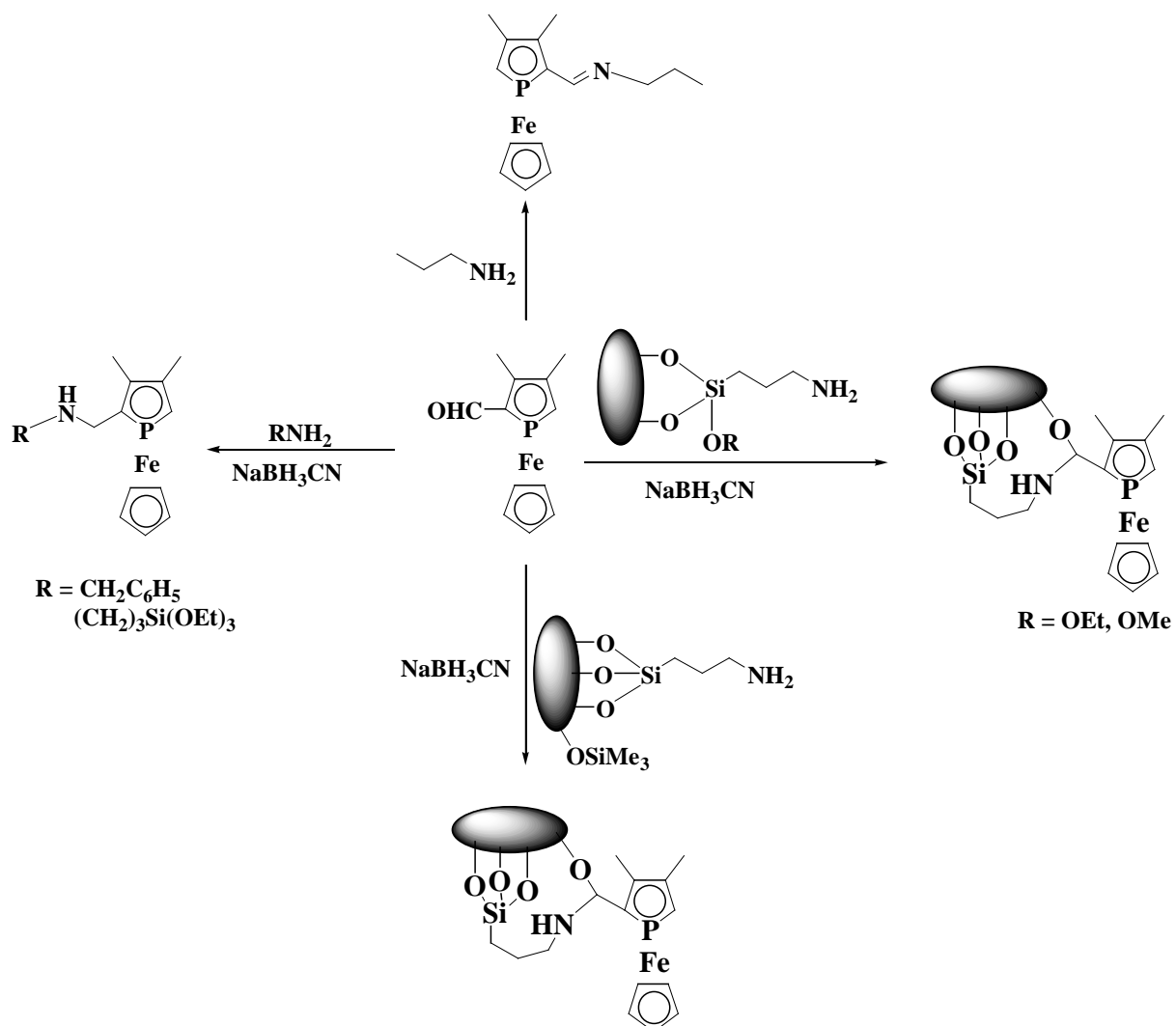
Outlook

The immobilisation of monophosphaferrocene can be extended further in future to other functional derivatives of monophosphaferrocene. The formyl derivative of monophosphaferrocene can be reduced to the corresponding alcohols which can be immobilised onto modified chloro functionalized silica surface as outlined below.
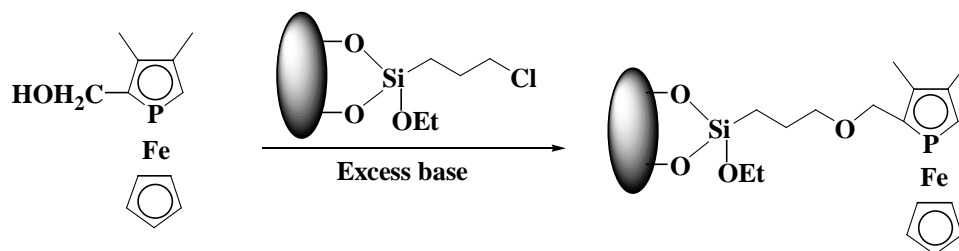
Further it is also proposed to develop some similar P/√N ligands with hydroxy functionality on the aromatic ring as outlined below, which can be used in future for immobilisation on halo alkyl functionalized silica by covalent tethering.
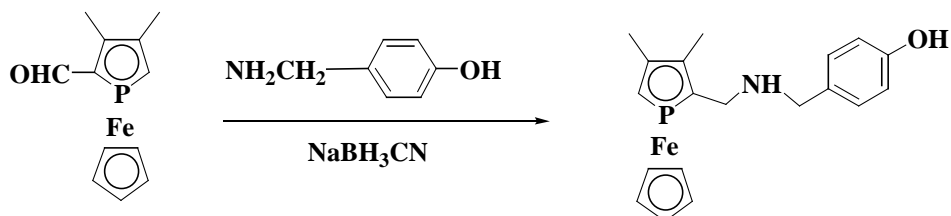
9. Zusammenfassung

Die vorliegende Studie hatte zum Ziel (i) Palladium-Catecholphosphane auf TiO_2 zu immobilisieren und die immobilisierten oder re-mobilisierten Spezies mittels HR MAS NMR-Spektroskopie zu untersuchen, (ii) neuartige funktionalisierte Phosphinine und deren Komplexe zu synthetisieren, die in der Lage sind, auf einem festen anorganischen Trägermaterial verankert zu werden, (iii) neuartige Gold(I)-Phosphininkomplexe und phosphininstabilisierte Gold-Nanopartikel zu entwickeln und die Art der Ligandenkoordination an der Goldoberfläche mittels ^{31}P CP MAS NMR-Spek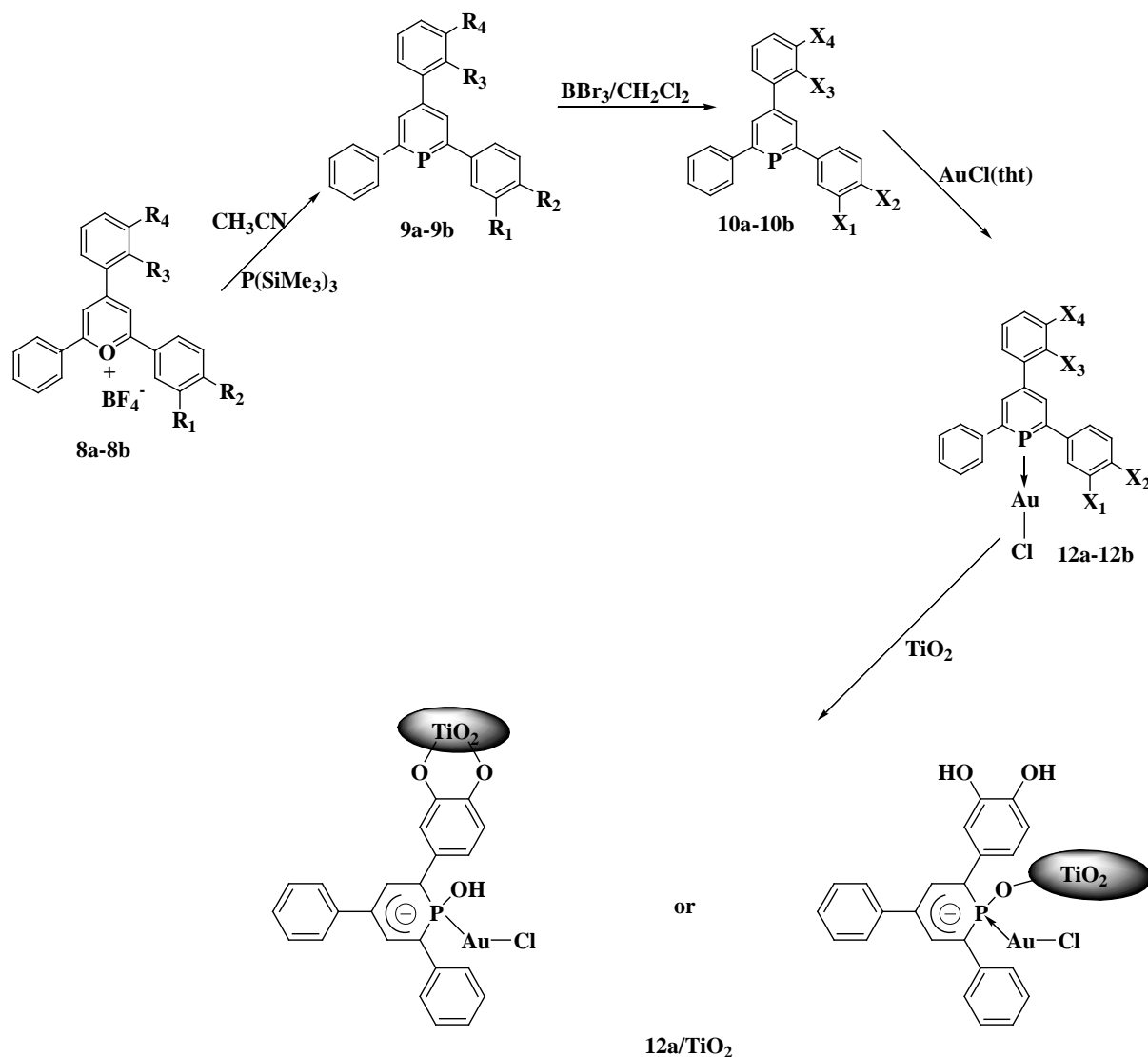troskopie zu untersuchen, (iv) funktionalsierte Derivate von Monophosphaferrocenen zu entwickeln und auf anorganischen Trägermaterialien zu verankern, sowie den Verankerungsprozess mittels CP MAS NMR-Spektroskopie zu untersuchen.

Im Rahmen des ersten Themas wurden zwei Isomere eines Palladium-Catecholphosphans zunächst in Bezug auf ihre Immobilisierung auf verschiedenen Arten von TiO_2 - neutralem und auf leicht sauren TiO_2-Nanopartikeln – zu untersuchen. Die erfolgreiche Ablagerung der Komplexe auf beiden Materialien wurde mit ^{31}P CP MAS NMR-Spektroskopie untersucht. Die Untersuchung von sowohl trockenen also auch in Lösemitteln suspendierten Proben mittels ^{31}P HR MAS NMR mit und ohne Kreuzpolarisation und „magic angle spinning" konnte aufklären, dass der Komplex, der auf neutralem TiO_2 immobilisiert war, sich in polaren Lösemitteln ablöste, und das die Mobilität dieser Spezies sehr von der Struktur der Liganden abhing. Die Untersuchungen zeigten, dass Komplexe, die auf leicht sauren TiO_2-Nanopartikeln immobilisiert waren, deutlich fester gebunden waren und keine Anzeichen für Auslaugen oder irgendwelcher baseninduzierter Reaktionen erkennen ließen. Die Verwendung der immobilisierten Komplexe als Katalysatoren in einer Kohlenstoff-Kohlenstoff-Kreuzkupplungsreaktion wurde ebenfalls demonstriert.
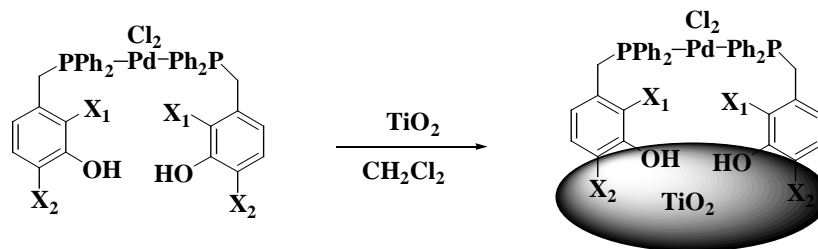
	X_1	X_2
2	OH	H
3	H	OH

Die erfolgreiche Fixierung von Phosphankomplexen auf TiO$_2$ regte dazu an, Phosphininkomplexe mit ähnlicher Funktionalität an der aromatischen Gruppe zu entwickeln, welche ebenfalls geeignet für die Immobilisierung auf TiO$_2$ sein könnten. In diesem Sinne wurden, ausgehend von den entsprechenden Pyryliumsalzen, mit Hilfe der modularen Prozedur von Vogt und Müller zwei isomere Formen neuartiger Phosphinine entwickelt, die OH-Funktionalität in den vicinalen Positionen der aromatischen Gruppe aufweisen.

	R₁	R₂	R₃	R₄		X₁	X₂	X₃	X₄
8a	OMe	OMe	H	H	**10a**	OH	OH	H	H
8b	H	H	OMe	OMe	**10b**	H	H	OH	OH
9a	OMe	OMe	H	H	**12a**	OH	OH	H	H
9b	H	H	OMe	OMe	**12b**	H	H	OH	OH

Diese Spezies dienten dann als Liganden für die Synthese von Gold(I)-Komplexen. Das Verhalten der so geformten Gold(I)-Phosphininkomplexe wurde während der Immobilisierungsversuche mittels ^{31}P CP MAS NMR-Spektroskopie überwacht. Spektrale Untersuchungen zeigten, dass die Liganden erfolgreich auf der TiO₂-Oberfläche abgelagert wurden, jedoch währenddessen strukturell modifiziert wurden. Auch Silika als festes Trägermaterial wurde untersucht: Eine funktionalisiertes Phosphinin wurde synthetisiert und auf der Silika-Oberfläche verankert. Die Charakterisierung mit Hilfe von ^{31}P MAS NMR-

151

Spektroskopie zeigte, dass fast 25% des Liganden seine Identität auf dem Träger bewahrt hatten, aber dennoch Abbauprodukte während der Immobilisierung entstanden waren.
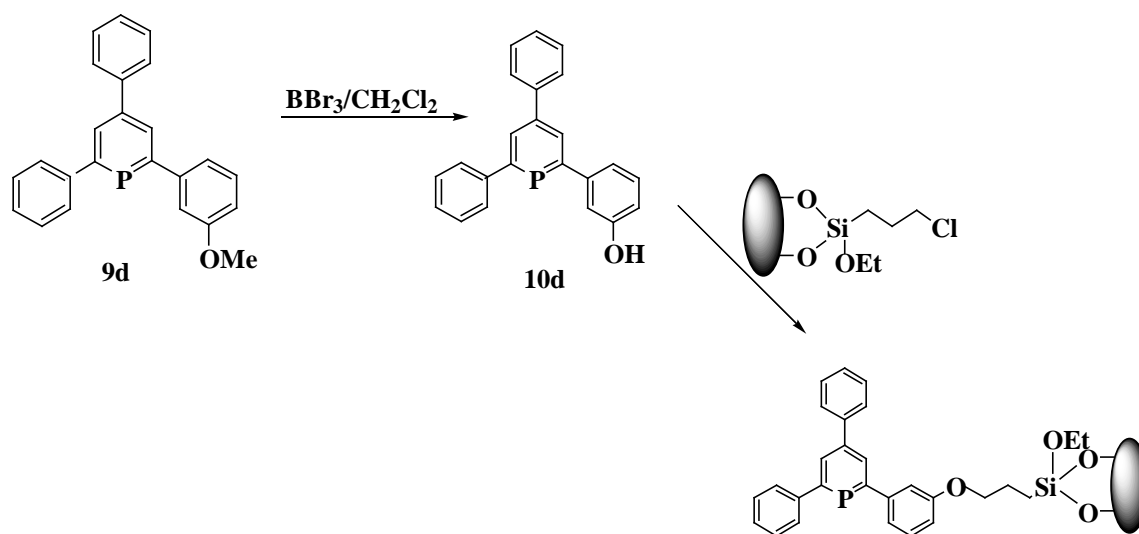
Gold-Nanopartikel von Phosphininen mit verschiedenen Gold-Phosphor-Verhältnissen wurden anhand einer bekannten Vorschrift dargestellt und mittels ^{31}P CP MAS NMR-Spektroskopie charakterisiert. Der Vergleich der Spektraldaten mit denen von echten Gold-Phosphininkomplexen und auch mit XPS-Messungen legte nahe, dass die Gold-Nanopartikel in Form von kationischen Clustern mit Chlorid-Gegenionen vorlagen, und dass sie terminal P-koordinierte Phosphininliganden an Gold(I)-Zentren enthielten, zusammen mit Abbauprodukten.

Ein Monophosphaferrocen wurde synthetisiert und Versuche unternommen, dies mit Hilfe von kovalenten Ankern via Schiff-Kondesation an aminofunktionalisierten HMS-Materialien zu immobilisieren. Festkörper-NMR-spektroskopische Untersuchungen gaben keine zufriedenstellende Aufklärung über den Immobilisierungsprozess. Deshalb wurde die Immobilisierung von Monophosphaferrocen mittels reduktiver Aminierung durchgeführt, und das so gewonnene Material mit Hilfe von NMR-Methoden untersucht und mit den entsprechenden löslichen Verbindungen verglichen. Festkörper-NMR-Studien zeigten, dass das immobilisierte Monophosphaferrocen in zwei diastereomeren Formen vorlag.

Weiterhin wurde die Verankerung von Monophosphaferrocen an verkapptes, amino-funktionalisiertes HMS mit Hilfe von Festkörper-NMR-Methoden untersucht, und auch hier zeigte sich, dass das verankerte Produkt in zwei Diastereomeren vorlag, aber die Verkappung im immobilisierten Material nicht beständig war.

R = CH₂C₆H₅
(CH₂)₃Si(OEt)₃

R = OEt, OMe

153
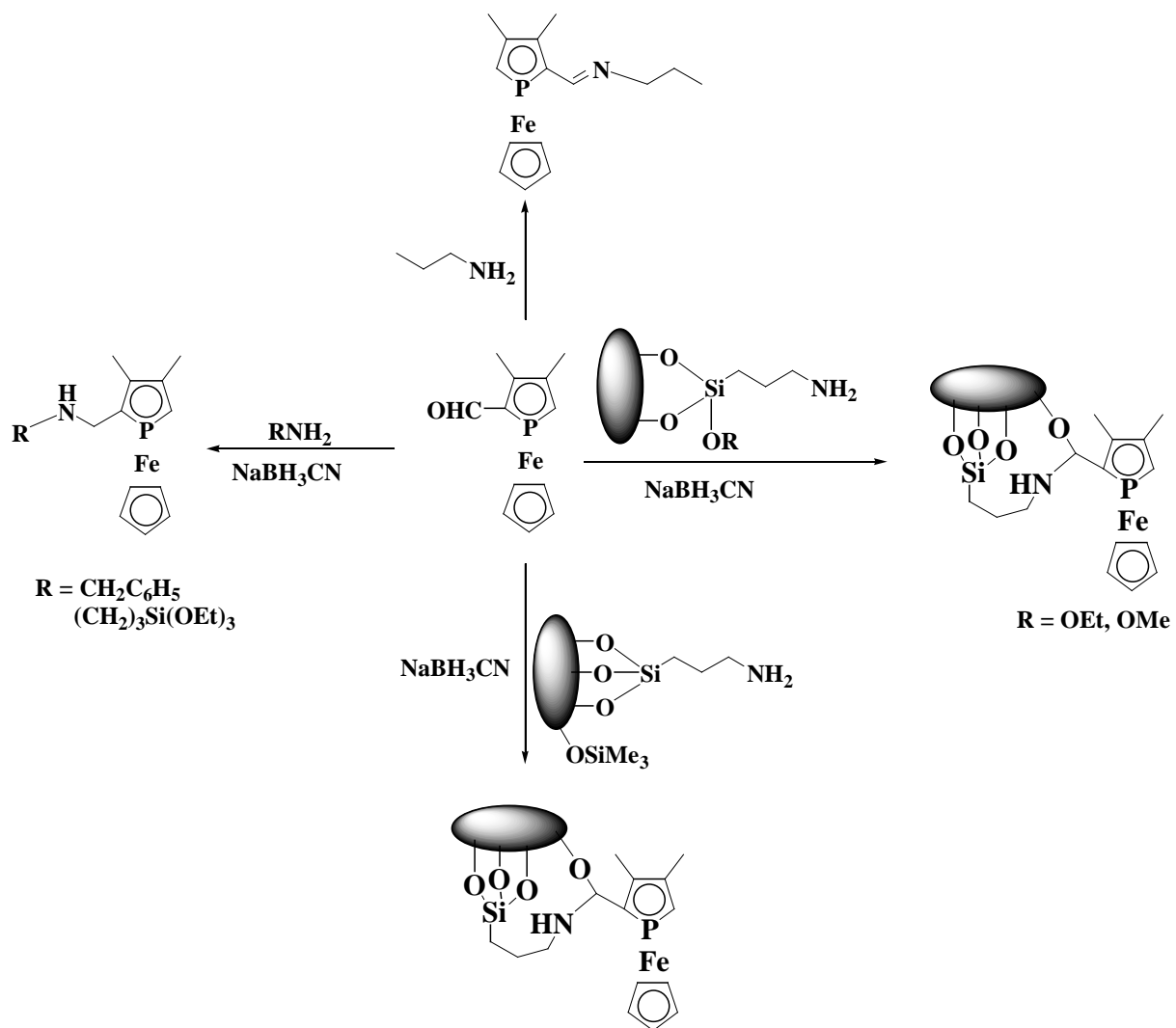
10. References

1 H. U. Blaser, B. Pugin and M. Studer, In Chiral Catalyst Immobilization and Recycling. D. E. De Vos, I. F. J Vankelecom, and P. A. Jacobs, (eds) Wiley-VCH, Weinheim. **2000**, 1-15.

2 W. C. Finch, R. D. Gillespie and D. Hedden, T. J. Marks, *J. Am. Chem. Soc*. **1990**, *112*, 6221.

3 S. Abramson, N. Bellocq and M. Lasperas, *Top. Catal*. **2000**, *13*, 339.

4 A. Kinting, H. Krause and M. Capka, *J. Catal*. **1985**, *25*, 152.

5 A. Corma, H. Garcia, A. Mousaif, M. J. Sabatier, R. Zniber and A. Redouane, *Chem Commun.* **2002**, 1058.

6 J. S. Albertus, Joost, N. H. Reek, Paul, C. J. Kamer and P. W. N. M van Leeuwen, *J. Am. Chem. Soc*. **2001**, *123*, 8468- 8476.

7 C. Baleizao, B. Gigante, M. J. Sabatier, H. Garcia and A. Corma, *Appl. Catal. A*. **2002**, *288*, 279.

8 C. Bianchini, P. Barbaro, V. Dal Santo, R. Gobetto, A. Meli, W. Oberhause, R. Psaro and F. Vizza, *Adv. Synth. Catal*. **2001**, *41*, 343.

9 J. M. Fraile, J. I. Garcia, J. A. Mayoral and T. Tarnai, *Tetra. Asym*. **1997**, *8*, 2089.

10 S. B. Ogunwami and T. Bein, *Chem. Commun*. **1997**, 901.

11 M. J. Sabatier, A. Corma, A. Domenech, V. Fornes and H. Garcia, *Chem. Commun*. **1997**, 1285.

12 P. M. Morn and G. J. Hutchings, *Chem. Soc. Rev*. **2004**, *33*, 108-122.

13 T.Lutz and H. Papp, *Kinteics and catalysis*. **2007**, *48*, 176-182.

14 J. M. Fraile, J. I. Garcia and J. A. Mayoral, *Coord. Chem. Rev*. **2008**, *252*, 624-646.

15 C. M. Crudden, D. Allen, M. D. Mikoluk and J. Sun, *Chem. Commun*. **2001**, 1154-1155.

16 Y. Wang and F. Caruso, *Chem. Mater*. **2005**, *17*, 953-961.

17 L. Berni, H. C. Clark, J. A. Davies, C. A. Fyfe and R. E. Wasylishen, *J. Am. Chem. Soc*. **1982**, *104*, 438.

18 C. Merckle, S. Haubrich and J. Blümel, *J. Organomet. Chem*. **2001**, *627*, 44-54.

19 P. Le Floch, *Coord. Chem. Rev*. **2006**, *250*, 627-681.

20 L. Weber, *Angew. Chem. Int. Ed*. **2002**, *41*, 563-572.

21 J. Waluk, H. P. Klein, A. J. Ashe, III and J. Michl, *Organometallics*. **1989**, *8*, 2804.

22 G. Märkl and C. Martin, *Angew. Chem. Int. Ed. Engl*. **1974**, *13*, 408.

23 A. J. Ashe III, *Acc. Chem. Res*. **1978**, *11*, 153.

24 T. C. Wong and L.S. Bartell, *J.Chem. Phys*. **1974**, *61*, 2840.

25 P. D. Burrow, A. J. Ashe, III, D. J. Belville, and K. D. Jordan, *J. Am. Chem. Soc*. **1982**, *104*, 425.

26 M. J. S. Dewar and A. Holder, *Heterocycles*. **1989**, *28*, 1135.

27 P. Rosa, N. Mezailles, F. Mathey and P. Le Floch, *J. Org. Chem*, **1998**, *63*, 4826.

28 L. Nyulazzi and G. Keglevich, *Heteroatom. Chem*. **1994**, *5*, 131.

29 H. Oehling and A. Schweig, *Phosphorus*. **1971**, 203.

30 D. J. Berger, P. P. Gaspar, and J. F. Liebman, *J. Mol. Struct. (Theochem)*. **1995**, *51*, 338.

31 A. Hettche and K. Dimroth, *Chem. Ber*. **1973**, *106*, 1001.

32 G. Märkl, *Angew. Chem. Int. Ed. Engl*. **1966**, *5*, 846.

33 K. Dimroth, N. Greif, W. Stade and F. W. Steuber, *Angew. Chem. Int. Ed. Engl*. **1967**, *6*, 711.

34 G. Märkl, F. Lieb and A. Merz, *Angew. Chem. Int. Ed. Engl*. **1967**, *6*, 458.

35 1) C. Muller, E. A. Pidko, A. J. P. M. Staring, M. Lutz, A. L. Spek, R. A. van Santen and D. Vogt, *Chem. Eur. J*. **2008**, *14*, 4899-4905. 2) C. Muller, L. G. Lopez, H. Kooijman, A. L. Spek and D. Vogt, *Tetra. Lett*. **2006**, *47*, 2017-2020.

36 C. Charrier, H. Bonnard and F. Mathey, *J. Org. Chem*. **1982**, *47*, 2376.

37 P. Le Floch and F. Marthey, *J. Chem. Soc., Chem. Commun*. **1993**, 1295.

38 N. Mezailles, N. Avarvari, L. Ricard, F. Mathey and P. Le Floch, *Inorg. Chem*. **1998**, *37*, 5313-5316.

39 N. Avarvari, P. Le. Floch and F. Mathey, *J. Am. Chem. Soc*. **1996**, *118*, 11978.

40 K. M. Doxsee and J. B. Farahi, *J. Am. Chem. Soc*. **1988**, *110*, 7239.

41 K. M. Doxsee and J. B. Farahi, *J. Chem. Soc, Chem. Commun*. **1990**, 1452.

42 K. M. Doxsee, J. B. Farahi and H. Hope, *J. Am. Chem. Soc*. **1991**, *113*, 8889.

43 K. M. Doxsee, J. J. J. Juliette, J. K. M. Mouser and K. Zientara, *Organometallics*. **1993**, *12*, 4682.

44 N. Avarvari, P. Le. Floch, L. Ricard and F. Mathey, *Organometallics*. **1997**, *16*, 4089.

45 J. Waluk, H. P. Klein, A. J. Ashe III, and J. Michl, *Organometallics*. **1989**, *8*, 2804.

46 T. Veszpremi, L. Nyulaszi, P. Varnai and J. Reffy, *Acta Chim. Hung.-Models Chem*. **1993**, *130*, 691.

47 P. D. Burrow, A. J. Ashe III, D. J. Belville, and K. D. Jordan, *J. Am. Chem. Soc*. **1982**, *104*, 425.

48 B. Breit, R. Winde, T. Mackewitz, R. Paciello and K. Harms, *Chem. Eur. J*. **2001**, *7*, 3106.

49 E. F. DiMauro and M. C. Kozlowski, *J. Chem. Soc. Perkin. Trans*. **2002**, *1*, 439.

50 C. Elschenbroich, M. Nowotny, A. Behrendt, W. Massa and S. Wocaldo, *Angew. Chem. Int. Ed.* **1992**, *31*, 1343.

51 C. Elschenbroich, S. Voss, O. Schiemann, A. Lippek and K. Harms, *Organometallics*, **1998**, *17*, 4417.

52 C. Elschenbroich, M. Nowotny, A. Behrendt, K. Harms, S. Wocaldo and J. Pebler, *J. Am. Chem. Soc.* **1994**, *116*, 6217.

53 P. L. Arnold, F. G. N. Cloke, K. Khan and P. Scott, *J. Organomet. Chem.* **1997**, *77*, 528.

54 F. Knoch, F. Kremer, U. Schimdt, U. Zenneck, P. Le. Floch and F. Mathey, *Organometallics*. **1996**, *15*, 2713.

55 P. Le. Floch, F. Knoch, F. Kremer, F. Mathey, J. Scholz, K. H. Thiele and U. Zenneck, *Eur. J. Inorg. Chem.* **1998**, 119.

56 N. Mezailles, L. Ricard, F. Mathey and P. Le. Floch, *Organometallics*. **2001**, *20*, 3304.

57 P. Le. Floch, L. Ricard and F. Mathey, *J. Chem. Soc., Chem. Commun*. **1993**, 789.

58 P. Le Floch, A. Kolb and F. Mathey, *J. Chem. Soc., Chem. Commun*. **1994**, 2065.

59 A. J. Arce, A. J. Deeming, Y. de Sanctis and J. Manzur, *J. Chem. Soc., Chem. Commun*. **1993**, 325.

60 K. Waschbusch, P. Le. Floch, L. Ricard and F. Mathey, *Chem. Ber. Recl*, **1997**, *130*, 843.

61 B. Breit, R. Paciello, B. Geisler and M. Röper, (BASF, A-G), Ger. Pat, 19621967, *Chem. Abstr*. **1999**, *130*, 129496.

62 D. Böhm, H. Geiger, F. Knoch, S. Kummer, P. Le Floch, F. Mathey, U. Schimdt and U. Zennck, *Phosphorus, Sulfur, Silicon*, **1996**, *109*, 173.

63 F. Mathey, *J. Organomet. Chem*. **1990**, *149*, 400.

64 F. Mathey, A. Mitschler and R. Weiss, *J. Am. Chem. Soc*. **1977**, *99*, 3537.

65 X. Sava, L. Ricard, F. Mathey and P. Le Floch, *Organometallics*. **2000**, *19*, 4899-4903.

66 F. Mathey, J. Fischer and J. H. Nelson, *Struct Bonding*. **1983**, *55*, 154.

67 G. deLauzon, B. Deschamps, J. Fischer, F. Mathey and A. Mitschler, *J. Am. Chem. Soc*. **1980**, *102*, 994.

68 G. deLauzon, B. Deschamps and F. Mathey, *Nouv. J. Chim*, **1980**, *4*, 683.

69 C. Ganter, L. Brassat, C. Glinsböckel and B. Ganter, *Organometallics*. **1997**, *16*, 2862-2867.

70 L. Brassat, B. Ganter, C. Ganter, *Chem. Eur. J.* **1998**, *4*, 2148-2153.

71 C. Ganter, L. Brassat and B. Ganter, *Chem. Ber*. **1997**, *130*, 1771-1776.

72 H. Willms, W. Frank and C. Ganter, *Organometallics*. **2009**, *28*, 3049-3058.

73 J. Bitta, S. Fassbender, G. Reiss, W. Frank and C. Ganter, *Organometallics*. **2005**, *24*, 5176-5179.

74 C. Ganter, *J. Chem. Soc., Dalton. Trans*. **2001**, 3541-3548.

75 C. Ganter, C. Kaulen and U. Englert, *Organometallics*. **1999**, *18*, 5444.

76 R. Shintani, M. M. C. Lo and G. C. Fu, *Org. Lett*. **2000**, *2*, 3695.

77 M. Ogasawara, K. Yoshida and T. Hayashi, *Organometallics*. **2001**, *20*, 3913.

78 X. Sava, M. Melaimi, N. Mezailles, L. Ricard, F. Mathey and P. Le. Floch, *New. J. Chem*, **2002**, *26*, 1378-1383.

79 R. M. G. Roberts, J. Silver and A. S. Wells, *Eur. J. Inorg. Chem*. **2003**, 2049-2053.

80 X. Sava, N. Mezailles, N. Maigrot, F. Nief, L. Ricard, F. Mathey and P. Le Floch, *Organometallics*, **1999**, *20*, 4205.

81 S. Qiao, D. A. Hoic and G. Fu, *Organometallics*, **1998**, *17*, 773.

82 X. Sava, L. Ricard, F. Mathey and P. Le. Floch, *Chem. Eur. J*. **2001**, 3159.

83 R. Shintani and G. C. Fu, *Org. Lett*. **2002**, *4*, 3699.

84 R. Shintani and G. C. Fu, *Angew. Chem. Int. Ed*, **2003**, *42*, 4082.

85 C. Merckle, S. Haubrich and J. Blümel, *J. Organomet. Chem*. **2001**, *44*, 627.

86 C. Merckle and J. Blumel, *Adv. Synth. Catal*. **2003**, *345*, 584.

87 C. Merckle and J. Blumel, *Top. Catal*. **2005**, *34*, 5.

88 G. Tsiavaliaris, S. Haubrich, C. Merckle and J. Blümel, *Synlett*. **2001**, 391.

89 F. Piestert, R. Fetouaki, M. Bogza, T. Oeser and J. Blümel, *Chem. Commun*. **2005**, 1481.

90 N. T. Lucas, J. M. Hook, A. M. Mc Donagh and S. B. Colbran, *Eur J. Inorg. Chem*. 2005, 496-503.

91 A. Moores, F. Goettmann, C. Sanchez and P. Le Floch, *Chem.Commun*. **2004**, 2842-2843.

92 S. A. Raynor, J. M. Thomas, R. Raja, B. F. G. Johnson, R. G. Bell and M. K. Mantle, *Chem. Commun*. **2000**, 1925-1926.

93 N. J. Meehan, M. Poliakoff, A. J. Sandee, J. N. H. Reek, P. C. J. Kamer and P. W. N. M. van Leeuwen, *Chem. Commun*. **2000**, 1497-1498.

94 A. J. Sandee, J. N. H. Reek, P. C. J. Kamer and P. W. N. M. van Leeuwen, *J. Am. Chem. Soc*. **2001**, *123*, 8468-8476.

95 C. Merckle and J. Blümel, *Chem. Mater*. **2001**, *13*, 3617-3623.

96 N. T. Lucas, A. M. McDonagh, I. G. Dance, S. B. Colbran and D. C. Craig, *Dalton Trans*. **2006**, 680-685.

97 S. Chikkali and D. Gudat, *Eur. J. Inorg. Chem*. **2006**, 3005-3009.

98 L. Bemi, H. C. Clark, J. A. Davies, D. Drexler, C. A. Fyfe and R. Wasylishen, *J. Organomet. Chem.* **1982**, *224*, C5.

99 J. P. Yesinowski, *J. Am. Chem. Soc*. **1981**, *103*, 6266.

100 J. Blümel, *Coord. Chem. Rev*. **2008**, *252*, 2410-2423.

101 S. Chikkali, D. Gudat and M. Niemeyer, *Chem. Commun*. **2007**, 981-983.

102 C. Merckle and J. Blümel, *Chem. Mater*. **2005**, *17*, 586.

103 C. Merckle and J. Blumel, *Chem. Mater*. **2001**, *13*, 3617.

104 D. J. Brauer, M. Hingst, K. W. Kottsieper, C. Liek, T. Nickel, M. Tepper, O. Stelzer and W. S. Sheldrick, *J. Organomet. Chem*. **2002**, 645, 14-26.

105 T. Posset and J. Blümel, *J. Am. Chem. Soc*. **2006**, *128*, 8394.

106 S. Brenna, T. Posset, J. Furrer and J. Blümel, *Chem. Eur. J*, **2006**, *12*, 2880.

107 F. J. LaRonde, A. M. Ragheb and M. A. Brook, *Colloid Polym Sci*. **2003**, *281*, 391-400.

108 Vogel, *Organic syntheses*. **1941**, *1*, 78.

109 P. Le Floch, D. Carmichael, L. Ricard and F. Mathey, *J. Am. Chem. Soc*. **1993**, *115*, 10665-10670.

110 P. Le. Floch, L. Ricard and F. Mathey, *Bull. Soc. Chim. F*r, **1996**, *133*, 691.

111 K. C. Dash, J. Eberlein and H. Schmidbaur, *Synth. Inorg. Met. Org. Chem*. **1973**, *3*, 375.

112 N. Mezailles, L. Ricard, F. Mathey and P. Le. Floch, *Eur. J. Inorg. Chem*. **1999**, 2233-2241.

113 M. Doux, L. Ricard, F. Mathey, P. Le. Floch and N. Mezailles. *Eur. J. Inorg. Chem*. **2003**, 687-698.

114 C. J. Jameson in Phosphorus-31 NMR spectroscopy in stereochemical analysis (Eds: J. Verkade, L. D. Quin), VCH Publishers, Inc, Deerfield Beach, Florida. **1987**, 205-230.

115 S. Attar, W. H. Bearden, N. W. Alock, E. C. Alyea and J. H. Nelson. *Inorg. Chem*. **1990**, *29*, 425.

116 P. Le. Floch, D. Carmichael, L. Ricard, F. Mathey, A. Jut and C. Amatore, *Organometallics*. 1992, 11, 2475.

117 A. J. Ashe III, W. Butler, J. C. Colburn and S. Abu-Orabi, *J. Organomet. Chem*. **1985**, *282*, 233.

118 N. J. Clayden, C. M. Dobson and K. P. H. D. Michael, *J. Chem. Soc. Dalton Trans*. **1985**, 1811-1814.

119 E. Deschamps, F. Mathey, C. Knobler and Y. Jeannin, *Organometallics*, **1984**, *3*, 1150-1157.

120 P. M. Price, J. H. Clark and D. J. Macquarrie, *J. Chem. Soc; Dalton Trans*. **2000**, 101-110.

121 K. Wilson, A. F. Lee, D. J. Macquarrie and J. H. Clark, *Appl. Cata, A*. **2002**, *228*, 127-133.

122 P. T. Panev and T. J. Pinnavaia, *Science*, **1995**, *267*, 865-867.

123 S. M. Bruno, A. C. Coelho, R. A. S. Ferreira, L. D. Carlos, M. Pillilnger, A. A. Valente, P. R. Claro and I. S. Goncalves, *Eur. J. Inorg. Chem*. **2008**, 3786-3795.

124 Sujandi, E. A. Prasetyanto, S. C. Lee and S. E Park, *Micropous and Mesoporous Materials*, **2009**, *118*, 134-142.

125 A. Mocanu, I. Cernica, G. Tomoaia, L. D Bobos, O. Horovitz and M. T. Cotisel, *Colloid and surfaces A : Physicochem, Eng Asp*. **2009**, *338*, 93-101.

126 M. A. Hayat, Colloidal Gold, Principles, method and application, edited by Academic Press, San Diego, **1991**.

127 R. C. Elder et al. *J. Am. Chem. Soc*. **1985**, *107*, 5024.

128 M. Faraday, *Philos*. *Trans*. **1857**, *147*, 145-181.

129 R. L. Kahn, Serum diagnosis for syphilis. In colloid chemistry, Alexander. J. Ed, The chemical catalog co, New York. **1928**, *11*, 757.

130 Hauser and E. A. Aurum Potabile, *J. Chem. Educ*. **1952**, 456-458.

131 D. H. Brown and W. E Smith, *Chem. Soc. Rev*. **1980**, *9*, 217-240.

132 Immuno gold electron microscopy in virus diagnosis and research, Hyatt. A. D, Eaton. B. T, Eds. CRC press : Boca Raton, FL, **1993**.

133 G. Schmid, In nanoscale materials in Klabunde. K. J. Ed Wiley, New York. **2001**.

134 G. Schmid and L. F. Chi, *Adv. Mater*. **1998**, *10*, 515-527.

135 G. Schmid, Clusters and colloids, Ed, VCH, weinheim. **1994**.

136 G. Schmid. *Chem. Rev*. **1992**, *92*, 1709-1727.

137 M. Brust and C. J. Kiely, *Colloids and Surfaces A. Physico Chem. Eng. Asp.* **2002**, *202*, 119-126.

138 J. Turkevitch, P. C. Stevenson and J. Hillier, *Discuss. Faraday Soc*. **1951**, *11*, 55-75.

139 G. Schimd, R. Pfell., R. Boese, F. Bandermann, S. Meyer, G. H. M. Calis and J. van der Velden, *Chem. Ber*, **1981**, *114*, 3634 - 3642.

140 G. Schön and U. Simon. *Colloid. Polym. Sci*. **1995**, *273*, 101.

141 L. Bronstein, D. Chernyshov, P. Valetsky, N. Tkachenko, H. Lemmetyinen, J. Hartmann and S. Forster, *Langmuir*. **1999**, *15*, 83-91.

142 M. Brust, M. Walker, D. Bethell, D. J Schiffrin and R. J. Whyman, *J. Chem. Soc. Chem. Commun*. **1995**, 1655-1656.

143 W. W. Walter, Scott, M. Reed, Marvin, G. Warner and E. Hutshison, *J. Am. Chem. Soc*, **2000**, 12890-12891.

144 M. C. Dainie. *Chem. Rev*. **2004**, *104*, 293-346.

145 F. A. Vollenbroek, P. C. Bouten, J. M. Trooster, J. P. van der Berg and J. J. Bour, *Inorg. Chem.* 1980, 19, 2685-2698.

146 M. Doux, L. Ricard, F. Mathey, P. Le. Floch and N. Mezailles, *Eur. J. Inorg. Chem*. **2003**, 687-698.

147 E. N. de Silva, G. A. Bowmaker and P. C.Healy, *J. Mol. Str*, **2000**, *516*, 263-272.

148 P. D. Boyle, B. J. Johnson, A. Buehler and L. H. Pignolet, *Inorg. Chem*, **1986**, *25*, 7-9.

149 J. G. Hexem, M. H. Frey and S. J. Opella, *J. Am. Chem. Soc*. **1981**, *103*, 224.

150 J. W. Diesveld, E. M. Menger, H. T. Edzes and W. S. Veeman, *J. Am. Chem. Soc*. **1980**, *102*, 7935-7936.

151 C. Olivieri Alejandro, *Solid State Magnetic Resonance*. **1992**, *1*, 345-353.

152 A. Breque, F. Mathey and P. Savignac, *Synthesis*. **1981**, 983-985.

153 F. Mathey, *Tetrahedron*. **1972**, *28*, 4171-4181.

154 A. R. Silva, K. Wilson, A. C. Whitwood, J. H. Clark and C. Freire, *Eur. J. Inorg. Chem*. **2006**, 1275-1283.

155 A. Tarafdar and P. Pramanik, *Microporus and mesoporus materials*. **2006**, *91*, 221-224.

156 G.Fan, S. Cheng, M. Zhu and X. Gao, *Appl. Organometal. Chem*. **2007**, *21*, 670-675.

157 J. C. Hicks, R. Dabestani, A. C. Buchanan III and C. W. Jones, *Inorg. Chim. Act*. **2008**, *361*, 3024-3032.

158 M. W. McKittrick and C. W. Jones, *J. Am. Chem. Soc*. **2004**, *126*, 3052-3053.

159 B. Buszweski , *Chromatographia*, **1989**, *28*, 574-578.

160 G. Becker, H. Schimdt, G. Uhl, M. Regitz, W. Rösch and U.J. Vogelbacher, *Inorg. Synth*, **1990**, *27*, 243-253.

161 R. Uson, A. Laguna and M. Laguna, *Inorg. Synth*, **1989**, *26*, 85.

11. CURRICULUM VITAE

SAMITH KOMATH MALLISSERY
Institute of Inorganic Chemistry
University of Stuttgart
Pfaffenwaldring 55
D-707569, Stuttgart

E mail : komath@iac.uni-stuttgart.de

ACADEMICS

Ph.D (Doctor of Philosophy)
(Organometallic chemistry)

- Nov 2005 onwards, Institute of Inorganic Chemistry, Stuttgart University, Thesis title: Synthesis and immobilisation of unsaturated, functional phosphorus ligands and their metal complexes.

  Supervisor: Prof. Dr. D. Gudat.

M.Tech (Master of Technology)
(Industrial Catalysis)

- 8.04 CGPA, A grade, 2002-2004, Cochin University of Science and Technology, Kerala, India.

M.Sc (Master of Science)
(Chemistry)

- 69.07%, First class, 1998-2000, Kannur University, Kerala, India.

B.Sc (Bachelor of Science)
Chemistry

- 85.5%, First class, 1995-1998, Calicut Univerity, Kerala, India.

AWARDS

GATE (Graduate Aptitude Test in Engineering)- Percentile score: 91.11%.

Second rank in M.Tech awarded by Cochin University of Science and Technology, Kerala, India.

PROJECTS

As Project Assistant:

'Synthesis of polypeptide (copaxane) via ring opening polymerization of N-carboxy

anhydrase of amino acids', National Chemical Laboratory, Pune.

M.Tech Project:

'Synthesis of ansa fluorenyl silyl and phosphanyl amido group (1V) metal complexes and their application as olefin polymerization catalysts', National Chemical Laboratory, Pune, India.

M.Sc Project:

'Nitration of triaryl-2-pyrazolines', S.N. College, Calicut university, Kannur, India.

RESEARCH/TEACHING EXPERIENCE

- As a Project Assistant, 2004 Nov – 2005 Sept at National Chemical laboratory, Pune, India.
- As a post graduate teacher, 2000 Aug – 2002 Aug in Central Board of Secondary Education, Kerala, India.

TECHNICAL SKILLS

Spectroscopy: 1D-2D, Solid state NMR, FTIR, MS.

Schlenk technique.

Experience in handling pressure polymerization reactors.

PUBLICATIONS

'On the immobilisation of catechol-phosphane palladium complexes on TiO_2', S. H. Chikkali, D. Gudat, S. K. Mallissery, *Eur. J. Inorg. Chem*, **2008**, 5603-5608.

ORAL PRESENTATIONS

- German-Austrian Scientific coworkers workshop on main group element chemistry 2006, Technical University of Graz, Austria; April 20-22nd
- GK workshop " New Developments in Magnetic Resonance Techniques" 2006, Blaubeuren, Germany, September 6-7th.
- 5th PhD workshop on phosphorus chemistry 2008, Regensburg, Germany; March 10-11th.
- German-Austrian Scientific coworkers workshop on main group element chemistry 2009, Tecklenburg, April 3-5th.

POSTER PRESENTATIONS

- Ampere NMR School 2007, Bukowina, Poland ; June 24-30th.
- 6th PhD workshop on phosphorus chemistry 2009, Florence, Italy; March 26-27th.